

TALLINN UNIVERSITY OF TECHNOLOGY
DOCTORAL THESIS
35/2018

Development of Cemented Carbides with High Chromium Iron Alloy Binder

MAREK TARRASTE



TALLINN UNIVERSITY OF TECHNOLOGY

School of Engineering

Department of Mechanical and Industrial Engineering

This doctoral thesis was accepted for the defence of the degree 03/05/2018

Supervisor:

Prof. Jakob Kübarsepp
School of Engineering
Tallinn University of Technology
Tallinn, Estonia

Co-supervisor:

Kristjan Juhani, PhD
School of Engineering
Tallinn University of Technology
Tallinn, Estonia

Opponents:

Igor Konyashin, PhD
Element Six GmbH, Burghaun, Germany
National University of Science and Technology MISiS,
Moscow, Russia

Ants Lõhmus, PhD
Institute of Physics, University of Tartu
Tartu, Estonia

Defence of the thesis: 20/06/2018, Tallinn

Declaration:

Hereby I declare that this doctoral thesis, my original investigation and achievement, submitted for the doctoral degree at Tallinn University of Technology, has not been previously submitted for doctoral or equivalent academic degree.

Marek Tarraste

signature



European Union
European Regional
Development Fund



Investing
in your future

Copyright: Marek Tarraste, 2018

ISSN 2585-6898 (publication)

ISBN 978-9949-83-277-4 (publication)

ISSN 2585-6901 (PDF)

ISBN 978-9949-83-278-1 (PDF)

TALLINNA TEHNIKAÜLIKOOL
DOKTORITÖÖ
35/2018

Kõrge kroomisisaldusega rauasulamsideainega kõvasulamite arendus

MAREK TARRASTE

Contents

FOREWORD	7
ABBREVIATIONS, TERMS AND SYMBOLS.....	8
LIST OF PUBLICATIONS.....	9
INTRODUCTION.....	10
1 LITERATURE REVIEW	13
1.1 Background of WC-based cemented carbides.....	13
1.1.1 Brief overview of history.....	13
1.1.2 Key properties.....	14
1.1.3 Applications.....	17
1.2 Binder systems in cemented carbides.....	17
1.2.1 Traditional binders.....	18
1.2.2 Alternative Fe-based binders.....	19
1.2.3 Composite systems with WC and FeCr(C).....	21
1.3 Thermodynamic background.....	22
1.3.1 Fe-Cr-C system.....	22
1.3.2 W-Fe-C system.....	23
1.3.3 W-Fe-Cr-C system.....	23
1.4 Objectives of the present work.....	25
2 EXPERIMENTAL.....	26
2.1 Materials.....	26
2.2 Processing.....	28
2.3 Characterization methods.....	29
3 DEVELOPMENT OF WC-FeCr(C) CEMENTED CARBIDES.....	31
3.1 Vacuum sintered WC-FeCr(C) cemented carbides.....	31
3.1.1 Densification.....	31
3.1.2 Microstructural investigation.....	32
3.1.3 Elemental distribution.....	37
3.1.4 Phase composition.....	42
3.1.5 Summary.....	43
3.2 Means of improving the homogeneity of the microstructure.....	44
3.2.1 Spark plasma sintering.....	44
3.2.2 Addition of strong carbide forming elements.....	46
3.2.3 Summary.....	50
3.3 Properties of WC-FeCr(C)-(M) cemented carbides.....	50
3.3.1 Mechanical performance.....	51
3.3.2 Corrosion and oxidation resistance.....	53
3.3.3 Abrasive-erosion wear resistance.....	54
3.3.4 Summary.....	55
CONCLUSIONS.....	56
REFERENCES.....	58
ACKNOWLEDGEMENTS.....	63
ABSTRACT.....	64

LÜHIKOKKUVÕTE.....	66
APPENDIX.....	69
CURRICULUM VITAE.....	106
ELULOO KIRJELDUS.....	107

FOREWORD

This thesis is continuation of decades-long research on hard materials at Tallinn University of Technology (TUT). One of the key research objects in the Department of Mechanical and Industrial Engineering and its predecessors has been cemented carbides and cermets with alternative compositions – utilization of titanium and chromium carbides instead of tungsten carbide, substitution of conventional binder metals with experimental iron alloys.

Author of the doctoral thesis has worked in the cemented carbide (hardmetal) research group since bachelor studies and has been involved in various projects where the development of cemented carbides for wear applications and extreme conditions has been the main objective.

The topic of this thesis is derived from the ever-increasing requirements on both chemical composition and performance of engineering materials. Besides the common motivators in materials research (constant demand for more durable tools and assemblies, the need to reduce the price and supply risk of raw materials) the field is also being guided by regulations on the use of chemical elements and compounds. This thesis considers today's necessity and focuses on the development of competitive cemented carbides with economical and environmental friendly composition.

ABBREVIATIONS, TERMS AND SYMBOLS

Abbreviations

a.u.	arbitrary units
CC	Cemented Carbide
CI	Cast Iron
DSC	Differential Scanning Calorimetry
EDS	Energy Dispersive X-ray Spectroscopy
HV30	Vickers Hardness, load 298 N (30 kgf)
LPS	Liquid Phase Sintering
OM	Optical Microscope
TG	Thermogravimetry
TRS	Transverse Rupture Strength
SEM	Scanning Electron Microscope
SPS	Spark Plasma Sintering
vol%	volume percent
wt%	weight percent
XRD	X-ray Diffraction

Terms

binder pool	Distinct area in microstructure where concentration of binder phase elements is increased.
mixed carbide	Carbide phase with two or more carbide forming elements.

Symbols

α -Fe	Iron with body centred cubic (bcc) structure
α -Co	Cobalt with face centred cubic (fcc) structure
γ -Fe	Iron with face centred cubic (fcc) structure
ε -Co	Cobalt with closed packed hexagonal (cph) structure
η (η -phase)	Mixed carbide, either M_4C or M_6C ($M=W$ and binder metals Fe, Co or Ni)
Σl	Sum of crack lengths emanating from Vickers indentation corners
K_{Ic}	Fracture toughness

LIST OF PUBLICATIONS

- Paper I M. Tarraste, K. Juhani, J. Kübarsepp, J. Pirso, V. Mikli, The Effect of Cr and C on the Characteristics of WC-FeCr Hardmetals, *Proceedings of Euro PM2015*. (2015).
- Paper II M. Tarraste, J. Kübarsepp, K. Juhani, A. Mere, M. Kolnes, M. Viljus, B. Maaten, Ferritic chromium steel as binder metal for WC cemented carbides, *Int. J. Refract. Met. Hard Mater.* (2018) 73, 183–191.
- Paper III M. Tarraste, J. Kübarsepp, K. Juhani, T. Suurkivi, J. Pirso, Spark plasma sintering of WC hardmetals with Fe-based binder, *Proceedings of World PM2016*. (2016).
- Paper IV M. Tarraste, J. Kübarsepp, K. Juhani, A. Mere, M. Viljus, Effect of Carbon Stabilizing Elements on WC Cemented Carbides with Chromium Steel Binder, *Materials Science (Medžiagotyra)*, (XXXX) XX. (Accepted)

Author's contribution

The author of the doctoral thesis planned, prepared and conducted the experiments, analysed the results and was responsible for writing and publishing of the articles.

INTRODUCTION

Over ninety years have passed since the novel cutting tools composed of hard tungsten carbide (WC) particles embedded in ductile cobalt (Co) matrix (cemented carbides) were introduced to the general public. It is next to impossible to underestimate the importance of implementation of WC-Co cemented carbides (CCs). The following increase of output in metal working, mining and construction that occurred in the 1930s and 1940s can be described as a breakthrough on a par with The Industrial Revolution. Although CCs with optimal composition and properties were developed already in the 1930s [1], several major trends have shaped further research and development, namely substitution of WC with other hard phases, reduction of carbide grain size, application of thin coatings (PVD and CVD) and last but not least – finding competitive replacement for cobalt [2, 3].

Cemented carbides with cobalt binder (matrix) attained major attention in the early years. This is due to the superior combination of properties that are achievable with the WC-Co system – high hardness coupled with relatively high toughness and strength and overall excellent performance in various wear situations. Historically, the “second best” choice for binders has been nickel (Ni). While mechanical and wear properties of the WC-Ni system fall short when compared with WC-Co, the improved corrosion and oxidation resistance of CCs with Ni-based binders prove valuable for certain applications [4]. The unprecedented properties of CCs are attributed to their unique microstructure, where homogeneous distribution of hard particles is imperative and generally two-phased composition is favoured. Introduction of additional ceramic or metallic compounds usually deteriorates the properties of the composite.

The motivation of searching for replacements for cobalt and even nickel does not stem from insufficient properties, but instead from economical and healthcare considerations.

Issues with raw material supply and price

World’s largest mineral deposits of cobalt are in the Democratic Republic of the Congo and local political and civil unrests (i.e., Congo crisis in 1960-1965) have affected cobalt supply and price greatly [5]. The fluctuations of cobalt price from 1970 onward are exhibited in Fig. 1. European Commission has classified cobalt as one of the critical raw materials (CRMs) for EU [6]. CRMs are raw materials of high importance to the EU economy that possess high risk associated with their supply. In order to achieve greater independence regarding CRMs, the development of advanced recycling methods and substitution of given materials are being imposed.

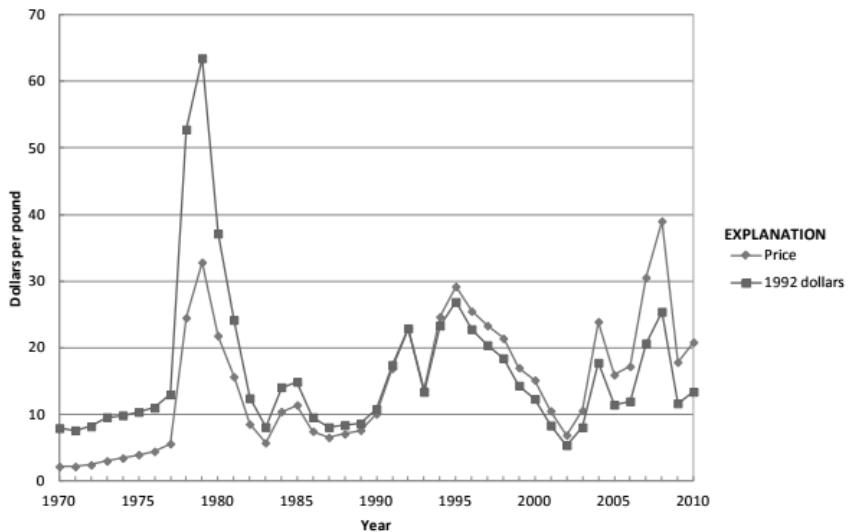


Figure 1. Average annual cobalt prices [7].

Health and safety issues

In recent decades, various legislations concerning chemicals and their safe use have put pressure on CCs with Co and Ni binder as well. REACH program in EU [8] and National Toxicology Program in US [9] classify both cobalt and nickel as carcinogens and therefore harmful for human health.

Most promising metal-systems for partial or complete substitution of Co/Ni are Fe-based alloys. At the beginning of implementation of CCs, Fe as a binder was largely discarded because its mechanical properties were found inferior to those of Co [10]. Two decades after the revelation of CCs, the viability of Fe-based binders was confirmed when Agte addressed the importance and impact of carbon balance in the WC-Fe system [11,12]. Since then, comprehensive research has focused on binder systems FeNi and FeNiCo [13,14]. However, completely Co and Ni free CCs, with only few examples of the reports on the WC-FeMn and WC-FeAl, have received much less attention.

Therefore, the doctoral thesis addresses the following problem: which cemented carbide compositions could satisfy today's requirements regarding raw material and health aspects?

The main goal of the thesis is to develop cemented carbide compositions that neglect the problem discussed above.

The research objects are cemented carbide with Co and Ni free chemical compositions, with the main focus on the microstructure, phase composition and performance (mechanical and tribological).

The hypothesis posed by the author:

If the iron-chromium-based (FeCr) alloys are successfully employed as a binder metal in WC cemented carbides, the resulting composite would be free of expensive and harmful elements. In addition, WC-FeCr composite would have the potential to perform competitively in corrosive and oxidative environments.

To achieve the goal established, the following tasks in the main body of the work were completed:

- literature research with the focus on trends in the cemented carbide industry and research on alternative binder systems (Chapter 1);
- thermodynamic overview of the W-Fe-Cr-C system to understand the conditions of various metallic and carbide phases in the system (Chapter 1);
- specific technical tasks formulated based on *Introduction* and *Literature Review* (Chapter 1, subsection 1.4);
- experimental preparation of WC cemented carbides with FeCr-based binder using powder metallurgical technologies and characterization of these composites (Chapters 2 and 3);
- determination of technological and chemical conditions that influence the structure and performance of WC-FeCr cemented carbides (Chapter 3).

The main body of the work is followed by the conclusions and the scientific novelty of the thesis and suggestions for future work regarding WC-FeCr cemented carbides.

Acknowledgements, abstract and copies of the articles are presented after the references.

Abbrobation

In addition to the international journal and conferences and respective proceedings where Papers I-IV were published, the scientific results of the present doctoral thesis have also been presented in *25th International Baltic Conference of Engineering Materials & Tribology*.

1 LITERATURE REVIEW

1.1 Background of WC-based cemented carbides

This section introduces the CCs to the reader. The history, especially the trends that have directed the development of CCs are discussed. Properties, performance and application fields are covered to demonstrate the importance of WC CCs in today's industry.

1.1.1 Brief overview of history

The advent of CCs (also known as hardmetals) began when the new material was proposed for wire drawing dies for tungsten filaments. Patent by Karl Schröter disclosed the novel composite materials of WC and iron-group metals in 1923 [10]. It was quickly realized that this novel material could be employed in metal cutting and the patent was sold to Friedrich

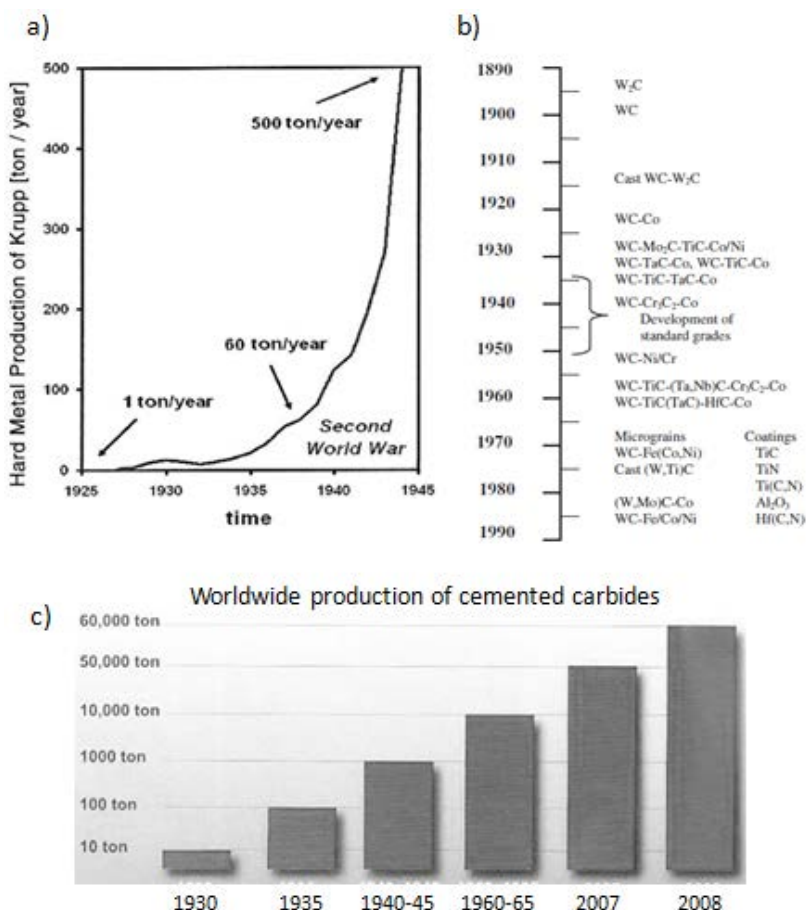


Figure 2. Hardmetal production of Krupp-WIDIA in the years of 1926-1945 (a), historical development of the cemented carbide cutting tools during the last century (b) and estimated worldwide production in 1930-2008 (c) [1, 15].

Krupp AG. Krupp created a trademark "WIDIA" ("wie" and "Diamant" together meaning "like diamond" in German) for CCs with the composition of WC-6 wt.% Co and presented the new material on Leipzig fair in 1927, thus beginning the triumph of CCs [1]. In the 1930s, majority of today's CC producers were founded and annual productions grew exponentially (Figs. 2a and 2c). The superiority of Co as a binder metal was claimed already in the original patent and research on an alternative to Co was minimal.

On the other hand, studies for substitution of the hard phase began early. Shortage of tungsten, especially during The Second World War, led to grades to be established where a portion of WC was substituted by other refractory metal carbides, mainly TiC and TaC (Fig. 2c). The addition of cubic carbides of Ti and Ta improved the strength and high temperature characteristics of WC CCs. Although CCs based on other carbides were also developed, today WC based systems remain most widely used, for example 95% of all CC cutting tools are WC-based [16]. Successive CC-based developments in the second half of the 20th century were aimed at improving coating technologies and refining grain size. Resulting from Agte's research, the potential of alternative Fe-based binders was introduced [11, 12]. The research and specific binder systems are discussed in subsection 1.2.2.

1.1.2 Key properties

Cemented carbides are mostly known as refractory composites with excellent performance in various wear conditions, especially under severe contact conditions [2,17]. Moreover, CCs are a very flexible group of materials – with simple change in the chemical composition or particle size, the values of different properties can be altered multiple times. Long-time researcher and consultant in the CC industry, K.J.A. Brookes, well-put phrase is "individual hardmetals may differ in composition and properties as strikingly as brass and high-speed steel". Below, the key properties of WC CCs are described in brief.

Hardness

Cemented carbides in general are foremost well known for their very high wear resistance. Wear resistance correlates relatively well with material hardness and the universal rule of thumb is that tool hardness must surpass workpiece's hardness. Hardness can be increased by decreasing carbide grain size and binder phase fraction. Typical value for WC CCs is between 800 and 2400 HV [2].

Transverse rupture strength

Transverse rupture strength (TRS), the commonest strength characteristic of CCs, functions efficiently as a quality measurement. While defects (pores) and detrimental structure constituents (brittle η -phase, free carbon) may not lower hardness values, they have notable negative effect on the strength of CCs. TRS test is also sensitive to the surface finish of the test sample. The TRS of samples with careful diamond polished surfaces can be nearly 1000 MPa higher than samples prepared otherwise identically, except without final surface polish [13,18]. The strength of CCs can be increased by decreasing carbide grain size down to nanoscale and increasing binder fraction up to 15–20 wt%. Typical value of WC CCs is between 1000 and 4000 MPa; however, some researchers have reported TRS values as high as 4500–5000 MPa [2].

Fracture toughness

Fracture toughness describes material's resistance to crack propagation, which influences strength and wear resistance. Because conventional fracture toughness testing of CCs has many obstacles, namely pre-cracking of specimen, the alternative non-destructive indentation test method has gained wide popularity [19]. Indentation fracture toughness test where toughness is evaluated by the length of cracks emanating from Vickers indentation was proposed by Palmqvist [20]. Since then, focus has been on the development of relations between Palmqvist toughness and plain strain fracture toughness and many models and equations have been reviewed [19, 21]. In conventional WC CCs, fracture toughness is known to increase as binder fraction and carbide grain size increases. Typical value of WC CCs is between 6 and 25 MPa · m^{1/2} [1].

Wear resistance

The most prominent attribute of WC CCs is its wear resistance which is defined as the attainment of acceptable tool life before the tool needs to be replaced [1]. Tool wear is a complicated phenomenon where many wear types (adhesion, abrasive, diffusion, oxidation etc.) act simultaneously. As a result of high hardness and toughness, WC-Co straight grades are most wear-resistant materials in severe abrasion and erosion environments. WC CCs with TiC and TaC additions possesses increased wear resistance in machining applications where high-temperature diffusive attack emerges [2].

Corrosion and oxidation resistance

Although corrosion and/or oxidation resistance is not a quality that CCs are usually designed for, major applications involve environments that are inherently corrosive [22]. For example, this occurs when coolants are used in extreme heat environment during metal cutting (machining), natural waters in mining and drilling [23]. Additionally, CCs are also used in "true corrosion applications" such as dental drills, spray nozzles, bearings. Still, even in highly corrosive situations, straight WC-Co grades are mostly used for their otherwise excellent properties and relatively satisfactory performance in alkaline media [22]. Increasing Ni and Cr fractions in the binder yields enhanced performance in acid media (Fig. 3) [24, 25].

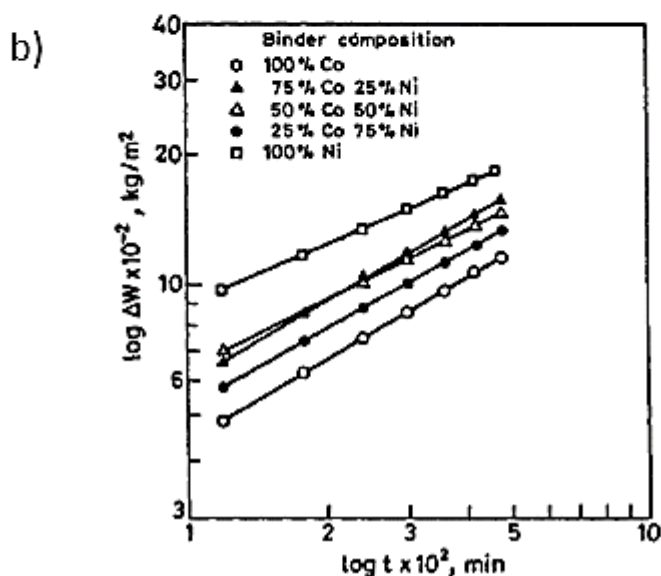
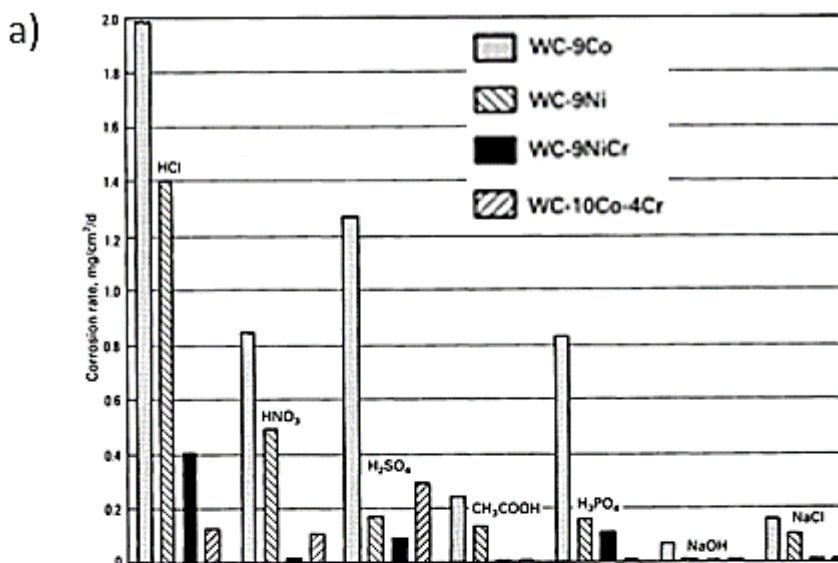


Figure 3. Corrosion and oxidation resistance of commercial cemented carbide compositions: a) corrosion rate in aqueous media at room temperature [25]; b) oxidation rate of WC-10Co/Ni hardmetals at 800 °C in air [26].

Since the binder phase in CCs is much more susceptible to corrosive attack, microstructural aspects, such as WC grain size and binder content, play an important role [22]. Corrosion resistance increases when both of the afore-mentioned characteristics decrease. Consequently, it is important that the microstructure of CCs is uniform in terms of phase distribution.

Although WC-Co CCs are reasonably resistant to oxidation, the practical working temperature limit is 500–600 °C. At higher temperatures, rapid oxidation on the WC phase (into WO₃) occurs. Oxidation resistance in WC CCs can be increased by increasing

the binder content and introducing beneficial carbide constituents (TiC, TaC and NbC) and alloying the binder with Cr [27, 28]. Interestingly, Ni has detrimental effect on the oxidation resistance (Fig. 3) [26, 29].

1.1.3 Applications

At large, CC applications can be divided in two large categories: machining application and other wear parts. The first category, which can be further divided between machining of ferrous and non-ferrous alloys, encompasses roughly two-thirds of CC worldwide turnover [1]. According to ISO standard, the WC-Co machining grades fall into the following classes: highly alloyed with TiC/TaC/NbC for fine machining of ferrous alloys at high speeds (“P series”); multipurpose, less alloyed grades for machining of ferrous alloys, ductile cast irons, non-ferrous alloys etc. (“M series”); straight WC-Co grades for machining cast irons, non-ferrous and non-metallic (“K series”) [30]. The revolutionary introduction of PVD and CVD hard coatings on CC tools started in the 1970s and today 85% of metal cutting tools are coated [31].

Besides metal cutting, CC wear parts with a wide range of shapes and sizes are employed in every industry, from construction and mining to electronics and aerospace. These applications generally require chemically simpler (less alloyed) CCs when compared with machining grades. However, due to diversity of working conditions, a wide range of binder fractions and carbide grain sizes find use. For example, wood working grades usually have 2–20 wt% binder and nano to submicron grain size while CC rolls have 6–30 wt% binder and their structure is medium or coarse [1].

1.2 Binder systems in cemented carbides

This section discusses the ductile component of the composite – metallic binder that “cements” WC particles. Schematic of the CC system is depicted in Fig. 4. Before review of specific binder systems, both traditional and more experimental alternative systems, the role and requirements for the binder are elaborated. Fully dense carbide-metal composites are achieved with liquid phase sintering (LPS) in protective atmospheres or with pressure assisted sintering, such as spark plasma sintering (SPS), hot pressing (HP), etc. However, only LPS under vacuum or inert gas atmosphere is industrially important.

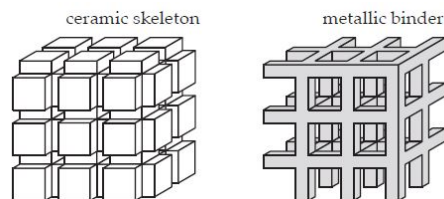


Figure 4. Structure of CCs and cermets composed of ceramic skeleton and metallic binder [32].

During LPS, metal constituent enters liquid phase and more refractory carbide phases remain solid. The result of LPS is a composite where solid grains are dispersed in a network of a solidified liquid. In 1951, Norton postulated that an optimal binder alloy would [33]:

- perfectly wet the refractory carbide;
- show a strong temperature dependent solubility for the carbide phase, being at the same time insoluble in the carbide;
- not be prone to form deleterious third phases and show compatible physico-chemical, thermal and mechanical properties that lead to the desired toughness and wear resistance of composite.

German discussed liquid phase sinterability and from the viewpoint of phase equilibria proposed the following conditions [34]:

- temperature difference between the melting point of base components and the eutectic should be as high as possible;
- the additive should have high solubility for the base component, rather than vice versa (Norton's second condition);
- the liquidus and solidus should decrease drastically in order to give rise to additive segregation at the interparticle interfaces, so as to enhance sintering.

Although all iron-group metals (Fe, Co, Ni) more or less meet the above mentioned requirements, it is no coincidence that cobalt satisfies those ideally.

1.2.1 Traditional binders

Cobalt

Cobalt is the most widely used binder metal in CCs. Due to secretive nature of the CC industry, it is always difficult to refer to exact numbers and figures; it is also complicated to estimate the exact market share of CCs with Co binder. However, only very few grades for niche applications, e.g. cutting blades for green wood, are completely Co free.

WC solubility in cobalt is highest amongst iron-group metals. During sintering of the WC CCs Co-based metallic phase with dissolved W and C rather than pure Co is formed. However, in the literature, this metallic binder phase is still commonly considered as cobalt. High solubility of WC in cobalt is directly connected with cobalt being predominant binder choice since W and C as solutes increase hardness and stabilise cubic cobalt phase (α -Co). α -Co, more ductile of the two cobalt allotropes (hexagonal ϵ -Co being the other), is usually stable at higher temperatures. Phase transformation α -Co \rightarrow ϵ -Co during mechanical loading is martensitic and further contributes towards excellent mechanical performance of WC-Co CCs [35, 36].

In addition to good wetting and dissolution of the WC phase, cobalt has excellent comminution characteristics, which contributes towards achieving good blend of phases during mechanical milling and thereby leads to desirable microstructure formation [35].

Nickel

WC CCs with plain nickel binder have considerably lower strength than with cobalt [37]. Unlike cobalt, nickel has no phase transformation and retains cubic structure at all temperatures, thus possessing lower work-hardening potential [38]. Although nickel has lower melting temperature than cobalt (1453 °C and 1495 °C, respectively),

different researchers report that liquid melt in the WC-Ni system forms at higher temperature and to obtain satisfactory density, prolonged sintering time and/or higher temperature are required [38, 39]. However, nickel based binders, especially those alloyed with Cr and Mo, perform significantly better in extreme corrosion applications involving acid media, e.g., sliding seals and bearings [37].

1.2.2 Alternative Fe-based binders

“Iron or nickel-bonded tungsten carbide exhibited not more than about 40–60% of the transverse rupture strength of Co-bonded material,...”

– Schwarzkopf and Kieffer, 1960 [40]

This subsection discusses major developments in the field of alternative binders where cobalt and/or nickel are mainly substituted with iron.

Fe

Following the studies by Agte [11], in 1971 Moskovitz reported that WC-Fe CCs possesses strength characteristics comparable with WC-Co [13]. With addition of 1.4–3 wt% carbon (relative to Fe), the WC-25Fe materials showed visually two phase (η and graphite free) structure, hardness of 86.6–88.0 (approx. 1050–1200 HV) and transverse rupture strength over 2500 MPa. The hardness increases quite linearly with the added carbon content and Moskovitz argued that this is due to the increased presence of iron carbide (Fe_3C) in the binder phase. However, CCs with purely Fe or Fe-C binder has not found commercial use, mainly because of its unsatisfactory toughness and because other binder systems composed of two or more metals possess better mechanical and tribological properties (e.g., FeNi binder that is discussed in next sections). The phase equilibria of the W-Fe-C system are reviewed in section 1.3.

FeNi

Resulting from the addition of nickel to the WC-Fe system, Moskovitz reported that to achieve η -phase free structure, 0.5–1 wt% added carbon (relative to FeNi) is required. The effect of nickel depends on its content. At 5 wt% of nickel in the FeNi binder, solid solution hardening and solid solution strengthening of ferrite takes place. When nickel content is raised over 10 wt%, martensite formation appears on cooling and further increase of nickel leads to nearly fully austenitic binder (>25 wt% of Ni in FeNi). When compared with WC-Fe, WC-FeNi CCs have increased strength and abrasive resistance, but likewise WC-Fe they have not found commercial value [41].

FeCoNi

FeCoNi is arguably the most well-known and studied binder system with considerable amount of iron. This binder system was extensively studied in the 1980s and onward. In addition, FeCoNi binder systems have been commercialized (e.g., AMPERSINT® grades by HC Stark). Prakash has published thorough review papers and his main conclusions are as follows [42, 43]:

- with careful carbon control it is possible to prepare composites with favorable two phase structure;
- varying chemical composition, the binder can be: martensitic, austenitic, ferritic or mixture of them;

- within the two phase region, changes in the carbon content can change the strength of the composite;
- the best combination of mechanical properties can be achieved with mainly martensitic binder;
- fully austenitic structure exhibits highest fracture toughness, but inferior hardness;
- irrespective of the binder composition, WC cemented carbides with FeCoNi binders have higher abrasive wear resistance than traditional WC-Co.

Schubert et al. argue that WC-FeCoNi CCs with low binder fraction (<10 wt%) have too narrow carbon window and technologically only higher binder content is feasible. In addition, due to low tungsten solubility, the solid-solution strengthening and therefore high temperature properties are inferior to those of WC-Co [5].

FeCrNi

Many studies have addressed WC CCs with the austenitic FeCrNi steel binder system. Fernandes et al. and Trung et al. have focused on the binder compositions equivalent to the AISI 304 stainless steel (Fe-18 wt% Cr-10wt% Ni) [44,45]. Fernandes et al. have prepared WC-FeCrNi CCs through conventional metallurgical route and have explored the coating of WC particles with steel to achieve high homogeneity of the binder [46,47]. Both groups report that addition of carbon is required to mitigate the formation of the η -phase during sintering, but exact suggested values are somewhat different [45,48]. However, results in [49] show that controlled inclusion of η -phase may have even a beneficial impact – increase in hardness without loss of toughness. Also, Fernandes demonstrates the possible formation of chromium carbide [50]. Both research groups conclude that austenitic stainless steel is a good candidate for replacing cobalt as a binder phase in WC CCs.

FeMn

The research of WC-FeMn CCs has been sparked by the carcinogenic behavior of cobalt and nickel. However, early research on the subject dates back to the last century when health concerns were not widely considered [42,51]. Since manganese is an austenite stabilizer like nickel, the WC-FeMn tends to have an austenitic binder, but FeMn alloys with intermediate Mn content (10–15 wt% in FeMn) exhibit martensitic phase transformation similar to Co. FeMn alloys can also dissolve carbon, thus acquiring properties similar to the Hadfield steel that is well-known for high workhardening rate. Hanyaloglu prepared WC-FeMn (Fe-13.5 wt% Mn) CCs with varying added carbon content to ensure two phase structure. He reported that competitive CCs with that composition are obtainable when strong carburizing sintering atmospheres are used [52]. Calculated and experimental results by Maccio [53] reveal that in the W-Fe-Mn-C system overstoichiometric carbon leads to the formation of M_3C iron carbide before formation of free graphite. In addition, Maccio proved that due to carbon solubility in the binder WC-FeMn CCs exhibit $\gamma \rightarrow \epsilon$ martensitic transformation that improves abrasive wear resistance. Another peculiarity of the WC-FeMn system is possible volatilization of Mn at sintering temperatures [54]. Resulting from the studies of sintering behaviour of WC CCs and Hadfield steel, Pascal et al. concluded that in order to minimize Mn loss through volatilization, fast sintering conditions and low temperatures (≤ 1300 °C) must be employed [55].

FeAl

Another class of completely Co/Ni free CCs are WC composites bonded with intermetallic iron aluminides (FeAl, Fe₃Al). In 1998, Subramanian reported that Fe₃Al could be effectively used in metal matrix composites with WC as a reinforcing phase [56]; many other researchers have shown promising mechanical properties, wear resistance and anti-corrosion behavior of WC-FeAl CCs [57–60]. Interestingly, presence of metal-oxides was found to have positive effect on the performance due to the refinement of WC grain size and reduction of the friction coefficient [60, 61].

1.2.3 Composite systems with WC and FeCr(C)

There is relatively scarce information available about WC-FeCr composites, especially about bulk materials. Humphry-Baker et al. proposed a WC-FeCr system as an alternative to WC-Co and studied thermophysical properties and means to employ it as substrate for a novel coating [62, 63]. Few papers have been published where WC used as the reinforcing phase in chromium cast irons (CI). In the WC-CI composition, the final microstructure consists of WC, α -Fe based binder phase and various M_xC_y metal carbides, where M=W, Fe, Cr, Co, Mo and x-y ratio is usually 7-3, 3-1, 6-1 (η), 2-1 or 23-6 [64, 65]. The complex chemical composition enables formation of various carbides, while in plain chromium-rich cast iron under normal conditions (without heat treatments) only eutectic carbide (Cr, Fe)₇C₃ and (Fe, Cr)₃C cementite are present [66]. Examples of the complex structure of WC-CI as well as WC-Fe-Cr-Si hard-facings are presented in Fig. 5. Chromium cast irons with WC reinforcement possess highly increased wear resistance.

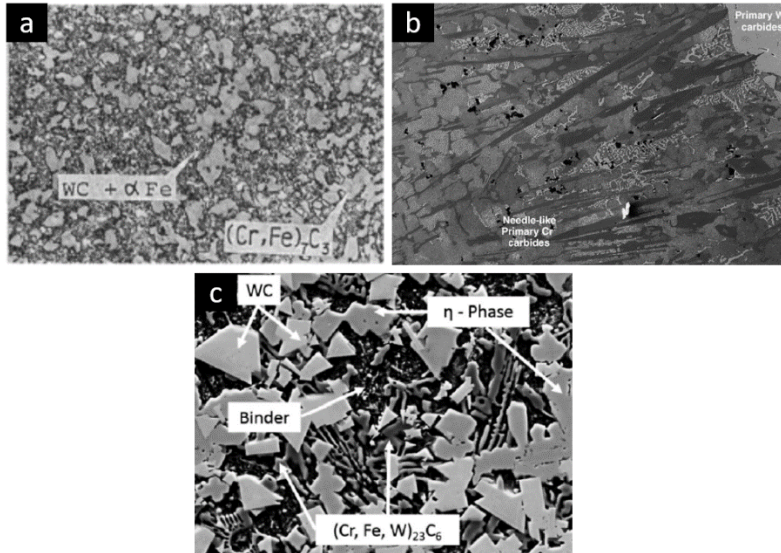


Figure 5. Various WC + FeCr(C) systems: a) WC cemented carbides with 40 wt% chromium cast iron (Fe-27Cr-3.1C) binder [64]; b) chromium cast iron (≈ 20 wt% Cr) reinforced with coarse WC particles [65]; c) WC-Fe-Cr-Si hard-facing obtained by PTA welding [67].

More common group of materials where either WC or other W containing carbides coexist with FeCr solutions are Fe-Cr-W-C hard-facings [68]. Various methods are used

for applying hard-facings (conventional welding, plasma transferred arc welding, brazing, laser-cladding, plasma, spraying, etc.) and two principal approaches are used – *ex-situ* route, where reinforcing particles are added to the metal matrix directly and *in-situ* route, where hard phase particles are synthesized in the metallic matrix by chemical reactions [69]. *In-situ* approach yields more uniform and fine structure of hard-facing composites with better adhesion between hard particles and matrix. Konyashin et al. have patented a method for preparing promising WC-Fe-Cr-Si system hard-facings [70]. They report that a novel hard-facing with a structure composed of a Fe-based binder, carbide grains and nano-precipitates in the binder (η -phase and CrFe carbides) possesses highly increased wear resistance [67].

1.3 Thermodynamic background

Since the WC-Fe-Cr(C) system is relatively complicated in regard to the elemental and phase composition, the understanding of phase equilibria is vital. In the following, elemental systems are evaluated in brief to give insight to the phase composition of WC-FeCr(C) cemented carbides.

1.3.1 Fe-Cr-C system

This system is of great importance for alloyed steels since Cr is one of the main alloying elements in both tool and stainless steels. The system involves three carbides that show extensive metal solid solubilities ((Fe, Cr)₃C – cementite, (Cr, Fe)₇C₃, (Cr, Fe)₂₃C₆) and chromium carbide Cr₃C₂ that does not dissolve Fe and therefore does not precipitate in ternary Fe-Cr-C alloys, which is of minor importance (Fig. 6).

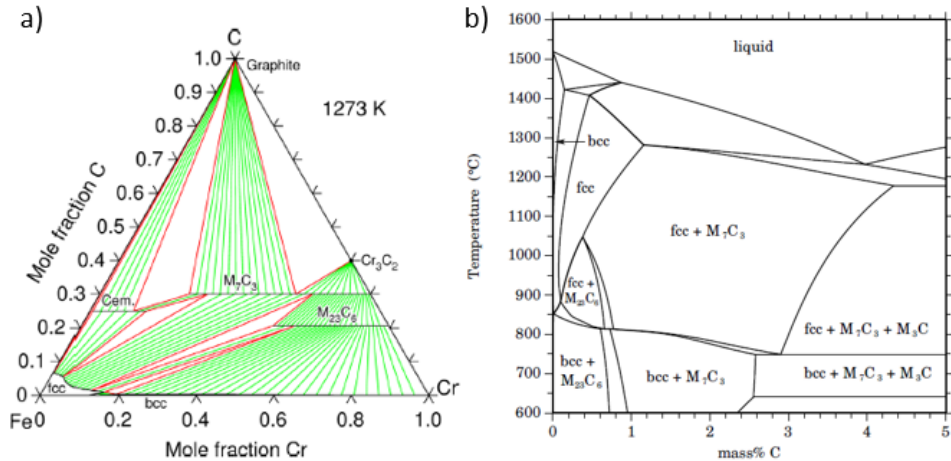


Figure 6. Fe–Cr–C phase diagram: a) Isothermal section at 1273 K [72]; b) isopleth at 13 wt% Cr [73].

Increasing the carbon content, the carbides with higher carbon/metal ratio become stable. Two solid solution metal phases are exhibited in the system – body centred cubic (bcc, α -Fe) that is stabilized by Cr and face centred cubic (fcc, γ -Fe) that is stabilized by C. Bcc phase is stable at lower temperatures [71]. With higher carbon content (>4 wt%), the bcc \leftrightarrow fcc transformation takes place at around 740 °C, which is close to the γ -Fe formation in binary Fe-C alloys.

1.3.2 W-Fe-C system

The layout of the W-Fe-C system is in many aspects similar to the W-Co-C system on conventional CCs. WC-Co and WC-Fe (with small fraction of Ni and Co) with 10 wt% of metal phase are presented in Fig. 7. The main differences are [74]:

- ternary eutectic liquid melt forms already at 1143 °C (1280 °C for W-Co-C);
- higher carbon content is needed for two phase structure and “carbon window” for two phase structure is much narrower;
- M_6C type η -phase is much more stable in the W-Fe-C system;
- possible formation of $(Fe, W)_3C$ cementite.

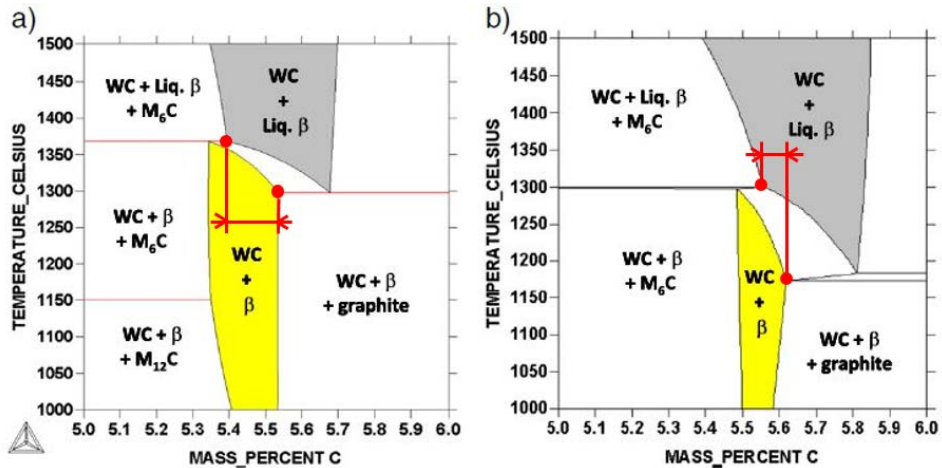


Figure 7. Calculated phase diagrams: a) WC–10 wt% Co; b) WC–7 wt% Fe–2 wt% Ni–1 wt% Co (M_6C , $M_{12}C = \eta$ -phase, β = binder phase) [3].

The narrow “carbon window” and tendency to form M_6C η -carbide is clearly represented in Fig. 7, where the two phase area is almost completely covered with WC+liquid+ M_6C field. In addition to the carbides mentioned, in the M_4C and $M_{23}C_6$ carbides are also reported in the W-Fe-C system [75].

1.3.3 W-Fe-Cr-C system

Unlike W-C-Co and W-C-Ni systems, where only one active carbide forming element (W) is present, the W-Fe-Cr-C system includes three elements with relatively high affinity for carbon. According to the investigation by Gustafson, all carbides that are included in the W-Fe-C system are also included in the W-Fe-Cr-C system (with the exception of M_4C) with some additions, such as M_2C and M_3C_2 [76]. M_2C can dissolve all metals and M_3C_2 dissolves Cr and W, but not Fe, as explained in subsection 1.3.2. Table 1 shows all metal carbides that this system contains.

Table 1. Carbide phases in the W-Fe-Cr-C system.

Carbide	Possible constituents
MC	W, C
MC _{1-x}	W, Fe, Cr, C
M ₂ C	W, Fe, Cr, C
M ₃ C	W, Fe, Cr, C
M ₆ C	W, Fe, Cr, C
M ₂₃ C ₆	W, Fe, Cr, C
M ₇ C ₃	W, Fe, Cr, C
M ₃ C ₂	W, Cr, C

One parameter that can be employed to evaluate which phases are more stable is the standard Gibbs energy of formation. Based on the Gibbs energy of transition metals (Fig. 8), the following carbon activity order can be estimated: $\text{Co} \cong \text{Ni} < \text{Fe} \leq \text{Mn} < \text{Mo} \cong \text{W} < \text{Cr} < \text{V} < \text{Ta} < \text{Ti} < \text{Zr} < \text{Nb}$. However, this is a rough estimation and as Fig. 8 shows, different carbides of one metal can have highly varying Gibbs energies. For example, Cr_7C_3 carbide is on par with well-known high stability carbides such as TiC .

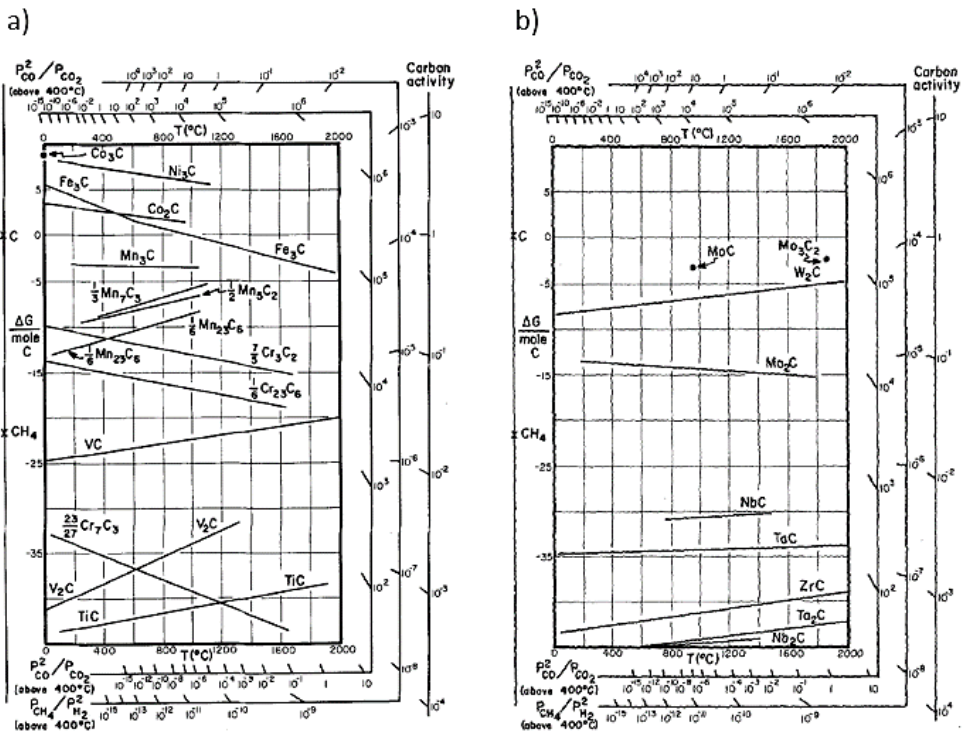


Figure 8. Ellingham diagrams where Gibbs energies are plotted as a function of temperature: a) first transition series carbides; b) second transition series carbides. Gibbs energies are normalized with respect to 1 mole of C [77].

Another consideration is that carbon activities derived from Gibbs energies may not entirely reflect a practical situation, e.g., sintering cycle of CC. In the preparation of materials, the parameters like heat treatment duration, cooling speed may prevent

reactions and phase transformations and leave materials in a meta-stable condition. Furthermore, carbide formation tendency is influenced by solid solubilities, e.g., Fe solubility in Cr_7C_3 .

1.4 Objectives of the present work

The *main goal* of the doctoral thesis is to develop novel CC compositions that are relieved from the economical and environmental problems encountered with conventional CC systems like WC-Co.

The hypothesis posed by the author:

If the iron-chromium-based (FeCr) alloys are successfully employed as a binder metal in WC cemented carbides, the resulting composite would be free of expensive and harmful elements. In addition, WC-FeCr composite would have the potential to perform competitively in corrosive and oxidative environments.

Following the author's *hypothesis* and peculiarities and thermodynamic background of the systems containing WC and FeCr(C) (discussed in Literature Review), the following scientific objectives are established:

- to reveal sintering features of high chromium FeCr(C) alloys bonded CCs;
- to reveal microstructure evolution and phase formation of WC-FeCr(C) composites;
- to identify possibilities for performance improvement using alloying and/or technological possibilities;
- to characterize the mechanical and tribological properties of the developed materials.

2 EXPERIMENTAL

Current chapter covers materials, the experimental procedures implemented for the investigation of WC cemented carbides with iron-chromium-based binder and their characterization techniques.

2.1 Materials

The studied materials were prepared from commercially available carbide and metal powders (Table 2) [Papers I, II and IV]. The goal was to employ powders with as similar powder size as possible. However, a compromise was done with WC powder – in most powder mixtures, fine grained (0.86 μm) carbide powder was mixed with relatively coarse iron or steel powders. However, with coarser (10 μm) carbide powder it was verified that initial WC powder particle size influences only the final WC grain size and not the overall morphology (see 3.1.2).

Table 2. Chemical composition and particle size of initial powders.

Material	Chemical composition, wt%	Powder particle size, μm	Supplier
WC	W – base; C – 6.13, oth. < 0.14	0.86	Wolfram Bergbau und Hütten AG
WC	W – base; C – 6.16, oth. < 0.14	10	H. C. Starck
Fe	Fe – 99.72; oth. – 0.28	<90*	Rio Tinto
Cr	Cr – 99.5; oth. – 0.5	6.65	PPM Ltd.
Co	Nb – 99.5; oth. – 0.5	5–6	PPM Ltd.
Ti	Ti – 99.7; oth. – 0.3	20	Baoji Ziyu Metal Materials CO., Ltd.
Nb	Nb – 99.5; oth. – 0.5	4–6	NPM Silmet
Ferritic steel AISI430L (1.4016; X3Cr17)	Fe – base; Cr – 16.8; Mn – 0.69; Si – 0.64; oth. \leq 0.05	10–45	Sandvik Osprey Ltd.
Austenitic steel AISI316L (1.4401; X4CrNiMo17-12-2)	Fe – base; Cr – 17.1; Mn – 1.2; Ni – 10.9; Mo – 2.3; Si – 0.67; oth. \leq 0.15	10–45	Realizer GmbH.
C	C – 99.9; ash \leq 0.1	3.4	Imerys Graphite & Carbon

*Sieved to achieve powder under 90 μm (original powder size from few μm up to 250 μm).

Four series of powder mixtures were prepared: E-series where the FeCr binder is prepared from elemental powders [Paper I]; S-series where ferritic chromium steel AISI430L (1.4016; X6Cr17) is employed as binder [Paper II]; A-series with AISI430L steel binder and strong carbide former additions [Paper IV]; R-series with pure Fe, Co and FeCrNi austenitic steel AISI316L (1.4401; X4CrNiMo17-12-2) binders for reference (Table 3). Hereafter the E and S-series are referred to also as WC-FeCr(C) and A-series is referred to as WC-FeCr(C)-M (“M” stands for metal addition). Binder content in volumetric percent (vol%) is calculated according to the rule of mixture. It is relevant only to materials without added carbon, since carbon can form various carbide phases besides compensating carbon deficiency in WC and a simple rule of mixture could not

yield reliable results. Experimental E and S materials have either 15 or 30 wt% binder. Although 30 wt% (nearly 50 vol%) binder is quite unusual for WC CCs, most of the characterizations were performed on materials with this binder fraction since early tests with 15 wt% FeCr(C) binder showed that metal fraction found in sintered composites was rather low. Therefore, author presumed that densification behaviour and the effect of carbon content can be more reliably characterized in composites with a larger fraction of metal phase [Paper II].

Table 3. Prepared experimental and reference powder mixtures.

Grade designation*	Composition	Added C content, wt%	Binder content		Comment
			wt%	vol%	
E0	WC-(Fe-18Cr)	-	15	26.1	1 wt% of Si in FeCr binder
E1	WC-(Fe-18Cr)-C	1	15	n/a	1 wt% of Si in FeCr binder
E2	WC-(Fe-18Cr)-C	2	15	n/a	1 wt% of Si in FeCr binder
S0	WC-AISI430L	-	30	46.1	Prepared with 0.86 and 10 μ m WC powders
S1	WC-AISI430L-C	1	30	n/a	
S1.5	WC-AISI430L-C	1.5	30	n/a	
S2	WC-AISI430L-C	2	30	n/a	
S2.4	WC-AISI430L-C	2.4	30	n/a	
ATi1.5	WC-AISI430L-C-Ti	1.5	25	n/a	5 wt% Ti in alloy
ANb1.5	WC-AISI430L-C-Nb	1.5	25	n/a	5 wt% Nb in alloy
R0	WC-Fe	-	15	25.9	ref. material – Fe binder
R1	WC-Fe-C	1	15	n/a	ref. material – Fe binder
R2	WC-Fe-C	2	15	n/a	ref. material – Fe binder
RS	WC-AISI316L	-	30	45.5	ref. material – FeCrNi binder
RCoL**	WC-Co	-	6	10.0	ref. material – Co binder
RCoM**	WC-Co	-	11	17.8	ref. material – Co binder
RCoH**	WC-Co	-	15	23.6	ref. material – Co binder

* Roman number in grade designation indicates the added carbon content in wt% relative to the whole powder mass.

** Letters L, M, H in WC-Co grade designations indicate low, medium and high binder fractions, respectively.

2.2 Processing

Powder preparation and compaction

All powder mixtures were prepared using the conventional ball milling technique (Table 4). After milling, the powders were dried in oven at 40–80 °C and sieved. Portion of each powder was mixed with a solution of paraffin wax and heptane to introduce 3 wt% wax as a binding agent and the other portions of powders were stored in inert atmosphere in glovebox. Powders with paraffin were pressed into rectangular specimens using uniaxial pressing at 60-100 MPa.

Table 4. Powder milling parameters.

Vessel	Balls	Atmosphere	Medium	Ball-to-powder ratio	Duration
Steel drum with WC-Co lining	WC-Co, \varnothing 10–14 mm	Air	Isopropyl alcohol	10:1 or 20:1	72–144 h

Vacuum sintering

Sinterings were carried out in R. D. Webb furnace Red Devil and in FCT Systeme GmbH furnace FPW 300/400 [Papers I–IV]. The first furnace was used for small scale screening experiments and the FPW 300/400 furnace was employed for larger specimen batches. Sinterings were conducted in one cycle and vacuum levels in both furnaces were similar, in the range of 0.05–0.5 mbar. Typical sintering conditions are shown in Fig. 9. The cooling usually was so-called uncontrolled cooling with furnace. Also, controlled cooling at 10 °C/min rate and longer sintering durations (up to 2.5 h at max. temp.) were tested, but they showed no effect on the performance of CCs.

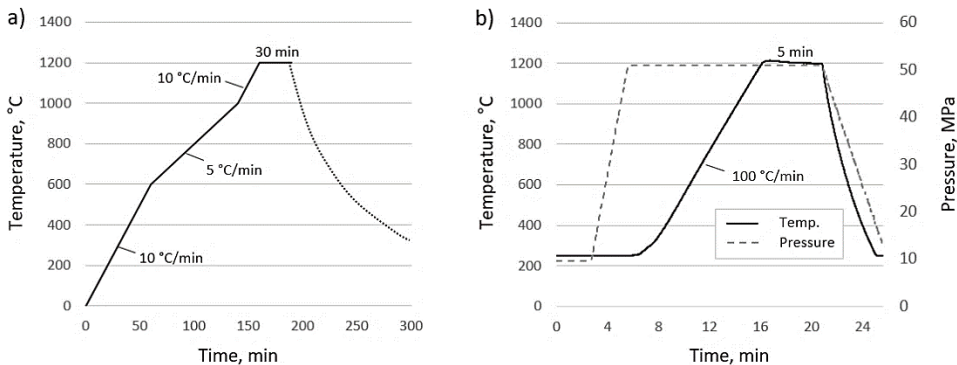


Figure 9. Typical sintering conditions: a) vacuum sintering; b) spark plasma sintering (SPS).

Spark plasma sintering

To investigate the impact of rapid sintering, the spark plasma sintering (SPS) technique was employed (furnace HPD 10-GB from FCT Systeme GmbH) [Paper III]. Powders that were kept in glovebox prior to sintering were placed in graphite die between two graphite punches. Pulsating current and uniaxial pressure were applied simultaneously. Vacuum level in the sintering chamber was kept around 1–2 mbar. The effect of temperature and pressure on the density of WC-Fe CCs was examined in [Paper III] and based on the results, the combination of 1100 ... 1200 °C and 50 MPa was chosen.

Similar to the vacuum sintering route, the cooling cycle was uncontrolled. The temperature was measured from the inside of the top graphite punch using a pyrometer (Fig. 10). In addition, the relative piston movement was recorded with the accuracy of 0.01 mm.

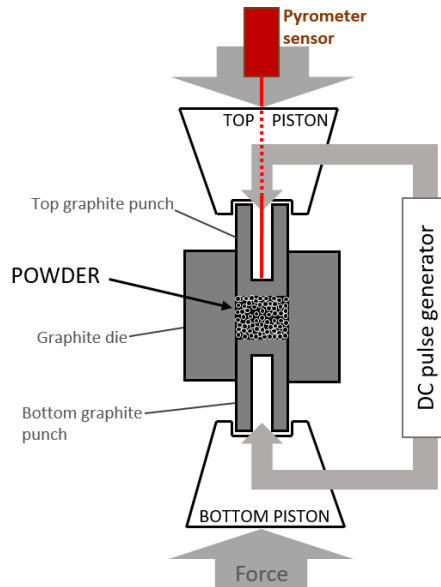


Figure 10. Schematic of SPS setup. The graphite die and bottom/top piston are in vacuum chamber.

2.3 Characterization methods

After sintering, specimens were ground with diamond wheel and polished. Density was measured using Archimedes method (Mettler Toledo ME204 analytical scale).

Microscopy

The porosity of sintered CCs was evaluated using optical microscope (OM) Axiovert 25 and Buehler Omnimet software. For microstructure investigation, a scanning electron microscope (SEM) Zeiss EVO MA15 was used.

Phase and elemental composition assessment

Phase composition was evaluated with X-ray diffraction (XRD) technique on a Rigaku Ultima IV diffractometer with monochromatic Cu $K\alpha$ radiation ($\lambda=1.5406 \text{ \AA}$). In order to understand the distribution of elements in the microstructural components and in specific phases energy-dispersive X-ray spectroscopy (EDS) system INCA was utilized.

Simultaneous thermal analysis

For thermal analysis, the CC grade S0 was analysed using a NETZSCH STA 449 F3 Jupiter® TG-DSC apparatus. The sample was heated in a pure argon (5.0) atmosphere from 40 °C to 1200 °C with the heating rate set at 10 °C/min and protective gas flow of 25 mL/min.

Determination of mechanical properties

Hardness (HV30) was measured with a hardness tester Indentec 5030 KV. Toughness of CCs was evaluated with the indentation method (Palmqvist method), where crack lengths emanating from Vickers indentation corners were measured. Throughout research for fracture toughness K_{IC} , the following equation was used:

$$K_{IC} = 0.15 \sqrt{\frac{HV_{30}}{\Sigma l}},$$

where Σl is the sum of crack lengths [19].

Corrosion and oxidation tests

The corrosion of investigated CCs was evaluated with a simple immersion test, thoroughly elaborated in [78]. Specimens were immersed in saline solution (3.5 wt% NaCl in H₂O). Weight of specimens was measured before and after the test. Before second measuring, the specimens were cleaned to remove corrosion products.

To assess oxidation resistance, the mass gain of specimens after heating in muffle in the presence of air was measured.

Abrasive-erosion wear test

The performance of CCs in abrasive-erosion conditions was investigated with the help of the four channel centrifugal high temperature erosion wear tester described in [79]. During all tests the atmosphere was air to simulate erosion-oxidation conditions. Before erosion tests at elevated temperatures, the specimens were oxidized in oven at respective temperatures and weighed directly before the erosion test to exclude weight change that occurs solely due to oxidation. Silica particles with an average size of 0.3 mm were chosen as erodent. Particles with the velocity of 80 m/s hit specimens at the angle of 30°.

3 DEVELOPMENT OF WC-FeCr(C) CEMENTED CARBIDES

This chapter discusses the results of the experimental work. The first part of the chapter focuses on the microstructural characteristics and problems of vacuum sintered WC-FeCr(C) CCs. In the following chapter, the means of improving the microstructure are considered. In the final part, the performance of WC-FeCr(C) CCs is assessed.

3.1 Vacuum sintered WC-FeCr(C) cemented carbides

3.1.1 Densification

To investigate consolidation during sintering and to ascertain optimal sintering temperature, various densification measurements were carried out [Paper II]. The density and percentage of theoretical density of WC-FeCr(C) CC grade with high (30 wt%) steel fraction (S0) during liquid phase sintering is presented (Fig. 11a). Sinterings at different temperatures were performed with a constant heating rate of 10 °C/min and 30 min holding time at target temperature. Rapid increase in density started between 1100 and 1150 °C and at 1150 °C liquid phase was clearly present. This is in agreement with liquid phase formation temperature in the W-Fe-C system (1143 °C) [74]. However, even 30 min holding at 1150 °C yielded CCs with only 80% of theoretical density. Theoretical density for this composition is 12.02 g/cm³ and although this value does not take into consideration possible chemical and phase composition changes (formation of η -phase, solubility of WC in binder, etc.), it is evident that near full density is achieved at 1200 °C. This is also confirmed by the low porosity of WC-FeCr grade S0 sintered at 1200 °C and at 1300 °C that was below 0.2 %. Low liquid phase formation temperature shows that forming liquid melt is rich in carbon (close to eutectic). This, in turn, indicates that during sintering of purely WC and steel mixture (powder mixture of grade S0 has no added carbon) considerable amount of WC is dissolved in the metal phase. Therefore, liquid melt in the W-Fe-Cr-C system resembles more cast iron rather than steel. When grade S0 was sintered at 1400 °C, the shape of the specimen began to deteriorate and therefore higher sintering temperatures for S-series were not considered further. However, the E-series with lower binder fraction (15 wt% of FeCr) required sintering temperatures near 1400 °C for near full density.

Thermogravimetric (TG) measurements on grade S0 were also performed and mass change is plotted against temperature in Fig. 11b [Paper II]. Noticeable mass loss of ~2 wt% between 200 and 250 °C is the result of the removal of paraffin wax. The second larger mass loss between ~780 and ~1020 °C can be attributed to the reduction of oxides. The XRD measurements that are discussed in detail in subsection 3.1.4 shows that before 800 °C, the formation of chromium based carbide and W-Fe mixed carbide (η -phase) starts. This proves that native oxide layers covering powder particles are at least partially destroyed, as a result, carbon oxides are formed. Formation of carbon oxides causes removal of carbon, which leads to notable mass reduction.

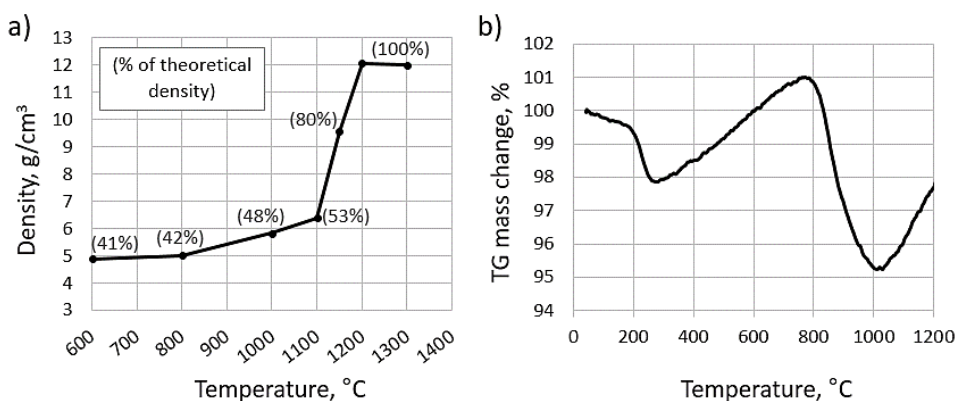


Figure 11. WC-FeCr(C) grade S0 vacuum sintering: a) density; b) mass change.

WC-FeCr(C) CCs with different fractions of added carbon were prepared to investigate the effect of added carbon fraction on the microstructure and phase composition. From the densification point of view, it can be observed that increasing carbon reduces density; however, only grade with the highest added carbon value (S2.4) exhibits extensive porosity that is arguably due to free graphite precipitation (Fig. 12e). Polished surface porosity measurements showed that grades S0–S2 have porosity under 0.2%, while porosity of S2.4 is over 1%. This demonstrates that a considerable amount of carbon can be added to the WC-FeCr(C) composition before carbon starts to manifest as a separate phase in the microstructure.

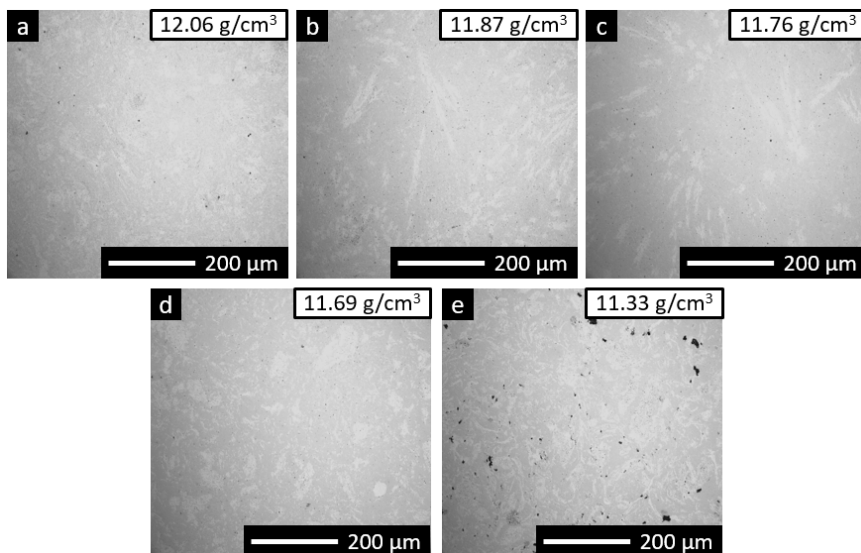


Figure 12. Microstructure images (OM) with corresponding densities of WC-FeCr(C) CC S-series: a) S0; b) S1; c) S1.5; d) S2; e) S2.4.

3.1.2 Microstructural investigation

In this subsection, the microstructure of WC-FeCr(C) CCs is discussed. Backscatter scanning electron microscope (BS-SEM) images of CCs with various chemical compositions are presented in Figs. 13, 14, 16 and 17. The phases present in all the images were confirmed by X-ray diffraction (XRD), but an in-depth discussion regarding

the phases is given in subsection 3.1.4. In the BS-SEM images, generally three phases are discernible: light grey – WC grains, medium grey – η -phase, dark grey – binder phase (Fig. 14). Binder phase in WC-FeCr(C) CCs is not solely metallic and contains a notable fraction of metal carbides. The nature of the binder phase is further considered in the next subsections.

Figure 13 presents the microstructure of reference WC-Fe(C) (R0, R1, R2) and experimental WC-FeCr(C) (E0, E1, E2) CCs with 15 wt% of calculated binder fraction. With pure Fe binder, the microstructure follows a logical trend depending on the added carbon content. No additional carbon causes formation of η -phase (R0). Extra 1 wt% carbon relative to the whole powder mass (E1) retards η -phase formation and the structure is essentially two-phased and resembles a common two-phased microstructure of WC-Co CCs. The necessity for extra carbon in WC CCs with a Fe-based binder to avoid detrimental phases is in good accordance with literature [11]. Further increase of carbon caused the appearance of free graphite (E2) [Paper I].

The η -phase fraction in WC-FeCr(C) CCs without added carbon (E0) is remarkably higher when compared with WC-Fe (R0) and η -phase remains in the structure even when 1 wt% of extra carbon is introduced (E1). Therefore, even a higher amount of added carbon is necessary in order to eliminate η -phase (E2); however, the resulting microstructure presents highly uneven distribution of phases. Areas with even WC+binder structure (structure schematic presented in Fig. 4) are interrupted with large binder rich zones – *binder pools* (grade E2 in Fig. 13f). The formation of *binder pools* is even more distinct with WC-FeCr(C) CCs with higher binder content (see Fig. 14) [Paper I].

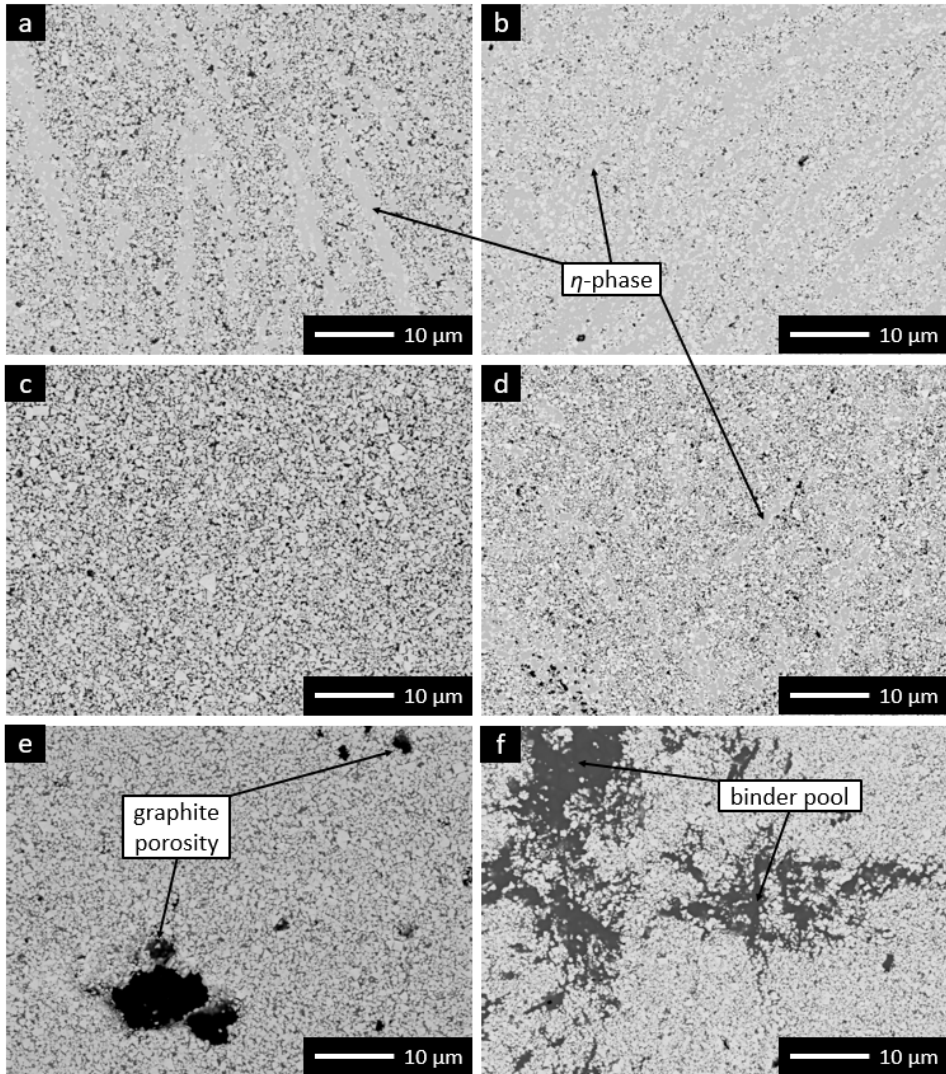


Figure 13. Microstructures of WC-Fe(C) and WC-FeCr(C) CCs: a), c), e) – R0, R1, R2, respectively; b), d), f) – E0, E1, E2, respectively.

The microstructure of WC-FeCr(C) CCs with higher volume of binder (S-series grades in Table 3) exhibits η -phase and *binder pools* simultaneously (Fig. 14). Since employed FeCr alloy (AISI430L ferritic steel) had powder particle size range 10–45, which is relatively large, the S0 grade was prepared using WC powders with extra coarse and fine WC particles. The main purpose of this experiment was to exclude the large difference in starting powder sizes (10–45 μm for steel and 0.86 μm for mainly employed WC) as the possible cause of uneven microstructure. As can be seen, different starting WC powder particle sizes have no effect on the morphology of the microstructure (Figs. 14a and 14b). However, the final WC grain size in the sintered CCs is different (Figs. 14c and 14d). In addition, this demonstrates that WC grain growth is considerably inhibited when using Fe alloys as binder, which is also in good accordance with literature [80].

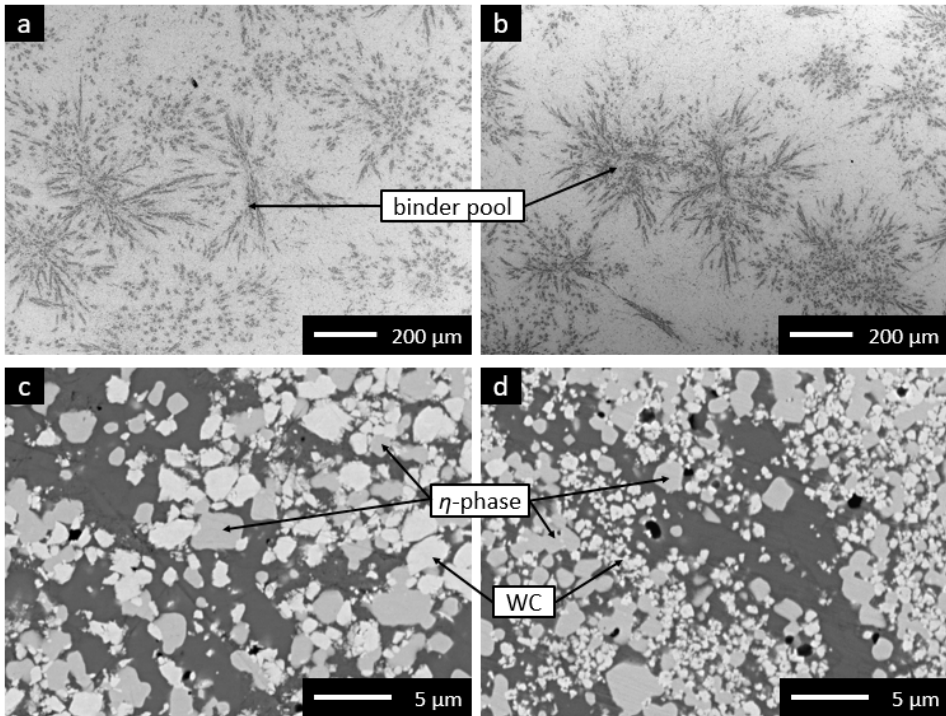


Figure 14. Microstructures of WC-FeCr(C) CC grade S0: a), c) – 10 μm WC starting powder; b), d) – 0.86 μm WC starting powder.

The appearance of *binder pools* is not entirely random. The pools with elongated shape mostly tend to originate from common locations, thus forming clusters with star or flower like pattern. This, in turn, implicates that these *binder pools* form during liquid phase sintering when a large fraction of liquid melt is present and following cooling [Paper II]. Formations with resembling shape were presented by Betts when he coated steel with laser deposited mixture of Cr_3C_2 and AISI316 (X5CrNiMo17-12-2; 1.4401) steel [81]. During the deposition, the majority of Cr_3C_2 particles were recrystallized and few remaining acted as nucleation centres for other chromium based carbides (Cr_7C_3 and Cr_{23}C_6) (Fig. 15). These chromium carbides created similar morphology as in our materials. Another important outcome from the microstructure investigation performed by Betts is that metal phase between larger carbide particles was actually a fine eutectic mixture of austenitic steel and carbides. The formation of such steel-carbide eutectic in rather short time during laser deposition demonstrates the rapid nature of structure formation in the Cr_3C_2 and Fe-based metal system.

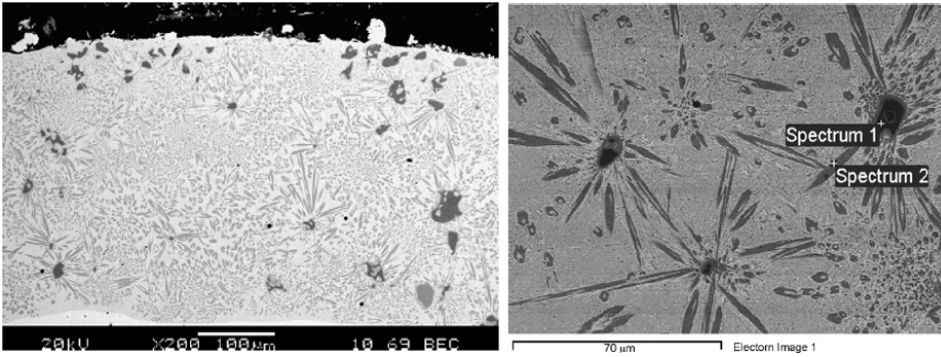


Figure 15. Cross-sections of laser deposited coatings from the powders of Cr_3C_2 and AISI316 steel. Residual Cr_3C_2 particles act as nucleation centers for other Cr-based carbides (Cr_7C_3 and $Cr_{23}C_6$) with elongated shape [81].

The low magnification BS-SEM images of WC-FeCr(C) CCs with high binder content (S-series) with different carbon content are exhibited in Fig. 16. The morphology of the *binder pools* is dependent on the carbon content. The microstructures of grades with lower added carbon amount (S1 and S1.5) resemble WC-FeCr(C) grade S0 without added carbon where binder rich areas demonstrate needle-like shape and form clusters (Fig. 16a,b). Increasing carbon content changes microstructure morphology entirely – *binder pools* acquire more equiaxed circular shape (Fig. 16c,d). The η -phase is relatively fine and cannot be visible in microstructures presented in Fig. 16, but closer examination revealed that grades with higher carbon content (S1.5, S2 and S2.4) appear to be η -phase free. This was also confirmed with XRD analysis (see discussion in 3.1.4.).

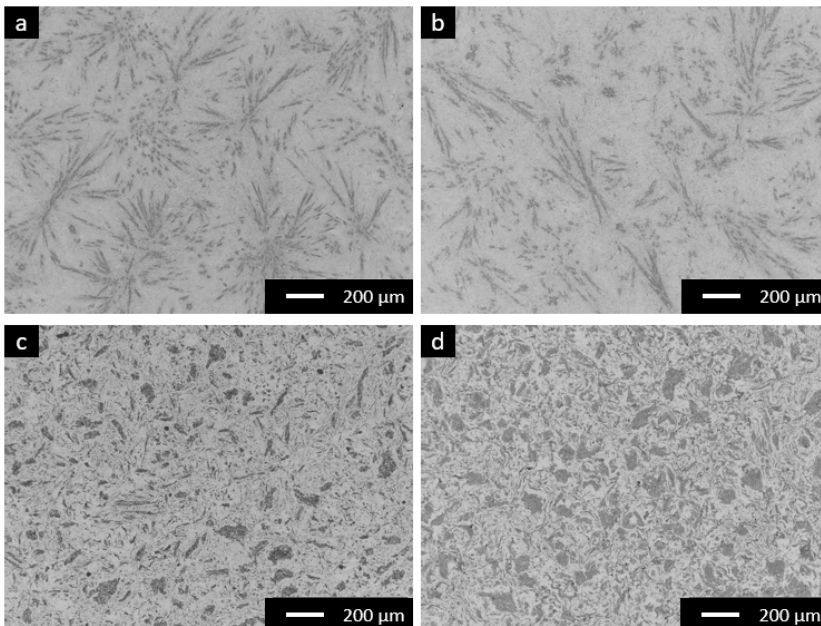


Figure 16. Microstructures of WC-FeCr(C) CC S-series grades with varying added carbon content: a – grade S1; b – grade S1.5; c – grade S2; d – grade S2.4.

The S-series WC-FeCr(C) CCs that have microstructures exhibited in Figs. 14 and 16 were sintered at 1200 °C, since this temperature is sufficient to achieve near full density with CCs that have high binder volume (Fig. 11). The increase in sintering temperature leads to enhanced growth of η -phase formations. The microstructure of the grade S0 sintered at 1200 °C exhibits relatively fine η -phase (Figs. 14c and 14d) while 100 °C increase in the sintering temperature yields η -phase areas already visible at low magnifications (Fig. 17b). The microstructure of grade S1.5 that appears to be η -phase free after sintering at 1200 °C exhibits scarce abnormally large η -phase formations at higher sintering temperature (Fig. 17c). The temperature sensitivity that manifests already at the difference of 100 °C in the sintering temperature suggests that WC-FeCr(C) CCs are heavily metastable and stability of η -phase increases with temperature.

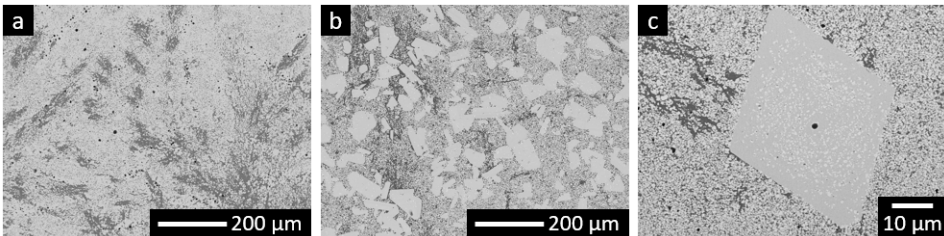


Figure 17. Microstructures of WC-FeCr(C) CCs: a) grade S0 sintered at 1200 °C; b) grade S0 sintered at 1300 °C; c) grade S1.5 sintered at 1300 °C.

3.1.3 Elemental distribution

In this subsection, the distribution of elements in phases is discussed. Main focus is on the *binder pools*. The Energy-dispersive X-ray spectroscopy (EDS) spot analysis as well as mappings and line scans with respective SEM images are presented. Due to the relatively large interaction volume of the EDS analysis method ($\varnothing \geq 1 \mu\text{m}$) coupled with submicron microstructure of experimental materials, the EDS spot analysis quantitative results (wt% of different elements) must be considered with caution. Only abnormally grown η -phase areas were characterized with relative accuracy (Fig. 17c).

The microstructure and elemental mappings of binder rich area in WC-FeCr(C) grade S0 are shown in Fig. 18. From EDS mapping (Fig. 18) and line-scan (Fig. 19), it is evident that the *binder pools* are composed of two zones: Cr-rich zones that are surrounded by Fe-rich one. Cr concentration outside *binder pools* is virtually nonexistent while the distribution of Fe is more uniform. Visibly different distribution of Cr and Fe is encountered also in WC CCs bonded with austenitic AISI304 (X5CrNi18-10; EN 1.4301) steel (WC-FeCrNi), reported by Marques et al. [46]. However, they did not examine the possible causes of such phenomena. Additionally, it is known that the binder phase in sintered CCs is usually in thermodynamic non-equilibrium state and composition gradients can be expected even in WC-Co CCs [82].

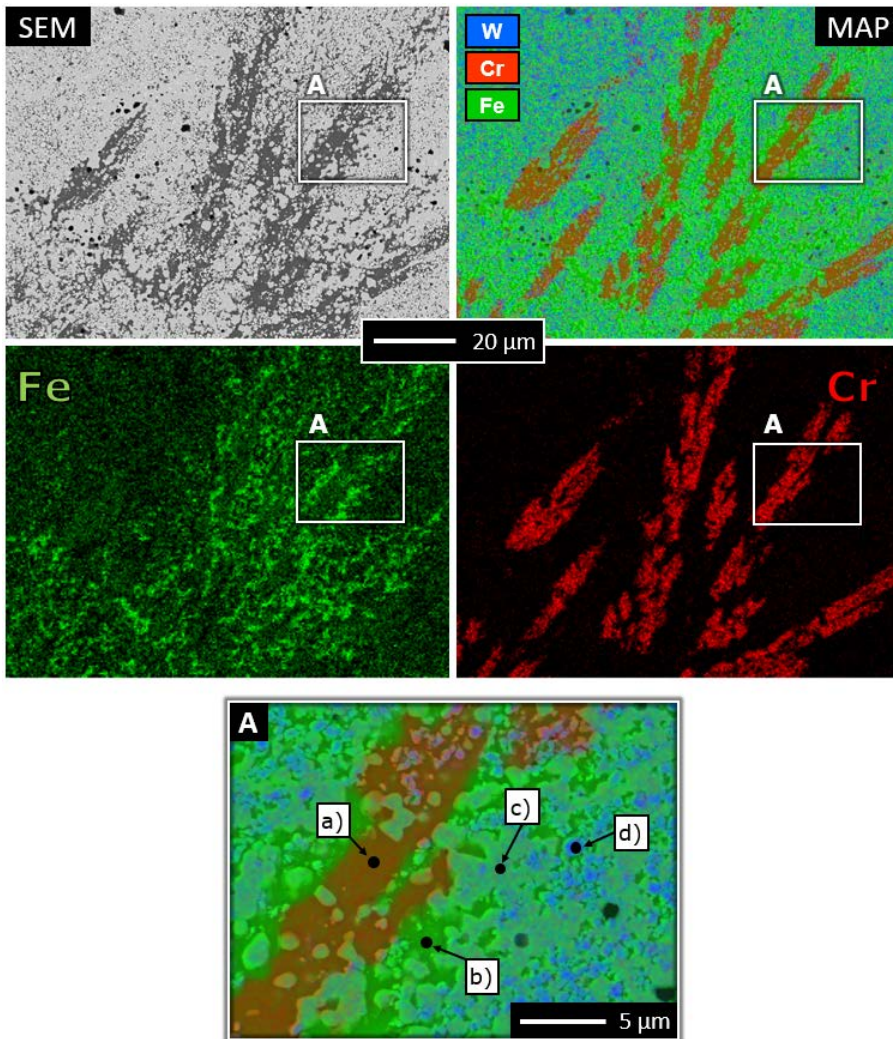


Figure 18. Microstructure and EDS elemental mappings of WC-FeCr(C) CC grade S0. The quantitative chemical analysis from locations (a–d) are given in Table 5.

Table 5. Results of the quantitative EDS spot analysis from locations exhibited in Fig 18.

	Content, wt%			
	W	C	Fe	Cr
Surface	65.1	4.9	24.4	5.6
Surface (calculated)	65.7	4.3	25.0	5.0
a)	13.5	9.5	41.2	35.8
b)	9.0	5.1	80.4	5.5
c)	67.9	4.6	23.0	4.5
d)	84.3	8.1	6.9	0.7

Elemental concentration measured from the surface and from locations exhibited in Fig. 18 are shown in Table 5. Elemental contents measured from the surface are in good agreement with calculated values. Spot analysis a-d (Fig. 18) represent four different phases encountered in the microstructure: a) Cr-rich zone of the *binder pool*; b) Fe-rich zone of the *binder pool*; c) η -phase; d) WC. The Cr-rich zone displays similar or even higher amounts of Fe and the highest C concentration. Since C solubility in Fe or Cr is very small (close to zero in Cr and α -Fe) [73], the Cr-rich zone is mainly composed of carbides. According to the literature, if possible, the formation of solid solution carbides or mixed carbides is favored. As stated in [83]: "... iron-based alloy containing Cr will contain complex carbide $(Cr, Fe)_x C_y$, rather than simple $Cr_x C_y$ carbide". The 5.1 wt% carbon signal from a Fe-rich zone can be largely attributed to the surrounding carbide phases and this zone is mainly composed of α -Fe(Cr). However, both Cr- and Fe-rich zones are probably fine eutectic mixtures of carbides and metallic phases and metal/carbide ratio is higher in the Fe-rich zone. The phenomenon of distinctive Cr- and Fe-rich zone formation was observed also in our research group's latest investigation on TiC-FeCr cermets [84].

W- and Fe-rich spot result (c) is arguably M_6C η -phase. EDS spot analysis was conducted also on WC-FeCr(C) CC with larger η -phase formations and the results were similar to those presented in Table 5. Weight fractions of approximately 70 and 21 of W and Fe respectively correspond closely to the atomic fraction of 1:1 and thus the η -phase has the composition of Fe_3W_3C with small Cr solubility. It has been shown that M_6C η -phase can have a composition range from Fe_2W_4C to Fe_4W_2C with possible Cr solubility up to 8 wt% [74, 76].

The final spot analysis result (d) is from a WC grain. Fe and Cr concentrations in this phase are attributed to the signal pick-up from surrounding phases due to relatively large interaction volume of the EDS method. It is well-known since the solubility of other metals in tungsten monocarbide is marginal [74].

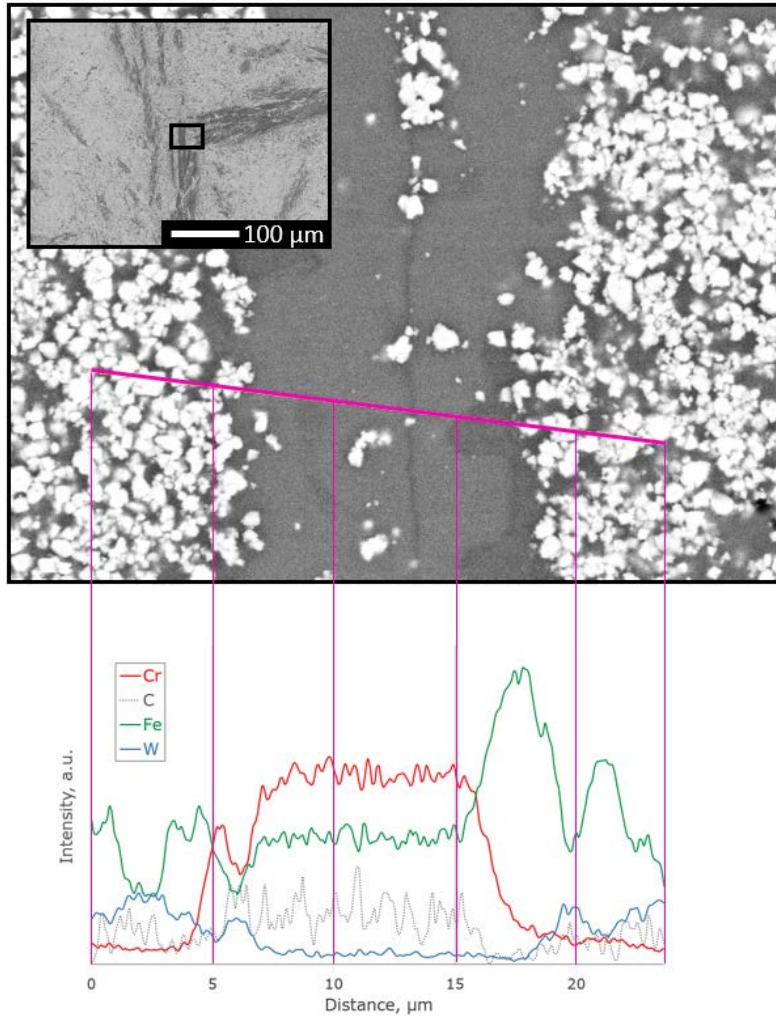


Figure 19. The EDS line-scan of binder pool in WC-FeCr(C) CC grade S0.

Binder pool in WC-FeCr(C) CCs was etched with common steel etchant (Nital solution) and common CC etchant (Murakami solution). BS-SEM images of the microstructure prior and after etching are given (Fig. 20). Etching with nitric acid solution (Nital) removed α -Fe based binder phase between ultrafine WC grains and around Cr-rich zones in *binder pools*. It revealed that the fraction of the remaining metal phase is relatively low, especially considering that the starting powder has nearly 50 vol% of steel. Murakami etchant revealed large grains in the Cr-rich zone that can be attributed to the $(\text{Cr,Fe})_x\text{C}_y$ carbides and are in strong contrast with ultrafine WC.

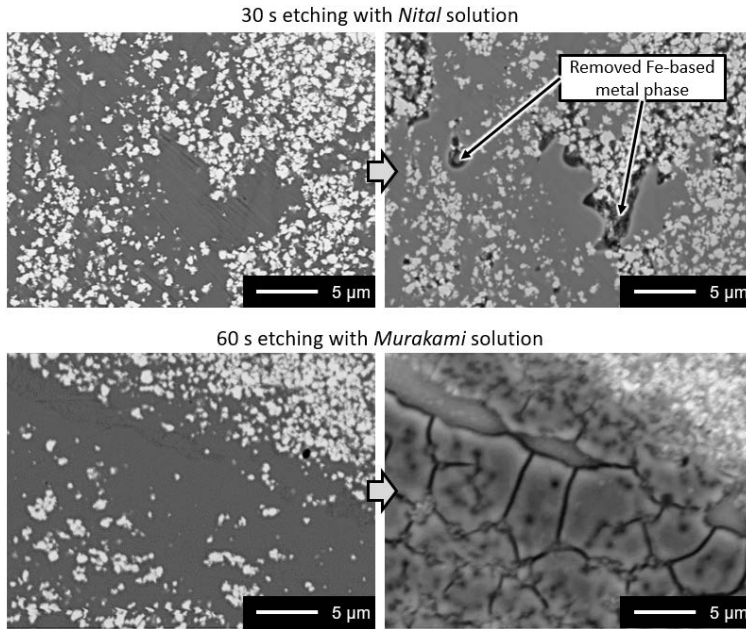


Figure 20. Microstructure of the binder pool in WC-FeCr(C) grade S1.5 before and after etching with *Nital* (top) and *Murakami* (bottom) solutions: a), c) before etching; b) d) after etching.

Besides changing or even improving the morphology of the microstructure, the introduction of extra carbon has a significant effect on the elemental distribution (Fig. 21). The signals of Fe and Cr in grade S2.4, with high added carbon, overlap almost completely. This suggests that Fe and Cr are distributed much more homogeneously and the phase composition, regarding Fe- and Cr-rich compounds, is different. Indeed, with the XRD analysis the difference of $(Cr,Fe)_x C_y$ mixed carbides present in grades S0 and S2.4 (see 3.1.4. *Phase composition*) was witnessed.

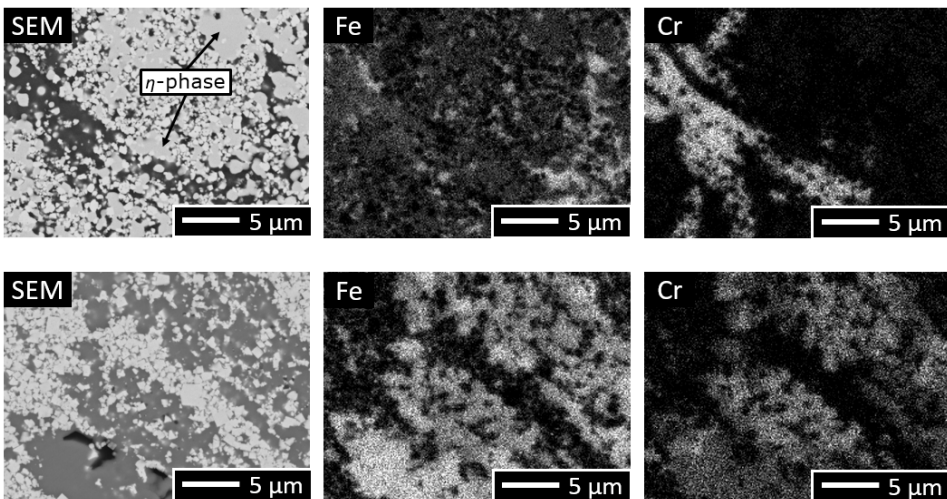


Fig. 21. Microstructure and EDS elemental mappings of WC-FeCr(C) grades S0 (top) and S2.4 (bottom).

3.1.4 Phase composition

WC-FeCr(C) CC grade S0 was investigated with X-ray diffraction after milling and after sintering at different temperatures (Fig. 22a). The diffraction patterns of the milled powder display two phases: WC and α -Fe (small peaks around 28.5 and 43.5 deg., which are visible in all XRD patterns, are K-beta peaks of WC). In the current study, α -Fe should be considered as Fe-Cr solid solution, since Cr solubility in ferrite is unlimited. The specimen sintered at 600 °C remains essentially two-phased, but at 800 °C new carbide phases are already present: M_6C type η -phase and $(Cr,Fe)_{23}C_6$ carbide. Differential scanning calorimetry (DSC) analysis confirms that endothermic reactions start before 800 °C (Fig. 22b). Lack of distinctive peaks in the DSC plot can be explained by the pronounced number of different reactions taking place simultaneously: reduction of oxides coupled with formation of carbides (metal oxide + carbon \rightarrow metal carbide + carbon oxides), Fe solid solution transformation (α -Fe \rightarrow γ -Fe), etc. At higher temperatures, especially at 1300 °C, the $(Cr,Fe)_{23}C_6$ carbide peaks are smaller, thus suggesting that the stability of Cr-Fe mixed carbide decreases. Another explanation would be that $(Cr,Fe)_{23}C_6$ dissolves readily in the liquid phase and during the following cooling, smaller carbide fraction forms [Paper II].

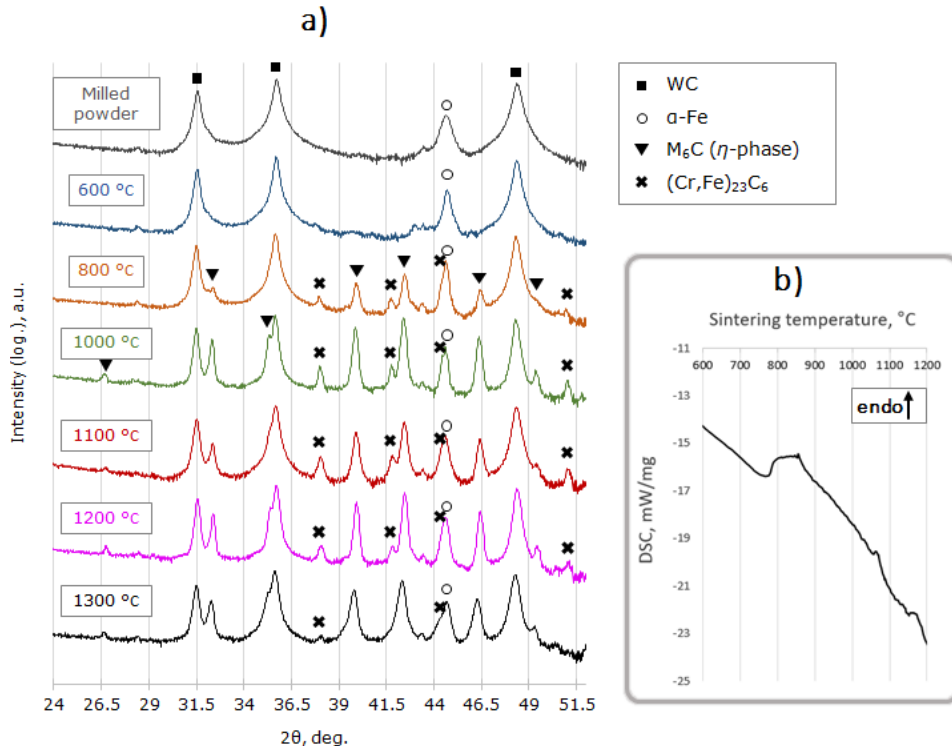


Figure 22. XRD diffractograms and DSC plot of WC-FeCr(C) CC grade S0: a) diffractograms of the milled powder and specimens sintered at different temperatures; b) DSC plot.

The influence of added carbon on the phase composition of WC-FeCr(C) CCs was investigated (Fig. 23). Introducing extra carbon to the powder mixture is common practice also with WC-Co CCs, when the precipitation of the η -phase is a problem. As expected, the addition of carbon retards the formation of the η -phase in CCs with FeCr

binder as-well; grades S1.5, S2 and S2.4 are free of M_6C carbide. Furthermore, the $(Cr,Fe)_{23}C_6$ peaks disappear and somewhat indistinct traces of M_2C and M_3C carbides emerge. The carbon/metal ratio in these carbides is higher when compared with $M_{23}C_6$, thus making their presence very plausible. Only the grade with the highest added carbon fraction (S2.4) shows extensive graphite porosity when inspected with an optical microscope (Fig. 12e). In the Fe-Cr-C system, Cr-based mixed carbides $(Cr,Fe)_{23}C_6$ and $(Cr,Fe)_7C_3$ and Fe-based $(Fe,Cr)_3C$ cementite can be stable (Fig. 6). The presence of $(Cr,Fe)_7C_3$ in WC-FeCr(C) cannot be disregarded, but a signal even in the logarithmic scale is too weak to confirm it. The trace signals of M_2C can be attributed to the $(W,Cr)_2C$ carbide, which is stable in the W-Cr-C system [76].

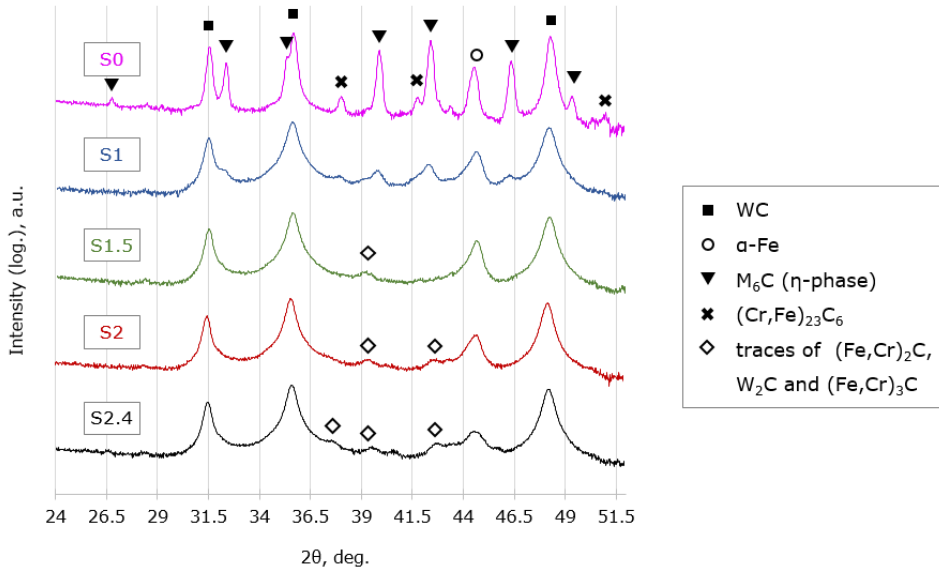


Figure 23. XRD diffractograms of the WC-FeCr(C) CC grades without added carbon (S0) and with different added carbon contents (S1 - S2.4) sintered at 1200 °C.

3.1.5 Summary

WC-FeCr(C) CCs can be consolidated close to full density at relatively low temperatures using vacuum sintering. The formation of the liquid phase close to the eutectic temperature has been reported in the W-Fe-C system. It suggests that the liquid phase is rich in carbon and therefore its composition resembles that of cast iron rather than steel. Even with considerable amount of added carbon, low porosity (under 0.2 %) is achievable.

With right carbon balance, the favorable two-phased microstructure of WC-Fe CCs is attainable. However, with a FeCr based binder, the situation is much more complicated. Experiments with 15 wt% and 30 wt% of calculated binder fraction showed that the microstructure of WC-FeCr(C) CCs consists of WC, η -phase and binder phase that forms *binder pools*, disrupting homogeneity of the microstructure. Increasing added carbon content changes the morphology of *binder pools* from elongated into more equiaxed shape.

The relatively large *binder pools* that form and disturb the homogeneity of WC-FeCr(C) CCs possess sophisticated structure in terms of phase and elemental composition. Elongated pools that are more common in CCs with lower added carbon fraction tend to be composed of Cr-rich core and Fe-rich shell. The core, in turn, with increased carbon content, consists largely of $(Cr,Fe)_x C_y$ mixed carbides. The increase of carbon content improves the homogeneity of elemental distribution.

X-ray diffraction investigations revealed that the microstructure of WC-FeCr(C) CCs consists of tungsten monocarbide, α -Fe-based binder phase and carbides that form during sintering above 600 °C: M_6C type η -phase and mainly Cr- and Fe-based $M_x C_y$ mixed carbides. Lower carbon contents favor the formation of Cr-based $(Cr,Fe)_{23}C_6$ carbide with lower carbon/metal ratio, while increasing the carbon content yields the formation of $(Fe,Cr)_3C$ and $(W,Cr)_2C$ carbides.

3.2 Means of improving the homogeneity of the microstructure

The SEM and EDS investigations showed that the microstructure of the WC-FeCr(C) CCs is highly heterogeneous due to the formation of large *binder pools* during liquid phase sintering. Furthermore, formed binder rich zones exhibit highly uneven distribution of elements (and therefore also phases). Therefore, the second part of the experimental work in the current thesis focuses on the improvement of the microstructure of WC-FeCr(C) CCs. Both processing methods and compositional changes are considered.

3.2.1 Spark plasma sintering

In this research, SPS was employed to investigate the effect of the rapid consolidation method [Paper III].

The densification of WC-FeCr(C) CC grade S0 with a high calculated binder fraction (30 wt%) during SPS is displayed through the piston movement (Fig. 10). Piston movement (Fig. 24) is practically the decrease of the distance between the pistons, thus indicating the densification of the powder mass. Initial change in piston positions occurs when the pressure of 50 MPa is applied, followed by two minute interval gap when the transformer is pre-heated. During the heating cycle, the compression is slow at the start and accelerates above 800 °C. The final temperature of 1100 °C (coupled with pressure) resulted in the density of 11.2 g/cm³, which is 93.3 % of the theoretical full density (12.02 g/cm³). Incomplete densification is also exhibited by residual porosity (Fig. 25). When the temperature was increased over 1100 °C, the liquid phase started flowing out, thus damaging the die. The experiments with WC-Fe(C) and WC-FeCr(C) CCs with lower binder fractions indicated that more desirable density can be acquired at higher sintering temperatures when the pressure is decreased [Paper III].

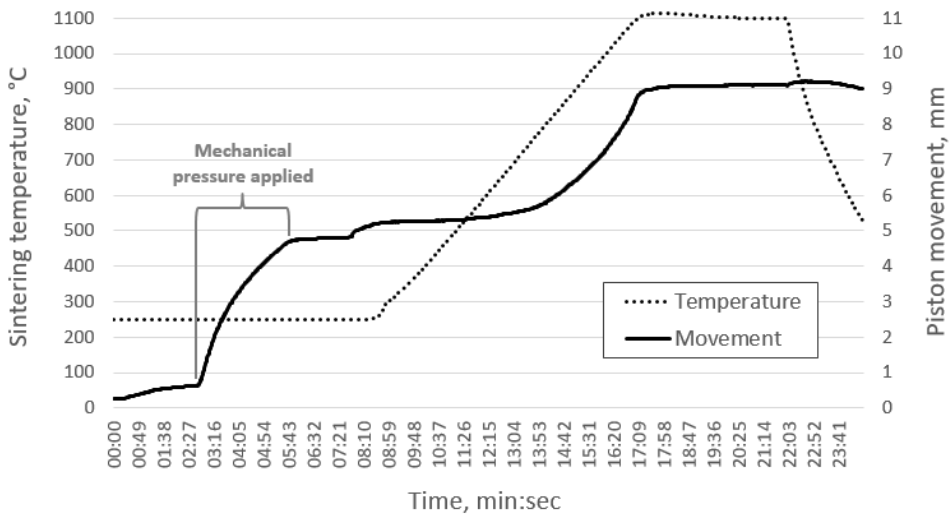


Figure 24. Sintering diagram of WC-FeCr(C) grade S0 during spark plasma sintering.

Figure 25 presents the microstructure of grade S0 after SPS at 1100 °C using 50 MPa pressure. Small porosity is visible at higher magnification (Fig. 25c). When compared with vacuum sintering (Fig. 14), the microstructure is considerably more homogeneous. However, binder rich areas are still discernible, but in the case of SPSed materials, they tend to be perpendicular to the pressing direction. Two conclusions can be drawn: a) the inherent nature of SPS (fast consolidation; lower temperature) does not allow extensive formation of the liquid phase and therefore rearrangement of the particles; b) the WC-steel powder remains somewhat heterogeneous after milling.

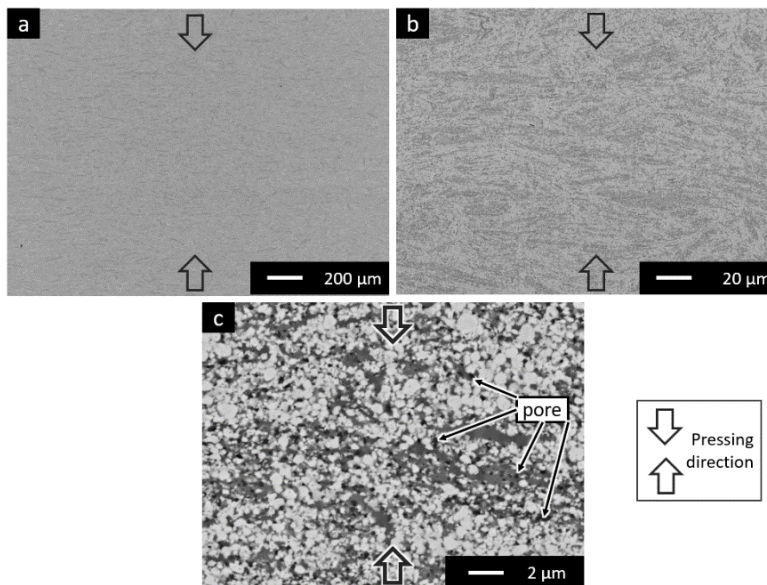


Figure 25. Microstructure of spark plasma sintered WC-FeCr(C) CC grade S0 at different magnifications.

The more uniform microstructure of SPSed WC-FeCr(C) CC grade S0 exhibits also relatively even distribution of binder metals (Fe and Cr in Fig. 26), especially when compared with the EDS results of vacuum sintered samples of the same grade (Fig. 18). However, there are still small areas that appear richer in either Fe or Cr (marked with circles in Fig. 26). This implies that some fraction of the liquid phase is formed and due to the instability of the W-Fe-Cr-C system, phase transformations can take place in very short time at elevated temperatures. Also, it is important to note that during the SPS process, the temperature was measured from a slight distance (inside graphite punch) and the actual temperature inside the powder mass may be somewhat higher.

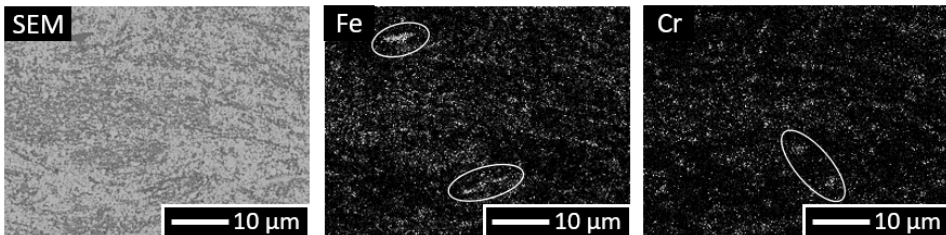


Figure 26. Microstructure and EDS elemental mappings of spark plasma sintered WC-FeCr(C) grade S0.

The XRD results of vacuum sintered and SPSed WC-FeCr(C) grade S0 are compared in Fig. 27. SPS yields sintered CC with nearly two-phased structure. No η -phase signal was detected and only small trace signals of Fe-based carbides were present. Yet, these signals were distinct enough to be attributed to the $(\text{Fe,Cr})_3\text{C}$ cementite phase. In terms of phase composition, the diffractogram of SPSed grade S0 resembles the diffractogram of vacuum sintered grade S2.4 with a considerable amount of extra carbon (Fig. 23). The absence of both η -phase and Cr-based $(\text{Cr,Fe})_{23}\text{C}_6$ mixed carbide after SPS suggests that these compounds require extended time to form.

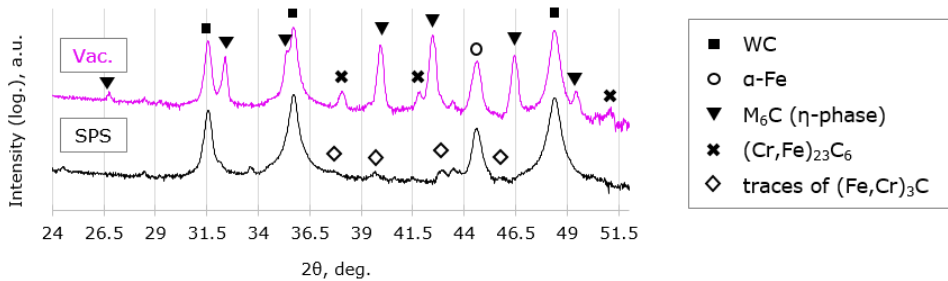


Figure 27. XRD diffractograms of the WC-FeCr(C) CC grade S0 – vacuum sintering at 1200 °C (top) and spark plasma sintering at 1100 °C (bottom).

3.2.2 Addition of strong carbide forming elements

The *binder pools* that disrupt the homogeneity of the microstructure of WC-FeCr(C) CCs are composed largely of $(\text{Cr,Fe})_x\text{C}_y$ carbides. For that reason, altering the chemical composition to reduce the stability of such metal carbides could lead to enhanced homogeneity. In stainless steels, the formation of unwanted carbides (mainly $(\text{Cr,Fe})_{23}\text{C}_6$ due to the relatively small amount of carbon present) can be avoided with the addition of carbon active metals that form MC monocarbides [85]. Titanium and niobium are most frequently used monocarbide formers and they were employed as additions in the current research as well [Paper IV].

In the experimental A-series (Table 3), a part of FeCr alloy was substituted by either Ti or Nb. Extra carbon was included in those grades since the XRD analysis showed that, of the S-series, the S1.5 grade (with 1.5 wt% extra carbon) has almost desired two-phase composition (Fig. 23).

The microstructures with corresponding elemental mappings of WC-FeCr(C)-M grades ATi1.5 with Ti and ANb1.5 with Nb are shown in Figs. 28 and 29, respectively. In the material with addition of Ti (ATi1.5), the η -phase manifests as large, often elongated, but scarce formations. However, with Nb addition, the particles of the η -phase are relatively fine (0.5–3 μm) and very evenly distributed in the microstructure. The EDS spot analysis proved that the η -phase has roughly the same composition as in WC-FeCr(C) grade S0 (Fig. 18 and Table 5).

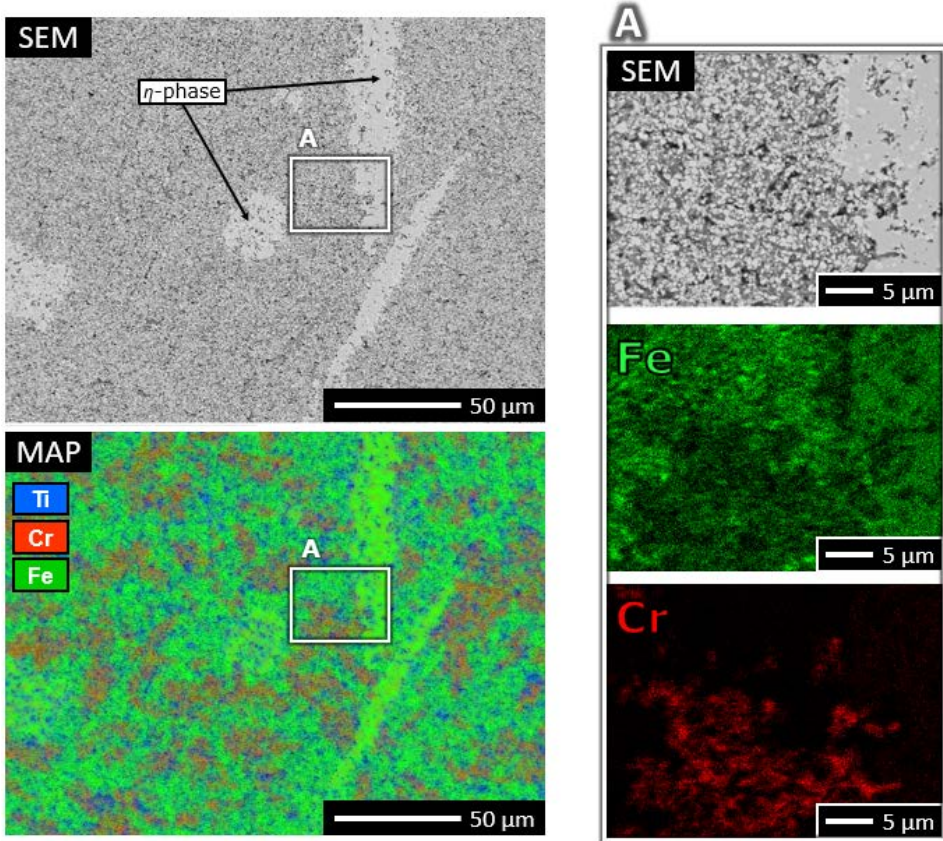


Figure 28. Microstructure and EDS elemental mappings of WC-FeCr(C)-M CC grade ATi1.5 with Ti addition.

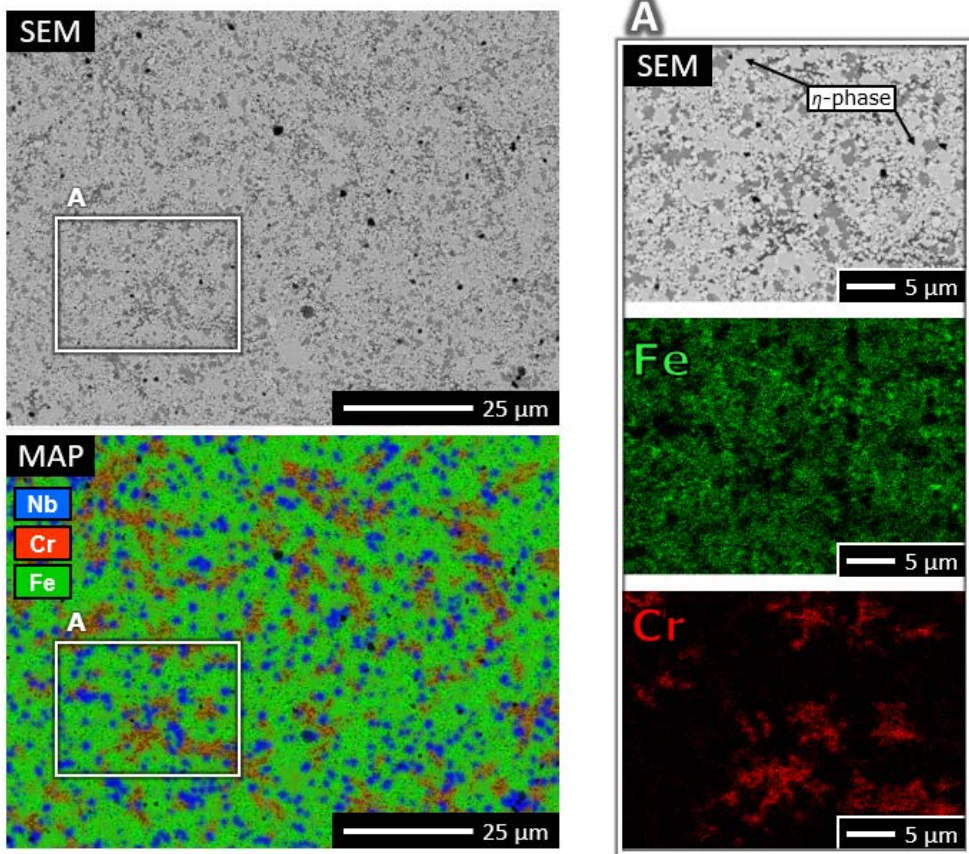


Figure 29. Microstructure and EDS elemental mappings of WC-FeCr(C)-M CC grade ANb1.5 with Nb addition.

From the EDS mappings (Figs. 28 and 29), the Ti- and Nb-rich areas are visible. With the XRD analysis, the presence of Ti and Nb carbides was confirmed (Fig. 30). The EDS spot analysis results exhibit the elemental distribution in Ti- and Nb- rich areas (Table 6). Again, it should be emphasized that the EDS spot analysis must be taken as approximations due to the very fine microstructure. The large fraction of W in Ti-rich spots implies that (Ti, W)C solid solution carbide is present. Nb-rich spots yield considerably larger Nb signal, which suggests that Nb monocarbide has formed.

Table 6. Results of the quantitative EDS spot analysis from WC-FeCr(C)-M grades ATi1.5 and ANb1.5.

	Content, wt%					
	W	C	Fe	Cr	Ti	Nb
ATi1.5 – surface	65.1	5.9	19.2	4.1	5.7	-
ATi1.5 – Ti-rich area	49.0	11.5	11.1	7.6	20.6	-
ANb1.5 – surface	65.6	6.1	16.4	3.6	-	8.4
ANb1.5 – Nb-rich area	20.2	17.1	2.6	0.8	-	59.3

It is evident that the addition of strong carbide formers has positive effect on the distribution of phases and chromium. Cr-rich areas are still visible on the EDS mappings, but they appear significantly smaller and more homogeneously distributed than Cr-rich areas present in WC-FeCr(C) CCs without Ti or Nb addition (Fig. 18). Furthermore, there are no distinctive *binder pools* present in A-series grades as compared with grade S1.5 without Ti and Nb additions (Fig. 16b).

Figure 30 compares the experimental WC-FeCr(C) and reference materials. The positive effect of the rapid consolidation method and alloying on the morphology of the microstructure is observable. The microstructures of WC-FeCr(C)-M grades, especially with Nb addition, are similar to those of WC-FeCrNi and WC-Co.

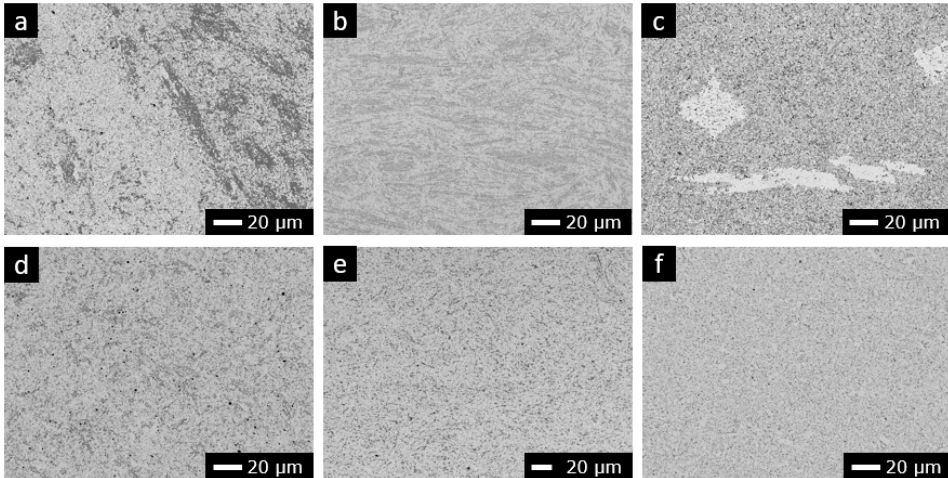


Figure 30. Comparison of the microstructures of the WC CCs: a) vacuum sintered WC-FeCr(C) grade S1.5; b) spark plasma sintered WC-FeCr(C) grade S0; c) vacuum sintered WC-FeCr(C)-M grade ATi1.5 with Ti addition; d) vacuum sintered WC-FeCr(C)-M grade ANb1.5 with Nb addition; e) reference material – vacuum sintered WC-FeCrNi grade RS (AISI316 as binder); f) reference material – WC-Co grade RCoH.

The XRD analysis of WC-FeCr(C)-M grades ATi1.5 and ANb1.5 demonstrates that the addition of Ti and Nb yielded the formation of respective carbides (Fig. 31). Interestingly, the diffractogram of CC with Ti addition demonstrated rather complicated phase composition – alongside WC, η -phase, α -Fe and TiC the traces of Cr-based carbides, Fe-based carbides and γ -Fe (austenite) are detectable. Thus, six different ceramic and metallic compounds are present. Therefore it is plausible that the WC-FeCr(C)-M grade ATi1.5 is rather metastable and the structure could be altered easily with processing parameters. Grade ANb1.5 with Nb addition mainly consists of four phases – WC, η -phase, α -Fe and NbC.

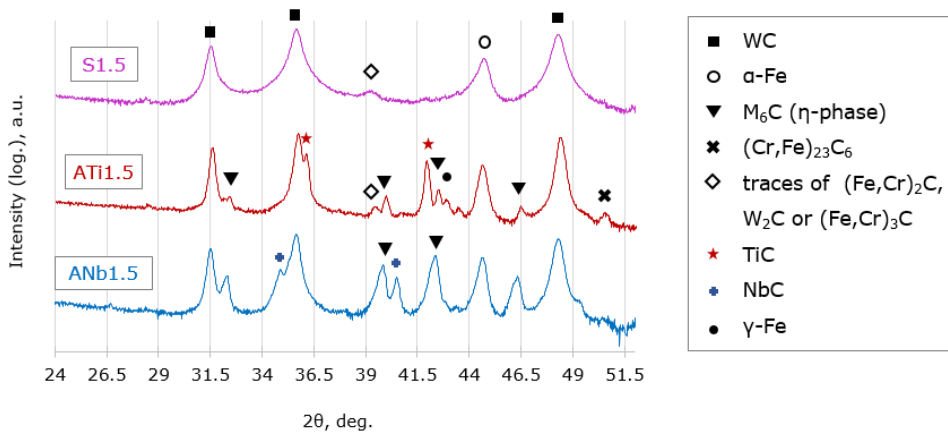


Figure 31. XRD diffractograms of the WC-FeCr(C) CC grade S1.5 compared with WC-FeCr(C)-M CC grades ATi1.5 (with Ti) and ANb1.5 (with Nb).

3.2.3 Summary

The homogeneity of the microstructure of WC-FeCr(C) CCs can be enhanced with both employing rapid sintering conditions and with alloying (Fig. 30). When spark plasma sintering is used, the enhancing effect comes from considerably shorter processing duration and reduced temperature. Both of these factors contribute towards retarding the formation of unwanted phases and microstructural constituents (*binder pools*). To reduce the lamellar binder rich areas that are characteristic of the SPSed alloys (Fig. 31b), the processing parameters, especially powder preparation (milling), should be further investigated.

The alloying approach relies on the formation of monocarbides and therefore is suppressing the formation of unwanted $(Cr,Fe)_x C_y$ mixed carbides. The carbides of alloying elements appear in the structure as evenly dispersed constituents and exhibit no abnormal growth. Although the areas of high Cr concentration are still present, the overall morphology of the microstructure is improved.

The microstructures of experimental WC-FeCr(C)-M CCs are already comparable with reference materials (WC-FeCrNi and WC-Co) in terms of the homogeneity of the microstructure.

3.3 Properties of WC-FeCr(C)-(M) cemented carbides

In this section, the performance of WC-FeCr(C) CCs is discussed. Mechanical properties (hardness and toughness) of experimental materials are compared with conventional CCs. As reference, from the literature, the properties of CCs with other Fe-based binders are presented.

The serviceability of WC-FeCr(C)-(M) in corrosive and oxidative environments is assessed through corrosion and oxidation tests and abrasive-erosion test results at room and elevated temperatures demonstrate wear resistance in the conditions where oxidation is an important factor.

3.3.1 Mechanical performance

A comprehensive overview of the correlation between hardness and fracture toughness is presented in Fig. 32.

E grades

WC-FeCr(C) CC E-series with low calculated binder content (15 wt%; ~26 vol%) exhibit high hardness, but rather low toughness values when compared with WC-Co grade RCoH with similar binder fraction [Paper I]. The addition of 1% carbon increases toughness slightly. The reference grades R0 and R1 with the same binder fraction and pure Fe binder possess considerably lower hardness and slightly higher toughness. Therefore, it is evident that introducing Cr into the binder makes CCs more brittle.

Another consideration is the actual binder fraction. With the formation of extensive η -phase in WC-FeCr(C) grades E0 and E1 (Fig. 13b and 13d), it is evident that in sintered CCs, the metallic binder fraction is noticeably lower than calculated. Moreover, the hardness of E-series grades is comparable with WC-Co grade RCoL that has only 6 wt% (10 vol%) binder. The small residual binder fraction is the reason that majority of phase and microstructure studies in this research were carried out on WC-FeCr(C) CCs with higher calculated binder volume (S-series grades).

S grades

Firstly, the substantial uncertainty of the values of WC-FeCr(C) S-series grades must be addressed. The reason behind considerable fluctuations of the hardness and toughness is the highly heterogeneous microstructure (Figs. 14 and 16). The effect of the uneven microstructure is observable in Fig. 33a. Another attribute of S grades is the formation of multiple crack from one indentation corner (Fig. 33b), which complicates the toughness measurements via the indentation method. Of the vacuum sintered S grades, only S2 (with 2 wt% added carbon) exhibited repeatedly the formation on four distinct crack per indentation and showed relatively small uncertainty values. The microstructure of S2 (Fig. 16c) grade is notably less heterogeneous as compared with the microstructures of the S0 (Fig. 14), S1 (Fig. 16a) and S1.5 (Fig. 16b). Spark plasma sintered S0 grade with a much more homogeneous microstructure (Fig. 25) yielded also repeatable results with low scattering. However, toughness of this grade is relatively low. Due to the extensive porosity, the properties of the E, S and R-series grades with the highest added carbon values (E2, S2.4 and R2) could not be accurately measured [Paper II].

Even when considering the high uncertainty, it is evident that sintering temperature has a marked effect on the mechanical properties. Grade S0 sintered at 1300 °C (S0^b in Fig. 32) shows higher toughness than S0 sintered at 1200 °C (S0^a in Fig. 32). It is difficult to give indisputable explanation for this, but it is most probably connected with the major change in the microstructure that occurred when S0 was sintered at higher temperature – extensive formation of large η -phase areas.

In general, the positive effect of the extra carbon on the fracture toughness is apparent in all CCs grades with Fe-based binder (E, S and R-series). This can be attributed to the reduction of η -phase and is in accordance with the properties reported by Vilhena et al. [86]. In contradiction, Trung et al. reported the increase in hardness and toughness simultaneously with 1.5 and 2 wt% of extra carbon and argued that this is due to higher relative density [45].

A grades

WC-FeCr(C)-M grades with Ti and Nb addition (Figs. 28 and 29, respectively) exhibit acceptably low uncertainty of mechanical properties, but the toughness of these grades is relatively low. A grades have lower calculated binder content (25 wt%) than the “unalloyed” S grades [Paper IV]. However, grade ATi1.5 with Ti addition has uncompetitive fracture toughness and in terms of toughness is on par with brittle E grades.

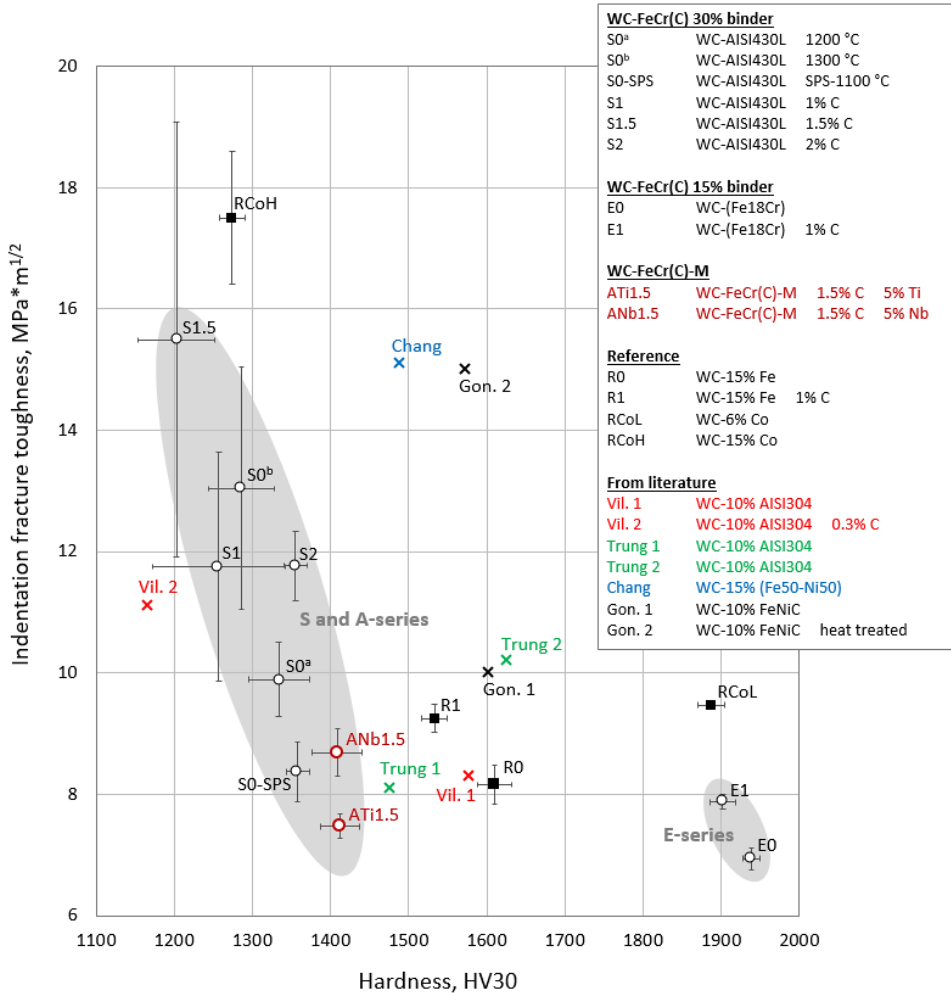


Figure 32. Comprehensive overview of mechanical properties of CC grades studied in this work. The properties of reference CCs, WC-FeNi and WC-FeCrNi, are taken from the works of Vilhena et al. [86], Trung et al. [45], Chang et al. [88] and Gonzales et al. [87].

The mechanical characteristics of the experimental WC-FeCr(C) CCs, especially S-series, are comparable with CCs from literature reports where AISI304 (X5CrNi18-10) Cr-Ni austenitic steel is employed as binder. Still, the mechanical performance of well-studied WC-Co is superior. The hardness of S- and A-series is comparable with WC-Co grade RCoH and the hardness of E-series is comparable with WC-Co grade RCoL, but toughness of CCs with Co binder is in both cases notably higher. The toughness of Cr

free WC-FeNi CC also surpasses the toughness of CCs with FeCr(Ni) binder at equal hardness. Gonzales et al. demonstrated also the possibility of improving the properties of WC-FeNi through heat treatment [87].

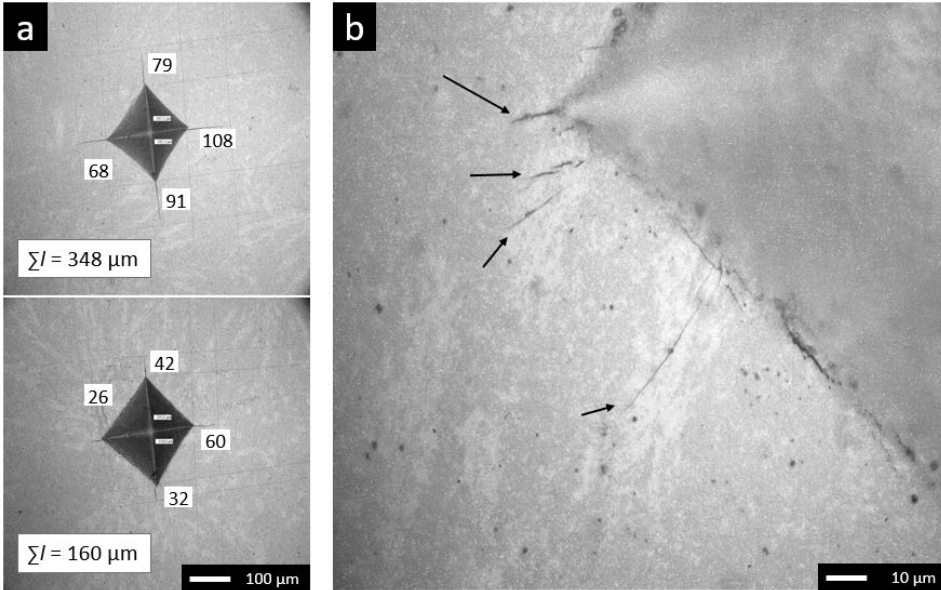


Figure 33. Optical microscope images of WC-FeCr(C) CC grade S1.5: a) example of inconsistent indentations with a sum of crack lengths; b) multiple crack formations from the indentation corner.

3.3.2 Corrosion and oxidation resistance

The robust laboratory oxidation and corrosion test results are exhibited in Fig. 34. The WC-Co grade RCoH with 15 wt% of binder with comparable hardness and therefore similar metal phase fraction was used as reference. The corrosion rate in alkaline condition (NaCl solution) is nearly equal among investigated CC grades; however, a vast difference over order of magnitude between WC-Co and WC-FeCr(C) was revealed in the oxidation test. It has been reported that WC-Fe has better oxidation resistance than WC-Co and addition of Cr enhances it even further [89], but such drastic difference was somewhat unexpected.

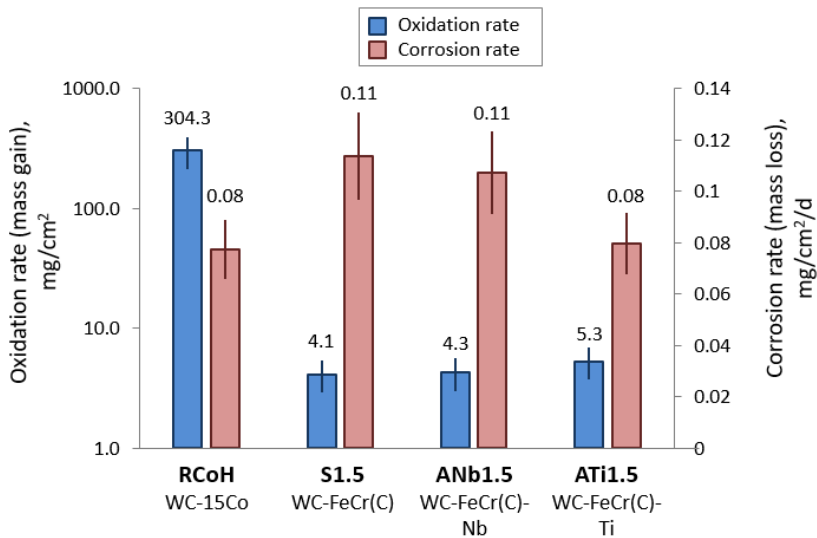


Figure 34. Oxidation rate (mass gain after 2 h heating at 900 °C) and corrosion rate (mass loss after 42 h immersion on 3.5 wt% NaCl solution) of WC-FeCr(C)-(M) CCs and WC-Co reference grade.

3.3.3 Abrasive-erosion wear resistance

As expected, the abrasive-erosion wear resistance of WC-FeCr(C) CCs at room temperature is comparable with WC-Co that has similar hardness (RCoH). WC-Co CCs with lower binder fraction (RCoL and RCoM with binder weight fractions 6% and 11%, respectively) showed notably lower volume loss. At 350 °C, the situation was similar, only the wear rates were increased. From 450 °C onward, the resistance of WC-Co grades started to deteriorate. The increase of volume loss of WC-FeCr(C) grades with an increase of temperature is fairly linear and at higher temperatures, they outperform conventional WC-Co materials considerably, regardless of hardness. Thus, it is evident that employing FeCr-based binder systems in WC CCs enhances the temperature stability of these composites remarkably.

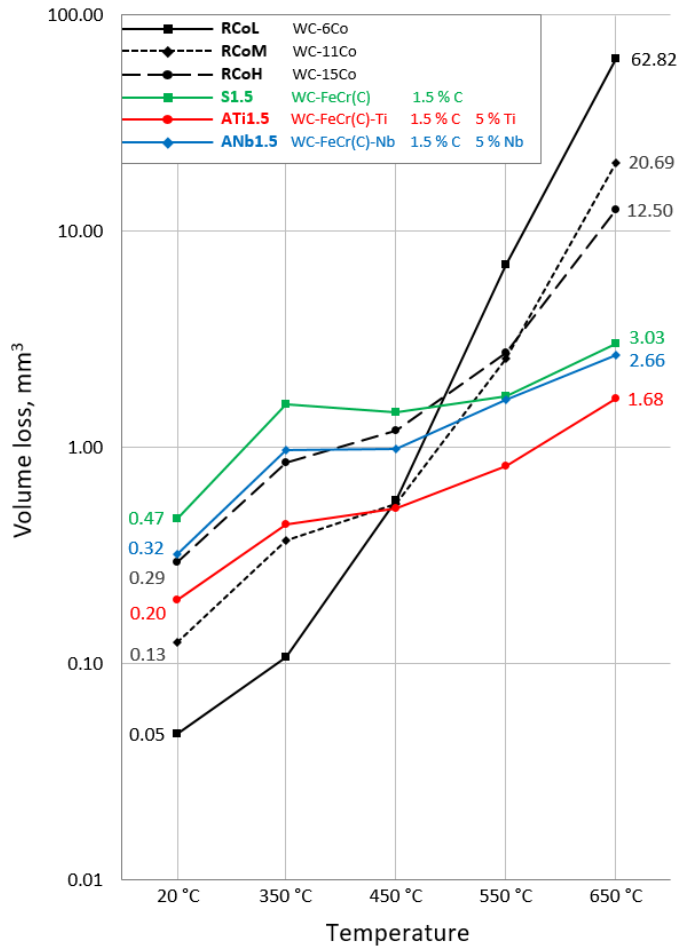


Figure 35. Erosion wear of WC-FeCr(C) and WC-Co CCs at room and elevated temperatures (the uncertainty (error bars) is not presented since average uncertainty was relatively low, under 7% of measure value).

3.3.4 Summary

The highly heterogeneous microstructure of WC-FeCr(C) CCs impacts the mechanical performance. The uneven microstructure causes high fluctuations in hardness and toughness and even complicates the measuring process. Cemented carbides with enhanced homogeneity of the microstructure through increased carbon content, use of rapid sintering method and alloying exhibited more stable mechanical properties. Comparison of the mechanical properties with reference materials and literature gave evidence that the experimental WC-FeCr(C) CCs are on a par with WC-FeCrNi CCs, but exhibits lower toughness than more conventional compositions (WC-Co, WC-FeNi).

The initial corrosion resistance assessment in alkaline environment showed that CCs with FeCr-based binder are comparable with WC-Co. However, tests in oxidation and erosion-oxidation conditions demonstrated advantageous performance of WC-FeCr(C) compositions.

CONCLUSIONS

The main goal of the research was to develop cemented carbide compositions that would satisfy today's requirements, in particular, avoiding the use of expensive and harmful elements. The objects of the research were Co and Ni free CCs and the focus was on two aspects: microstructural characteristics and means of improving its homogeneity; mechanical and tribological performance.

In the experimental part of the thesis, the WC-FeCr(C) CCs were studied in detail and the following conclusions can be drawn:

- Densification. The WC-FeCr(C) CCs can be sintered to near full density at relatively low temperature. Sintering in vacuum at 1200 °C yields CCs with density of approximately 100% of the theoretical density and porosity under 0.2%. The liquid phase is formed between 1100–1200 °C which is in good accordance with the liquid phase formation temperature in the W-Fe-C system (1143 °C). When extra carbon is introduced, the density of the WC-FeCr(C) CCs decreases, but the porosity remains low until 2.4 wt% of extra carbon. This demonstrates that the added carbon readily dissolves in metallic or ceramic phases.
- The microstructures of WC-FeCr(C) CCs is heterogeneous. The areas with homogeneous tungsten carbide + binder distribution are interrupted by extensive and mostly elongated *binder pools*. From their shape and sheer size it is evident that these formations are the result of liquid phase sintering. The extra carbon content affects the shape of *binder pools*. With carbon addition of 2 and 2.4 wt%, the *binder pools* are more equiaxed and overall heterogeneity of the microstructure is reduced. It was demonstrated that these pools tend to be composed of Cr-rich core and Fe-rich shell. The Cr-rich zone possesses also increased carbon content and is therefore rich in (Cr,Fe)_xC_y mixed carbides. The increase of carbon content improves the homogeneity of Cr and Fe distribution.
- The phase composition investigations revealed that during processing (sintering) of WC-FeCr(C) CCs, two types of mixed carbides form above 600 °C – the (W,Fe)₆C type η -phase and Cr- or Fe-based M_xC_y carbides. The carbon content has the following effects on the phase composition:
 - Increased carbon contents decrease (W,Fe)₆C type η -phase fraction.
 - Smaller carbon content favors the formation of Cr-based carbides with lower carbon:metal ratio.
 - Higher carbon content (1.5 wt% of added carbon and higher) favors the formations of mixed carbides with higher carbon:metal ratio.
- Enhancing the homogeneity of the microstructure. Since the *binder pools* are clearly the result of vacuum sintering and are rich in Cr- or Fe-based mixed carbides, two approaches were considered for reducing the heterogeneity of the microstructure: the use of rapid sintering (SPS) and introducing strong monocarbide formers (Ti and Nb). Both approaches had positive effect. With

SPS, the microstructure was free of *binder pools* that are characteristic of vacuum sintered WC-FeCr(C); however, somewhat uneven distribution was caused by nonoptimal milling. As expected, the addition of Ti and Nb yielded the formation of respective monocarbides and the resulting microstructure is homogeneous. Morphology of the microstructures of the WC-FeCr(C) grades with Ti and Nb addition are comparable with WC-FeCrNi and WC-Co CCs.

- Performance. The mechanical performance of WC-FeCr(C) CCs is on a par with WC CCs with austenitic FeCrNi binder. However, at comparable hardness, the toughness of WC-FeCr(C) CCs is lower than toughness of WC-Co and WC-FeNi. When compared with WC-Co, the WC-FeCr(C) CCs exhibits similar resistance to corrosion, but excel in oxidation resistance. The increased oxidation resistance was further demonstrated in erosion-oxidation conditions, where WC-FeCr(C) proved to be superior to WC-Co.

Scientific novelty

The novelty of the research can be outlined as follows:

- Ascertainment of microstructure evolution and phase transformation features of high-chromium WC-FeCr cemented carbides.
- Proposed technological and chemical opportunities for the improvement of structural homogeneity and performance.

Future research

To further increase the serviceability of WC cemented carbides with high chromium FeCr binder, the following future research topics are proposed:

- Revealing the possibilities to achieve corrosion resistance that is comparable with WC-Ni cemented carbides;
- Study of carbon balance of WC-FeCr(C) cemented carbides with Ti and/or Nb additions to retard different carbide phase formations during sintering;
- Study of WC-FeCrMn(C) cemented carbides with austenitic or austenitic-ferritic structure of metallic binder with the aim to increase toughness of such composites;
- Assessment of the wear performance of developed composites in true abrasive and sliding wear conditions as well as in corrosive environments.

REFERENCES

- [1] *Comprehensive Hard Materials - 1st Edition*, Elsevier, 2014.
- [2] K.J.A. Brookes, *World Directory and Handbook of Hardmetals: And Hard Materials, 6 edition*, Metal Powder Industry, East Barnet, Hertfordshire, 1997.
- [3] S. Norgren, J. García, A. Blomqvist, L. Yin, Trends in the P/M hard metal industry, *Int. J. Refract. Met. Hard Mater.* (2015) 48, pp. 31–45.
- [4] V.A. Tracey, Nickel in hardmetals, *Int. J. Refract. Met. Hard Mater.* (1992) 11, pp. 137–149.
- [5] W.D. Schubert, M. Fugger, B. Wittmann, R. Useldinger, Aspects of sintering of cemented carbides with Fe-based binders, *Int. J. Refract. Met. Hard Mater.* (2015) 49, pp. 110–123.
- [6] A.N. Løpvik, C. Hagelūken, P. Wäger, Improving supply security of critical metals: Current developments and research in the EU, *Sustain. Mater. Technol.*
- [7] USGS Scientific Investigations Report 2012–5188: Metal Prices in the United States Through 2010, <https://pubs.usgs.gov/sir/2012/5188/> (accessed March 30, 2017).
- [8] REACH - Chemicals - Environment - European Commission, http://ec.europa.eu/environment/chemicals/reach/reach_en.htm (accessed March 30, 2017).
- [9] National Toxicology Program, <https://ntp.niehs.nih.gov/> (accessed March 30, 2017).
- [10] K. Schröter, Gesinterte harte Metalllegierungen und Verfahren zu ihrer Herstellung, DRP 420689, 1923.
- [11] C. Agte, Die neue Hochleistungshartsmetallsorte S6HL, *Neue Hütte*, (1956) 1, p. 333.
- [12] C. Agte, Entwicklung der Hartmetalltechnik während der letzten Jahre in der Deutschen Demokratischen Republik, *Neue Hütte*, (1957) 2, pp. 537–544.
- [13] D. Moskowitz, M.J. Ford, M.H. Jr, High-Strength Tungsten Carbides, in: H.H. Hausner (Ed.), *Mod. Dev. Powder Metall.*, Springer US, 1971, pp. 225–234.
- [14] L. Prakash, H. Holleck, F. Thümler, P. Walter, The influence of the binder composition on the properties of WC-Fe/Co/Ni cemented carbides, *Modern Developments in Powder Metallurgy*. (1980) 14, pp. 255–268.
- [15] H. Pastor, Centenaire de la découverte du carbure de tungstène par Henri Moissan ; historique du développement de ce matériau, *Rev. Métallurgie*. (1997) 94, pp. 1537–1552.
- [16] Z. Yao, J. Stiglich, T. Sudarshan, Nano-grained tungsten carbide-cobalt (WC/Co), *Mater Modif.* (1999), pp. 1–27.
- [17] O.J. Ojo-Kupoluyi, S.M. Tahir, B.T.H.T. Baharudin, M.A.A. Hanim, M.S. Anuar, Mechanical properties of WC-based hardmetals bonded with iron alloys – a review, *Mater. Sci. Technol.* (2017), pp. 507–517.
- [18] J. Gurland, *Powder Metall. Leszynski W Ed Intersci.* (1961), p. 661.
- [19] R. Spiegler, S. Schmauder, L.S. Sigl, Fracture Toughness Evaluation of WC-Co Alloys by Indentation Testing, *J. Hard Mater.* (1990) 1, pp. 147–158.
- [20] S. Palmqvist, Method att bestamma segheten hos sproda material sarskilt hardmetaller, *Jernkontorets Ann.* (1957) 141, pp. 300–307.
- [21] F. Sergejev, M. Antonov, Comparative study on indentation fracture toughness measurements of cemented carbides, *Est. J. Eng.* (2006) 12, pp. 388–398.

- [22] S.D. Cramer, *ASM Handbook: Volume 13B: Corrosion: Materials, 10th Ed edition*, ASM International, Materials Park, Ohio, 2005.
- [23] R.S. Montgomery, The mechanism of percussive wear of tungsten carbide composites, *Wear*. (1968) 12, pp. 309–329.
- [24] S. Ekemar, L. Lindholm, T. Hartzel, Aspects on Nickel as a Binder Metal in WC-Based Cemented Carbides, (1981), pp. 477–492.
- [25] E. Kny, L. Schmid, New Hardmetal Alloys with Improved Erosion and Corrosion Resistance, *Int J Refract Mater Met Hard*. (1987) 6, pp. 145–148.
- [26] G.S. Upadhyaya, S.K. Bhaumik, Sintering of submicron WC-10wt.%Co hard metals containing nickel and iron, *Mater. Sci. Eng. A*. (1988) 105–106, pp. 249–256.
- [27] S. Huang, J. Xiong, Z. Guo, W. Wan, L. Tang, H. Zhong, W. Zhou, B. Wang, Oxidation of WC-TiC-TaC-Co hard materials at relatively low temperature, *Int. J. Refract. Met. Hard Mater*. (2015) 48, pp. 134–140.
- [28] M. Jafari, M.H. Enayati, M. Salehi, S.M. Nahvi, C.G. Park, Comparison between oxidation kinetics of HVOF sprayed WC–12Co and WC–10Co–4Cr coatings, *Int. J. Refract. Met. Hard Mater*. (2013) 41, pp. 78–84.
- [29] V.B. Voitovich, V.V. Sverdel, R.F. Voitovich, E.I. Golovko, Oxidation of WC-Co, WC-Ni and WC-Co-Ni hard metals in the temperature range 500–800 °C, *Int. J. Refract. Met. Hard Mater*. (1996) 14, pp. 289–295.
- [30] E. Oberg, *Machinery's Handbook, 29 edition*, Industrial Press, South Norwalk, Connecticut, 2012.
- [31] V.P. Astakhov, *Tribology of Metal Cutting*, Elsevier, 2006.
- [32] K. Buss, *High temperature deformation mechanisms of cemented carbides and cermets*, PhD thesis, École polytechnique fédérale de Lausanne, 2004.
- [33] J.T. Norton, *Powder Met Bull*. 6 (1951) 75–78.
- [34] R.M. German, *Liquid Phase Sintering*, Springer US, 1985.
- [35] G.S. Upadhyaya, *Cemented Tungsten Carbides: Production, Properties and Testing*, William Andrew, 1998.
- [36] Z. Nishiyama, *Martensitic Transformation*, Academic Press, 2012.
- [37] W. Schatt, E.P.M. Association, K.-P. Wieters, *Powder metallurgy: processing and materials*, European Powder Metallurgy Association, 1997.
- [38] T.W. Penrice, Alternative binders for hard metals, *J. Mater. Shap. Technol*. (1987) 5, pp. 35–39.
- [39] A. Gabriel, H. Pastor, D.M. Deo, S. Basu, C.H. Allibert, New Experimental Data in the C-Fe-W, C-Co-W, C-Ni-W, C-Fe-Ni-W and C-Co-Ni-W Systems Application to Sintering Conditions of Cemented Carbides Optimization of Steel Binder Composition by Partial Factorial Experiments, in: *Sintering'85*, Springer, Boston, MA, (1987), pp. 379–393.
- [40] P. Schwarzkopf, R. Kieffer, *Cemented Carbides*, Collier Macmillan Ltd, 1960.
- [41] D. Moskowitz, M.J. Ford, M. Humenik Jr., Abrasion resistant iron–nickel bonded tungsten carbide, *Modern Developments in Powder Metallurgy*. (1977) 10, pp. 543–551.
- [42] L. Prakash, A review of the properties of tungsten carbide hardmetals with alternative binder systems, *Proc. 13th Plansee Seminar*, (1993), pp. 80–109.
- [43] L. Prakash, G. Benno, WC Hardmetals with Iron based Binders, *Proc. 17th Plansee Seminar*, (2009) 2.

- [44] C.M. Fernandes, A. Rocha, J.P. Cardoso, A.C. Bastos, E. Soares, J. Sacramento, M.G.S. Ferreira, A.M.R. Senos, WC-stainless steel hardmetals, *Int. J. Refract. Met. Hard Mater.* (2018) 72, pp. 21–26.
- [45] T.B. Trung, H. Zuhailawati, Z.A. Ahmad, K.N. Ishihara, Sintering characteristics and properties of WC-10AISI304 (stainless steel) hardmetals with added graphite, *Mater. Sci. Eng. A.* (2014) 605, pp. 210–214.
- [46] B.J. Marques, C.M. Fernandes, A.M.R. Senos, Sintering, microstructure and properties of WC-AISI304 powder composites, *J. Alloys Compd.* (2013) 562, pp. 164–170.
- [47] C.M. Fernandes, A.M.R. Senos, M.T. Vieira, Study of Sintering Variables of Tungsten Carbide Particles Sputter-Deposited with Stainless Steel, *Mater. Sci. Forum.* (2004) 455–456, pp. 295–298.
- [48] C.M. Fernandes, A.M.R. Senos, M.T. Vieira, Control of eta carbide formation in tungsten carbide powders sputter-coated with (Fe/Ni/Cr), *Int. J. Refract. Met. Hard Mater.* (2007) 25, pp. 310–317.
- [49] C.M. Fernandes, A.M.R. Senos, M.T. Vieira, J.V. Fernandes, Composites from WC powders sputter-deposited with iron rich binders, *Ceram. Int.* (2009) 35, pp. 1617–1623.
- [50] C.M. Fernandes, V. Popovich, M. Matos, A.M.R. Senos, M.T. Vieira, Carbide phases formed in WC–M (M = Fe/Ni/Cr) systems, *Ceram. Int.* (2009) 35, pp. 369–372.
- [51] J.D. Bolton, C. Hanyaloglu, (1992) p. 21.
- [52] C. Hanyaloglu, B. Aksakal, J.D. Bolton, Production and indentation analysis of WC/Fe–Mn as an alternative to cobalt-bonded hardmetals, *Mater. Charact.* (2001) 47, pp. 315–322.
- [53] M.R. Maccio, H. Berns, Sintered hardmetals with iron–manganese binder, *Powder Metall.* (2012) 55, pp. 101–109.
- [54] E. Klar, P.K. Samal, *Powder Metallurgy Stainless Steels: Processing, Microstructures, and Properties*, ASM International, 2007.
- [55] C. Pascal, A. Thomazic, A. Antoni-Zdziobek, J.-M. Chaix, Investigation on pressureless cosintering behaviour of Hadfield steel/cemented carbide bimetals, *Powder Metall.* (2012) 55, pp. 110–117.
- [56] R. Subramanian, J.H. Schneibel, *Mater Sci Eng A.* (1998) 244, p. 103.
- [57] A.Y. Mosbah, D. Wexler, A. Calka, Tungsten Carbide Iron Aluminide Hardmetals: Nanocrystalline vs Microcrystalline, *J. Metastable Nanocrystalline Mater.* (2001) 10, p. 649.
- [58] M. Ahmadian, D. Wexler, T. Chandra, A. Calka, Abrasive wear of WC–FeAl–B and WC–Ni₃Al–B composites, *Int. J. Refract. Met. Hard Mater.* (2005) 23, pp. 155–159.
- [59] R. Furushima, K. Katou, K. Shimojima, H. Hosokawa, A. Matsumoto, Effect of Sintering Techniques on Mechanical Properties of WC–FeAl Composites, in: *TMS 2015 144th Annu. Meet. Exhib.*, Springer, Cham, (2015), pp. 1091–1095.
- [60] Y. Liu, J. Cheng, B. Yin, S. Zhu, Z. Qiao, J. Yang, Study of the tribological behaviors and wear mechanisms of WC–Co and WC–Fe₃Al hard materials under dry sliding condition, *Tribol. Int.* (2017) 109, pp. 19–25.
- [61] I.-J. Shon, Rapid consolidation of nanostructured WC–FeAl hard composites by high-frequency induction heating and its mechanical properties, *Int. J. Refract. Met. Hard Mater.* (2016) 61, pp. 185–191.
- [62] S.A. Humphry-Baker, J.M. Marshall, G.D.W. Smith, W.E. Lee, Thermophysical properties of Co-free WC–FeCr hardmetals, *Proc. 19th Plansee Seminar.* (2017).

- [63] S.A. Humphry-Baker, K. Peng, W.E. Lee, Oxidation resistant tungsten carbide hardmetals, *Int. J. Refract. Met. Hard Mater.* (2017) 66, pp. 135–143.
- [64] S. Sakaguchi, S. Imasato, H. Ito, R. Nakamura, Some Properties of Sintered WC-(Fe-Cr-C) Alloys, *J. Jpn. Soc. Powder Powder Metall.* (1989) 36, pp. 908–912.
- [65] K. Kambakas, P. Tsakirooulos, Solidification of high-Cr white cast iron–WC particle reinforced composites, *Mater. Sci. Eng. A.* (2005) 413–414, pp. 538–544.
- [66] J.-O. Andersson, A thermodynamic evaluation of the Fe-Cr-C system, *Metall. Trans. A.* (1988) 19, pp. 627–636.
- [67] H. Hinnert, I. Konyashin, B. Ries, M. Petrzehik, E.A. Levashov, D. Park, T. Weirich, J. Mayer, A.A. Mazilkin, Novel hardmetals with nano-grain reinforced binder for hard-facings, *Int. J. Refract. Met. Hard Mater.* (2017) 67, 98–104.
- [68] M. Hajihashemi, M. Shamanian, G. Azimi, Physical, Mechanical, and Dry Sliding Wear Properties of Fe-Cr-W-C Hardfacing Alloys Under Different Tungsten Addition, *Metall. Mater. Trans. B.* (2015) 46, pp. 919–927.
- [69] S. Chatterjee, J.D. Majumdar, K. Singaiah, S.M. Shariff, G. Padmanabham, A.R. Choudhury, Performance evaluation of laser surface alloyed hard nanostructured Al₂O₃–TiB₂–TiN composite coatings with in-situ and ex-situ reinforcements, *Surf. Coat. Technol.* (2011) 205, pp. 3478–3484.
- [70] I.Y. Konyashin, B.H. Ries, F.F. Lachmann, Polycrystalline Material, Bodies Comprising Same, Tools Comprising Same and Method for Making Same, WO2013178552 (A1), (2013).
- [71] M.F. McGuire, *Stainless Steels for Design Engineers*, ASM International, (2008).
- [72] A.V. Khvan, B. Hallstedt, C. Broeckmann, A thermodynamic evaluation of the Fe–Cr–C system, *Calphad.* (2014) 46, pp. 24–33.
- [73] P. Franke, H.J. Seifert, eds., Binary Systems and Ternary Systems from C-Cr-Fe to Cr-Fe-W: Thermodynamic Properties of Inorganic Materials Compiled by SGTE, Subvolume C: Ternary Steel Systems, *Phase Diagrams and Phase Transition Data*, Springer-Verlag, Berlin Heidelberg, (2012).
- [74] C.M. Fernandes, A.M.R. Senos, Cemented carbide phase diagrams: A review, *Int. J. Refract. Met. Hard Mater.* (2011) 29, pp. 405–418.
- [75] P. Gustafson, A thermodynamic evaluation of the C–Fe–W system, *Metall. Mater. Trans. A.* (1987) 18, pp. 175–188.
- [76] P. Gustafson, A thermodynamic evaluation of the c-cr-fe-w system, *Metall. Trans. A.* (1987) 19, pp. 2547–2554.
- [77] S.R. Shatynski, The thermochemistry of transition metal carbides, *Oxid. Met.* (1979) 13, pp. 105–118.
- [78] J. Covino, B. S, 13A: *ASM Handbook: Corrosion: Fundamentals, Testing, and Protection, 10 edition*, ASM International, Materials Park, Ohio, (2003).
- [79] M. Antonov, I. Hussainova, J. Pirso, O. Volobueva, Assessment of mechanically mixed layer developed during high temperature erosion of cermets, *Wear.* (2007) 263, pp. 878–886.
- [80] B. Wittmann, W.-D. Schubert, B. Lux, WC grain growth and grain growth inhibition in nickel and iron binder hardmetals, *Int. J. Refract. Met. Hard Mater.* (2002) 20, pp. 51–60.
- [81] J.C. Betts, The direct laser deposition of AISI316 stainless steel and Cr₃C₂ powder, *J. Mater. Process. Technol.* (2009) 209, pp. 5229–5238.
- [82] H.-O. Andrén, Microstructures of cemented carbides, *Mater. Des.* (2001) 22, pp. 491–498.

- [83] B. Fahlman, *Materials Chemistry, 2nd ed.*, Springer Netherlands, 2011.
- [84] M. Kolnes, A. Mere, J. Kübarsepp, M. Viljus, B. Maaten, M. Tarraste, Microstructure evolution of TiC cermets with ferritic AISI 430L steel binder, *Powder Metall.* (2018) 0, pp. 1–13.
- [85] K.H. Lo, C.H. Shek, J.K.L. Lai, Recent developments in stainless steels, *Mater. Sci. Eng. R Rep.* (2009) 65, pp. 39–104.
- [86] L.M. Vilhena, C.M. Fernandes, E. Soares, J. Sacramento, A.M.R. Senos, A. Ramalho, Abrasive wear resistance of WC–Co and WC–AISI 304 composites by ball-cratering method, *Wear.* (2016) 346–347, pp. 99–107.
- [87] R. González, J. Echeberría, J.M. Sánchez, F. Castro, WC-(Fe,Ni,C) hardmetals with improved toughness through isothermal heat treatments, *J. Mater. Sci.* (1995) 30, pp. 3435–3439.
- [88] S.-H. Chang, S.-L. Chen, Characterization and properties of sintered WC–Co and WC–Ni–Fe hard metal alloys, *J. Alloys Compd.* (2014) 585, pp. 407–413..
- [89] B. Wittmann, W.-D. Schubert, B. Lux, Hardmetals with Iron-Based Binder, *Proc. EURO PM2002.* (2002), pp. 303–308.

ACKNOWLEDGEMENTS

First and foremost, I would like to thank my supervisors, prof. Jakob Kübarsepp and senior researcher Kristjan Juhani for providing me an opportunity to do my doctoral study connected with one of the research topics in the Department of Mechanical and Industrial Engineering. I am grateful for their support and counsel during my studies. In addition, special thanks are due to senior researcher Jüri Pirso who possesses incredible knowledge in materials science and whom I can consider as my third, nonofficial supervisor.

My very special gratitude goes to all my colleagues at the Department of Mechanical and Industrial Engineering and Department of Materials and Environmental Technology who have helped me with my research. Furthermore, I am thankful to all the co-authors who contributed to publications related to my thesis. Also, the help of Väino Sammelselg and his research group in University of Tartu, Institute of Physics is greatly appreciated.

I will always cherish the long discussions on scientific matter and on other topics with my long-time friends and colleagues Marek Jöeleht, Märt and Mart Kolnes and with friends I made during my studies – Kaspar Kallip, Der-Liang Yung, Zorjana Mural, Yaroslav Holovenko and others. Without the technical assistance from engineer Hans Valner, my experimental work in the Laboratory of Powder Metallurgy would have been hindered.

My research was funded by institutional research fundings IUT (19-29) "*Multi-scale structured ceramic-based composites for extreme applications*" and IUT (19-4) "*Thin films and nanomaterials by wet-chemical methods for next-generation photovoltaics*", base funding by the Estonian Ministry of Education and Research, project number B56 "*Innovative polycrystalline diamond (PDC) drag bit for soft ground tunnel boring machines*", research grant ETF8817 "*Developing novel methods to enhance the reliability of WC-Co and TiC-NiMo cermets*" and partially by ASTRA "*TUT Institutional Development Programme for 2016-2022*" Graduate School of Functional Materials and Technologies.

And finally, last but by no means least, I would like to express my sincere gratitude to my family for supporting me through all those years.

ABSTRACT

Development of cemented carbides with high chromium iron alloy binder

The development of more economical and environment friendly material systems is one of the main research directions in materials science. The field of hard and wear resistant materials is not an exception. Cemented carbides that were developed in the 1920s quickly became irreplaceable in manufacturing industries. The properties of the combination of tungsten carbide (WC) and cobalt have been refined to excellence over the last ninety years. The motivation to alter the reliable WC-Co system stems from economic considerations, such as supply insecurity and high price of cobalt, and healthcare aspects – the carcinogenic nature of Co. Historically “second best” choice for a metal binder in cemented carbides, nickel, suffers also from toxicity.

Over the last decades, substantial research has been conducted to reduce, or even avoid, the usage of Co and Ni in cemented carbides. Iron-based alloys have shown most promising results. Iron-cobalt-nickel binder system has received most attention and WC-FeCoNi cemented carbides are also commercially available as alternatives to WC-Co. Other Fe-based binders have been employed in niche applications, for example, wood cutting.

Following the increasing necessity to develop Co and Ni free cemented carbides, the author of doctoral thesis posed the following hypothesis:

If the iron-chromium-based (FeCr) alloys are successfully employed as a binder metal in WC cemented carbides, the resulting composite will be free of expensive and harmful elements. In addition, WC-FeCr composite will have the potential to perform competitively in corrosive and oxidative environments.

The experimental cemented carbides with high chromium FeCr binder were prepared by standard powder metallurgy approach: mechanical milling of initial powders, mechanical uniaxial pressing and sintering. Two sintering methods, conventional vacuum sintering and rapid spark plasma sintering (SPS), were used. The microstructure and phase composition of cemented carbides with different chemical composition and processing routes were characterised with optical and electron microscopy, X-ray spectrometry, X-ray diffraction and differential scanning calorimetry (DSC). Hardness and fracture toughness were evaluated with Vickers hardness tests coupled with the Palmqvist toughness determination method. Corrosion resistance tests in saline medium and oxidation resistance tests in air were carried out in order to assess the performance of experimental cemented carbides in conditions that are inherently corrosive and/or oxidative. Additionally, the abrasive-erosion tests at room and at elevated temperatures were performed.

Chapter 3 discusses the results of the studies of the development of WC-FeCr(C) cemented carbides. The focus was on densification, microstructure evolution, phase composition, possibilities of enhancing the homogeneity of the microstructure and performance of cemented carbides. It was found that WC cemented carbides with FeCr binder can be sintered to near full density (under 0.2% residual porosity) at relatively low temperature of 1200 °C, thus implying that forming liquid phase is near eutectic and rich in carbon. The morphology of the microstructure was found heterogeneous where large *binder pools* are present and tend to form clusters. In addition, a common

constituent, brittle η -phase (W and Fe mixed carbide), appears in the structure. The shape of *binder pools* and overall morphology of the microstructure is influenced by added carbon fraction and sintering temperature. With higher added carbon fractions (2 wt% and 2.4 wt% relative to whole powder mass), the microstructure appears more homogeneous and the formation of η -phase is retarded.

X-ray spectrometry analysis showed that *binder pools* have notably uneven distribution of Cr and Fe. Fe-rich areas are arguably α -Fe based with some fractions of dissolved Cr, while Cr-rich areas with increased C content are M_xC_y mixed metal carbides. X-ray diffraction results confirmed the presence of both η -phase and Cr- or Fe-based carbides. These phases form during sintering above 600 °C. The increase of added C fraction retards the formation of η -phase, as was also observed with the microstructure studies, and favours the formation of M_xC_y carbides with higher carbon/metal ratio, namely M_3C – cementite.

The means of improving the homogeneity of the microstructure of WC-FeCr(C) cemented carbides were considered. Employing rapid sintering (SPS) and alloying with strong monocarbide formers (Ti and Nb) was found to enhance homogeneity. WC cemented carbides with FeCr binder and C and Nb additions resulted in the microstructure that is already comparable with well-studied WC-Co and WC-FeCrNi cemented carbides.

The experimental WC-FeCr(C) cemented carbides demonstrated mechanical properties that is on a par with WC-FeCrNi cemented carbides, but lower when compared with WC-Co. However, WC-FeCr(C) materials demonstrate promising results at elevated temperatures – low oxidation rate and high wear resistance in abrasive-erosion conditions at elevated temperatures.

The thorough ascertaining of microstructure evolution of WC-FeCr(C) cemented carbides and proposed means of improving microstructure homogeneity and overall performance can be highlighted as scientific novelty of the research.

LÜHIKOKKUVÕTE

Kõrge kroomisisaldusega rauasulamsideainega kõvasulamite arendus

Materjaliteaduses on üks läbivaid arendussuundi ökonoomsete ja keskkonnasõbralike materjalide arendus. Erandiks ei ole ka kõvasulamite ja kermistega seotud suuringud. 1920-ndatel aastatel väljatöötatud kõvasulamid said kiiresti asendamatuks tootvas tööstuses. Volframkarbiidist (WC) ja koobaltist koosnevate komposiitide omadused on viimase 90 aasta jooksul viidud märkimisväärsele tasemele. Vajadus muuta ennast tõestanud kõvasulamite (WC-Co) koostist tuleneb majanduslikest kaalutlustest (koobalti ebakindel kättesaadavus ja kõrge hind) ning koobalti ohtlikusest inimorganismile (kantserogeensus). Ajalooliselt „paremuselt teine“ metall kõvasulamite koostises, nikkel, on samuti tunnistatud toksiliseks.

Viimastel aastakümnetel on märkimisväärset tähelepanu pööratud viisidele, kuidas vähendada ja isegi vältida koobalti ja nikli kasutamist kõvasulamites. Rauasulamid on seni andnud kõige lootustandvamaid tulemusi ning välja on töötatud omadustelt WC-Co-ga võrdsed raud-koobalt-nikkel sideainega kõvasulamid. Teisi rauasulameid on vähem uuritud ja leidnud kasutust sideainena ainult üksikutes rakendustes.

Lähtudes järjest suuremast survest vähendada koobalti ja nikli kasutust on antud töö autor püstitanud järgneva hüpoteesi:

Kasutades sideainena raud-kroom (FeCr) sulameid on võimalik valmistada kõvasulamid, mis on vabad kulukatest ja toksilistest elementidest. Lisaks sellele on WC-FeCr kõvasulamid konkurentsivõimelised rakendades neid korrosiivsetes ja oksüdatiivsetes keskkondades.

Antud töös valmistati eksperimentaalsed kõvasulamid kõrge kroomisisaldusega rauasulamsideainega kasutades tüüpilist pulbermetallurgilist valmistusviisi: lähtepulbrite jahvatamine kuulveskis, jahvatatud pulbersegu pressimine ning paagutamine. Töös kasutati vaakumpaagutust ja plasmaaktiveeritud paagutust. Erinevate keemiliste koostistega ja erinevate paagutus parameetritega valmistatud kõvasulamite mikrostruktuuri ja faasilist koostist karakteriseeriti kasutades optilist- ja elektronmikroskoopiat, energia hajuvusspektroskoopiat, röntgendifraktsioon-analüüsi ja diferentsiaalset skaneerivat kalorimeetriat. Materjalide kõvaduse ja purunemissitkuse mõõtmiseks kasutati vastavalt Vickersi ja Palmqvisti meetodeid. Korrosioonikatse NaCl vesilahuses ja oksüdeerumiskatse õhu viidi läbi hindamaks kõvasulamite kasutatavust keskkondades, mis on loomu poolest korrosiivsed ja/või oksüdatiivsed. Vastupanu abrasiiv-erosioonkulumisele hinnati toa- ja kõrgendatud temperatuuridel.

Uurimistöö kolmas peatükk, „WC-FeCr(C) kõvasulamite arendus“, on pühendatud tulemustele ja diskussioonile. Fookuses on kõvasulamite paakuvus, mikrostruktuuri moodustumine, faasiline koostis, meetodid parandamaks struktuuri homogeensust ja mehaanilised ning triboloogilised omadused.

Suhteliselt madala paagutustemperatuuriga (1200 °C) on võimalik saavutada peaaegu täistihedus ja madal poorsus (alla 0.2 protsendi). Madal paagutus temperatuur viitab sellele, et tekkiv vedelfaas on eutektilisele koostisele väga lähedane ja seetõttu süsnikurikas. Peale paagutamist on kõvasulamite mikrostruktuur heterogeenne – struktuuris esinevad suured, enamasti pikliku kujuga, peamiselt sideainest koosnevad

alad. Samuti on mikrostruktuuris nähtav ka η -faas (volframi ja raua kaksikkarbiid). Sideainerikaste alade kuju ja struktuuri üldine morfoloogia sõltub süsiniku kogusest ja paagutustemperatuurist. Kui lisada algele pulbrisegule kaks massiprotsenti või rohkem süsinikku, siis sideaine alade kuju muutub rohkem võrdkülgsemaks ning struktuur ise rohkem homogeensemaks. Samuti vähendab süsiniku lisamine nähtavalt η -faasi osakaalu mikrostruktuuris.

Energia hajuvusspektroskoopia analüüsides leiti, et sideainerikkad alad koosnevad omakorda erineva keemilise koostisega piirkondadest. Selgesti on eristatavad alad, kus on kõrge raua kontsentratsioon ja alad, kus on kõrge kroomi kontsentratsioon. Kõrgendatud raua osakaaluga ala on metalliline tardlahus, samas kui kroomirikas ala koosneb peamiselt kroomi ja raua karbiididest. Röntgendifraktsioon-analüüs kinnitas, et WC-FeCr(C) kõvasulamid koosnevad peamiselt neljast faasist: volframkarbiid (WC), raua-baasil tardlahus (α -Fe), M_6C ($M = W, Fe$) η -faas ja M_xC_y ($M = Fe, Cr, W$) mitmikkarbiidid. Kui WC ja α -Fe tulenavad lähtepulbritest, siis η -faasist ja M_xC_y karbiidid moodustuvad paagutuse jooksul, kui temperatuur ületab 600 °C. Süsiniku lisamisega on võimalik η -faasi teket vältida ning mõjutada, millise keemilise koostisega M_xC_y mitmikkarbiidid tekivad.

Mikrostruktuuri homogeensuse parandamiseks uuriti kiire paagutustsükli ja legerimise mõjusid. Mõlemad meetodid, kiire plasmaaktiveeritud paagutamine ja titaani või nioobiumi lisamine, tõstsid märgatavalt kõvasulamite mikrostruktuuri ühtlust. Kui WC-FeCr kõvasulamile lisada süsinikku ja nioobiumi, siis paagutatud materjali mikrostruktuur on homogeensusel juba võrreldav põhjalikult uuritud WC-Co ja WC-FeCrNi kõvasulamitega.

Mehaaniliste omaduste (kõvadus ja purunemissitkus) poolest on eksperimentaalsed WC-FeCr(C) kõvasulamid võrreldavad WC-FeCrNi kõvasulamitega, kuid jäävad alla WC-Co kõvasulamitele. Samas, FeCr sideainega kõvasulamid näitasid silmapaitvaid tulemusi kõrgetel temperatuuridel – aeglane oksüdeerumine ja väike kulumine abrasiiv-erosioonkulumis tingimustes kõrgetel temperatuuridel.

Uurimistöö uudsus seisneb Ni- ja Co-vabade WC-FeCr(C) kõvasulamite põhjalikus mikrostruktuuri moodustumise selgitamises ning meetodite väljatöötamises, mille abil on võimalik tõsta nende komposiitide struktuuri ühtlust ja talitusomadusi.

APPENDIX

PAPER I

M. Tarraste, K. Juhani, J. Kübarsepp, J. Pirso, V. Mikli, The Effect of Cr and C on the Characteristics of WC-FeCr Hardmetals, *Proceedings of Euro PM2015*. (2015).

Manuscript refereed by Dr Leo Prakash, (Kyocera Unimerco, Denmark)

The Effect of Cr and C on the Characteristics of WC-FeCr Hardmetals

Marek Tarraste (Tallinn University of Technology, Ehitajate tee 5, 19086 Tallinn, Estonia) marek.tarraste@ttu.ee; Kristjan Juhani (Tallinn University of Technology, Ehitajate tee 5, 19086 Tallinn, Estonia) kristjan.juhani@gmail.com; Jakob Kübarsepp (Tallinn University of Technology, Ehitajate tee 5, 19086 Tallinn, Estonia) jakob.kubarsepp@ttu.ee; Jüri Pirso (Tallinn University of Technology, Ehitajate tee 5, 19086 Tallinn, Estonia) juri.pirso@ttu.ee; Valdek Mikli (Tallinn University of Technology, Ehitajate tee 5, 19086 Tallinn, Estonia) valdek.mikli@ttu.ee

Abstract

High price and toxicity of cobalt motivates the researchers to find alternative binder systems for WC hardmetals. Previous investigations have shown that iron based binders can be a viable alternative to cobalt. Focus in this research is on WC hardmetals with a 15wt.% iron-chromium binder. Different amounts of extra C were added to the powder mixture to compensate carbon loss during sintering and thus reduce the formation of η -phase. The effect of Cr introduction into a ferrous binder system on the binder phase composition and distribution as well as on the mechanical properties (hardness, indentation fracture toughness) was investigated.

1. Introduction

WC hardmetals are well known for excellent combination of hardness, toughness and wear resistance. Cobalt is widely used as the binder metal because of its good wetting behavior and good WC solubility in Co. WC-Co hardmetals are widely used as materials for cutting tools for machining of various materials, in the mining industry and for production of various wear parts. Main applications of WC-Co involve environments that are inherently corrosive. For example, in steel cutting where coolants are used, the corrosive attack of the coolant is a performance factor of a cutting tool. WC hardmetals are also employed where corrosion resistance is the main factor for material selection such as valve seats, spray nozzles, ball point pens, dental drills etc. [1]. Alternative binder systems such as Ni, Ni-Cr and Co-Cr can be used to obtain higher corrosion resistance than regular WC-Co. Further, in most aqueous media the addition of Cr to the Co and Ni binders improves corrosion resistance [2]. However, in applications where corrosion and wear occur simultaneously, the WC-Co composition is often used for its high wear resistance and excellent mechanical characteristics [1].

The high price and toxicity of cobalt and nickel have been motivating researchers to find suitable alternatives for binder metal in the last decades. Fe based binder systems have attracted interest because of their abundant availability, reduced price and non-toxicity compared to cobalt and nickel [3]. Regarding corrosion resistant binder solutions, Fe-Cr steels can offer an alternative to Co. Chromium acts as a ferrite stabilizer in steels. Ferritic steels with high Cr content (up to 30wt.%) are known for high oxidation resistance and corrosion resistance in saline environments [1]. It is known that high vapor pressure of Cr causes the evaporation of Cr during vacuum sintering of stainless steels at around 1200 °C [4]. Possible evaporation of Cr should be taken into consideration when sintering hardmetals with Cr additions. Another consideration is the effect of extra carbon content. According to previous research on hardmetals with Fe based binders, small amounts of carbon must be added to the powder mixture to prevent the formation of unwanted η -phase [5-8]. Knowledge of WC hardmetals with Fe-Cr binder is scarce. Previously sinterability and corrosion resistance of TiC base cemented carbides with FeCrSi binder have been studied in [9].

The aim of this work is to investigate the effects of chromium and extra carbon content on the microstructure formation and mechanical properties of WC-FeCr hardmetals with WC-Fe as reference.

2. Experimental procedure

WC hardmetal powder mixtures with binder compositions of Fe, Fe-18wt.%Cr and Fe-28wt.%Cr and with different extra carbon percentage (0, 1 and 2) were prepared by the conventional ball milling technique. Cr contents of 18 and 28 weight percent were based on commercial ferritic steel grades (AISI 430 and AISI 446, respectively). Overall binder content was kept at 15wt.%. Tungsten carbide powder (WC_{0,9µm} - Wolframite) and elemental powders of iron (ATOMET HP1001), chromium (Cr_{6,0µm} - PPM) and carbon black (TIMCAL Timrex KS75) were milled in a ball mill with hardmetal lining and balls for 72h with ball to powder weight ratio of 20:1. Isopropyl alcohol was used as milling liquid. 3%

Euro PM2015 – Hard Materials – Alternative Binders

of paraffin wax was added as a binding agent. Dried powders were compacted into green parts (5x5x20mm) using uniaxial pressing with a pressure of 95MPa. Green parts were sintered in a conventional vacuum furnace (FCT Systeme GmbH FPW 300/400) at 1390 °C. Hardmetal with high Cr content (28wt.% of Cr in initial binder) was sintered also at 1510 °C to examine the effect of possible Cr loss at higher temperature. Vacuum level in furnace during 30 min dwell at the end temperature was in the range of 0.04...0.08 mbar. Specimens were sintered on zirconia support to avoid the strong carbon pick-up of the iron matrix when sintering on conventional graphite support [10]. The compositions of initial powder mixtures and mechanical properties of sintered specimens are presented in Table 1.

Table 1. Material composition and mechanical properties

Powder mixtures					Mechanical properties of sintered samples	
Binder	Powder composition (wt.%)				Hardness, HV ₃₀	Indentation fracture toughness K _{1C} , MPa*m ^{1/2}
	WC	Fe	Cr	C		
Fe	85	15	-	-	1610	6.25
Fe	85	15	-	1	1533	7.88
Fe	85	15	-	2	n/a	n/a
Fe - 18wt.%Cr	85	12.3	2,7	-	1939	3.95
Fe - 18wt.%Cr	85	12.3	2,7	1	1902	5.19
Fe - 18wt.%Cr	85	12.3	2,7	2	n/a	n/a
Fe - 28wt.%Cr	85	10.8	4,2	-	1907	4.50
Fe - 28wt.%Cr	85	10.8	4,2	1	1782	5.94
Fe - 28wt.%Cr	85	10.8	4,2	2	n/a	n/a

Cross-sections of sintered parts were ground and polished. Zeiss Ultra 55 FEG-SEM scanning electron microscope (SEM) equipped with an energy dispersive X-ray spectrometer (EDS) Bruker Esprit 1.8 was used for microstructure observation and phase identification. Vickers hardness was measured in accordance with the ASTM Standard E384. The fracture toughness (K_{1C}) was determined by measuring the crack length from the tip of the indentation made by Vickers indentation (Palmqvist method). The toughness was calculated by the following equation [11]:

$$K_{1C} = 0.0726 \frac{P}{C^{3/2}},$$

where P is the load of Vickers indenter (N) and C is half of the diagonal + crack length (mm).

3. Results and discussion

3.1. Microstructures

Figs. 1 and 2 exhibit SEM images of WC hardmetals with Fe and Fe28Cr binders sintered at 1390 °C. The effect of 0%, 1% and 2% extra carbon additions is presented. In the case of the Fe binder, the effects of carbon additions followed a logical path: no carbon additions caused the formation of η -phase in the microstructure, 1% of extra carbon yielded a microstructure with homogenous distribution of two phases (light WC and darker Fe binder matrix) and in the material with 2% extra carbon, the free graphite phase is present. Both η -phase and free graphite are unwanted phases in the WC hardmetal since they deteriorate the mechanical properties of the material.

The microstructure of materials with high Cr content in the binder phase (Fig. 2) shows highly uneven distribution of phases. In addition to the vast share of η -phase at 0% carbon (Fig.2a), the Cr rich metal phase is present in materials with added carbon (Figs.2b and 2c). EDS analysis showed that the Fe and Cr ratio in this phase is nearly 1:1. Both the η -phase and the Cr rich phase contribute to the uneven allocation of WC grains. Dependant on the carbon content in sintered material the brittle η -phase in W-C-Fe-Cr system can compose of the M₂₃C, M₆C, M₄C carbides or of the mixture of these [12].

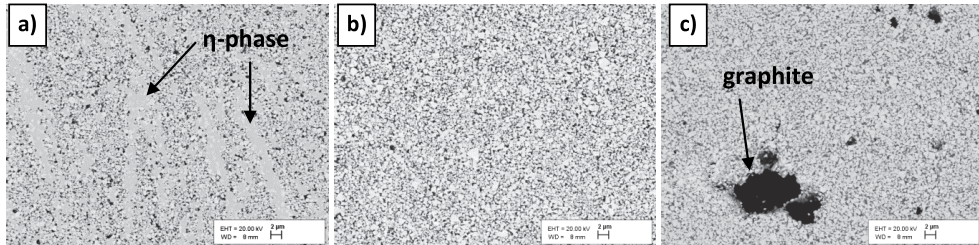


Figure 1. WC hardmetal with Fe binder with different extra carbon additions: a) 0%C, b) 1%C and c) 2%C.

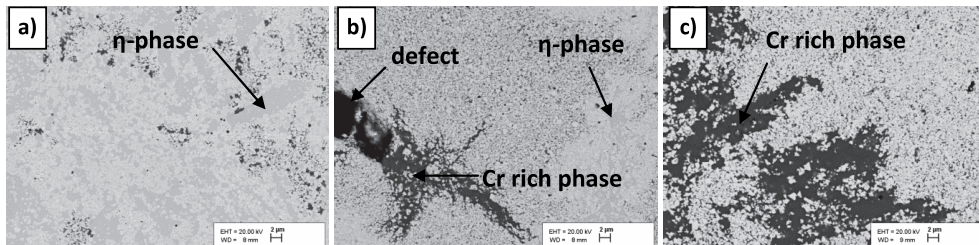


Figure 2. WC hardmetal with Fe28Cr binder with different extra carbon additions: a) 0%C, b) 1%C and c) 2%C.

Figure 3 shows the comparison of WC-Fe28Cr sintered at 1390 and 1510 °C. Increased temperature yielded more uniform microstructure (Fig.3b). The dark Cr rich phase is no longer present. The weight percentage of W, Fe, Cr and Co was determined with EDS equipment when a wide area was scanned. It should be noted that carbon was excluded from the current results and attention was on distribution of metals. The lack of uneven distribution of Cr and no formation of Cr rich phase in the microstructure can be attributed to the lower Cr content when sintered at higher temperatures.

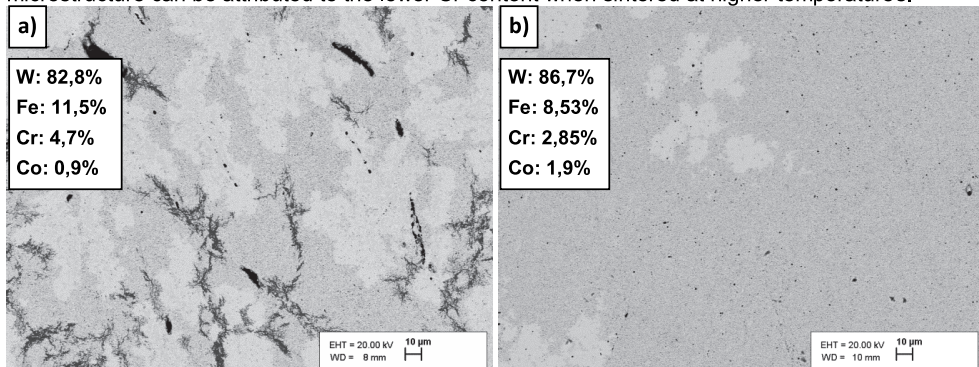


Figure 3. WC-Fe28Cr with 1%C of extra carbon sintered at a) 1390 °C and b) 1510 °C.

WC-FeCr hardmetals with 18wt.% of Cr in the initial binder phase were prepared and examined to verify the importance of Cr content on the phase distribution in the microstructure. Figure 4 shows SEM images of WC-Fe18Cr with different extra carbon additions sintered at 1390 °C.

c)

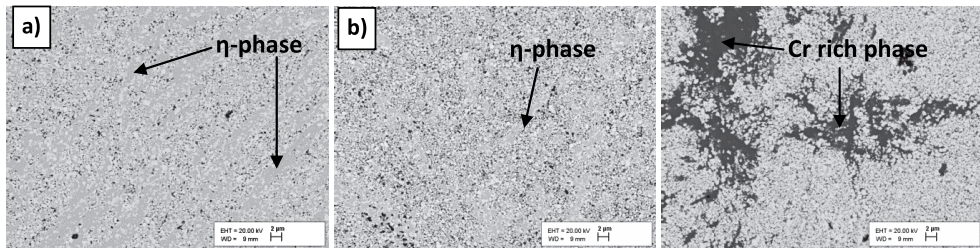


Figure 4. WC hardmetal with the Fe18Cr binder with different extra carbon additions: a) 0%C, b) 1%C and c) 2%C.

While η -phase is still present, no Cr rich phase was formed within materials 0% and 1% of carbon additions (Figs.4a and 4b). This correlates with the results of WC-Fe28Cr when sintered at 1510 °C and indicates that uniformity of phase distribution in the WC-based hardmetals with FeCr binder is connected with the Cr content. High Cr percentage in vacuum sintered WC-FeCr hardmetals can lead to the distortions in otherwise homogeneous microstructure. Optimal extra carbon content for Fe18Cr binder lies presumably between 1 and 2%.

3.2. Mechanical properties

Hardness and indentation fracture toughness of the prepared materials was measured and the results are presented in Table 1 and Figure 5. Materials with FeCr binder systems exhibit considerably higher hardness and lower toughness as compared with Fe binder. Surprisingly, the difference between the two FeCr binder systems is minimal - in a range of uncertainty. Carbon addition of 1% provides ~25...30% increase in toughness since extra carbon retards the formation of brittle η -phase (Figs.1b, 2b and 4b). Still, materials with the FeCr binder remain rather brittle when compared with WC-Co that have indentation fracture toughness (K_{IC}) values in range of 9...24 $\text{MPa}\cdot\text{m}^{1/2}$ [13].

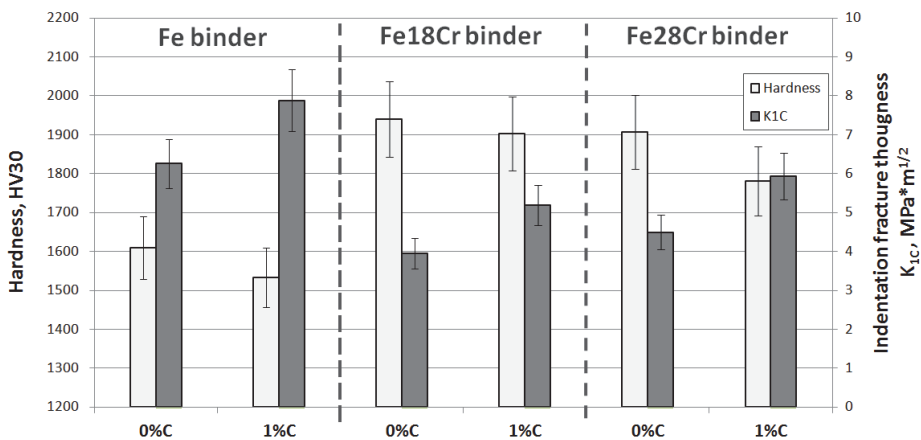


Figure 5. Dependence of hardness and indentation fracture toughness of the WC hardmetals on the Cr and C content.

4. Conclusions

- WC-Fe, WC-Fe18Cr and Fe-28Cr hardmetals with two Cr contents and different amounts of extra C additions were prepared with 15wt.% of binder content in the initial powder mixture.
- Additional carbon was found to have great impact on the microstructure. In the case of the Fe binder, materials with 0% and 2% extra carbon exhibited η -phase and free graphite, respectively, while 1% of additional carbon contributed to the formation of homogeneous two phase microstructure. Large amount of brittle η -phase was present in the WC hardmetal with Fe28Cr binder. The presence of η -phase was somewhat reduced with the binder system with a lower Cr content (Fe18Cr).

Euro PM2015 – Hard Materials – Alternative Binders

- Besides η -phase, the Cr rich phase was present when Cr was introduced to the system, especially with the Fe₂₈Cr binder. Cr rich phase with the Fe:Cr ratio nearly 1:1 caused major distortions in the uniformity of the microstructures, i.e. large metal rich areas were present. Higher sintering temperature was found to retard the formation of Cr rich phase.
- Hardmetals with FeCr binders are harder and therefore more brittle as compared to these with Fe binder. Toughness of materials is increased with 1% of extra carbon.
- Presently, it can be concluded that application of WC-FeCr hardmetals is limited due to their high hardness and brittleness. However, the performance of WC-FeCr hardmetals in corrosive environments must be examined in order to evaluate where FeCr binder systems could offer an alternative to Co.

Acknowledgments

This work was supported by institutional research funding IUT (19-29) of the Estonian Ministry of Education and Research.

References

- [1] ASM Handbook, volume 13 Corrosion, ASM International 1987.
- [2] E. Kny, L. Schmid, New Hardmetal Alloys with improved Erosion and Corrosion Resistance.
- [3] L. J. Prakash, Benno Gries, WC Hardmetals with Iron Based Binders, 17th Plansee Seminar, 2009, conference proceedings vol. 2, HM5.
- [4] Powder Metallurgy Stainless Steels: Processing, Microstructures and Properties, ASM International 2007.
- [5] C. Agte, Die neue Hochleistungshartmetallsorte, Neue Hütte 1, (1956), pp. 333-338.
- [6] C.M. Fernandes, V. Popovich, M. Matos, A.M.R. Senos, M.T. Vieira, Carbide Phases Formed in WC–M (M = Fe/Ni/Cr) Systems, Ceramics International, 35 (2009), pp. 369-372.
- [7] C. Hanyaloglu, B. Aksakal, J.D. Bolton, Production and Indentation Analysis of WC/Fe–Mn as an Alternative to Cobalt-bonded Hardmetals, Materials Characterization, 47 (2001), pp. 315– 322.
- [8] D. Moskowitz, M.J. Ford, M. Humenik, High-strength Tungsten Carbides, Int. J. Powder Metall, 6(4) (1970), pp. 55-64.
- [9] J. Kùbarsepp, V. Kallast, Stainless Hardmetals and Their Electrochemical Corrosion Resistance, Materials and Corrosion, 1994 (45), pp. 452-458.
- [10] B. Wittmann, W.D. Schubert, B. Lux, Hardmetals with Iron-Based Binder, Euro PM 2002, conference proceedings, pp. 303-308.
- [11] H.R. Lawn, E.R. Fuller, Equilibrium Penny-like Cracks in Indentation Fracture, J. Mater. Sci., 10 (1975), pp. 2016–2024.
- [12] C.M. Fernandes, A.M.R. Senos, Cemented carbide phase diagrams: A review, Int. Journal of Refractory Metals and Hard Materials, 29 (2011), pp. 405-418.
- [13] K.J.A. Brookes, World Directory and Handbook of Hardmetals and Hard Materials: Sixth Ed. International Carbide Data, 1996, pp. 99.

PAPER II

M. Tarraste, J. Kübarsepp, K. Juhani, A. Mere, M. Kolnes, M. Viljus, B. Maaten, Ferritic chromium steel as binder metal for WC cemented carbides, *Int. J. Refract. Met. Hard Mater.* (2018) 73, 183–191.



Contents lists available at ScienceDirect

International Journal of Refractory Metals & Hard Materials

journal homepage: www.elsevier.com/locate/IJRMHM

Ferritic chromium steel as binder metal for WC cemented carbides

Marek Tarraste^{a,*}, Jakob Kübarsepp^a, Kristjan Juhani^a, Arvo Mere^b, Märt Kolnes^a, Mart Viljus^a, Birgit Maaten^c

^a Department of Mechanical and Industrial Engineering, Tallinn University of Technology, Ehitajate tee 5, Tallinn 19086, Estonia

^b Department of Materials and Environmental Technology, Tallinn University of Technology, Ehitajate tee 5, Tallinn 19086, Estonia

^c Department of Energy Technology, Tallinn University of Technology, Ehitajate tee 5, Tallinn 19086, Estonia



ARTICLE INFO

Keywords:

Cemented carbides
Alternative binders
Phase formation
Microstructure evolution

ABSTRACT

Fe-based alloys as alternative binders of cemented carbides are of increased research interest. We used ferritic chromium steel AISI430L as metallic component in cobalt and nickel free WC-FeCr cemented carbides. Composites with relatively high binder content of 30 wt% were under investigation. Our focus was on the effect of sintering temperature on the densification and phase evolution and on the influence of extra carbon. With the liquid phase formation around 1150 °C, the near full density of the composites was achieved at 1200 °C. During sintering, M_6C η -phase and (Cr, Fe)_xC_y mixed carbides of different composition dependent on the carbon additions were formed. Addition of carbon to achieve over-stoichiometric carbon level proved opportunity to retard the formation of the η -phase and the (Cr, Fe)₂₃C₆ phase and favored microstructural homogeneity. However, final microstructure remained heterogeneous with binder rich areas consisting of Cr- and Fe-based carbides and α -Fe.

1. Introduction

Materials science is largely driven by a need for economical and environment friendly material systems. In the hardmetal industry, finding an alternative to cobalt has been a research challenge since WC-Co was established as an excellent engineering material. Relatively high and unstable price and availability of Co [1] have been common motivators whereas recently health and environment considerations have risen. The REACH programme (Registration, Evaluation, Authorisation and Restriction of Chemical substances) in Europe [2] and NTP (National Toxicology Program) in the United States [3] have classified cobalt as very toxic for the human health. Historically, the “second best” choice for a binder metal of nickel suffers also from high toxicity [4].

The use of iron as a binder metal was described already in an early patent by K. Schröter, but due to superior properties of the WC-Co system, further investigation of iron as an alternative was discontinued. Besides inferior mechanical properties, the properties of the W-C-Fe system made it difficult to achieve a favorable two phase structure [5,6]. In 1956, Agte pointed out the importance of carbon balance and a need for extra (overstoichiometric) carbon in the W-C-Fe system [7,8]. During the last three decades of the 20th century, the research of Fe-based binders increased. The potential, properties and, to some extent,

the commercial use of Fe-based binder systems have been overviewed in review papers by Norgren et al. [4] and Ojo-Kupoluyi et al. [9]. As compared to Co, traditional binder metal, Fe and Fe-based alloys introduce some distinctive characteristics and technological peculiarities:

- Theoretical calculations of phase diagrams (CALPHAD) by Guillermet [10–12] and experimental results from Schubert et al. [13] have demonstrated that increasing the Fe content in the binder will result in a narrower carbon window where the η -phase and free graphite are avoided.
- Another important conclusion from Guillermet is that it is very difficult to avoid the formation of M_6C mixed carbide, the η -phase, during sintering. Increasing the Fe content in the binder will cause the thermodynamical stability of the M_6C phase with stoichiometric carbon content when the temperature is raised above the solidus line. Following cooling will cause transformation of WC + liquid + M_6C → WC + fcc binder. Schubert explains that M_6C decomposition into a binder is most likely to cause the non-uniform distribution of the binder [13].
- Depending on the elemental composition, the Fe-based binders can be tailored to have different phase structures: ferritic, austenitic, martensitic and austenitic/martensitic, and exhibit different qualities in terms mechanical properties, wear resistance and corrosion-

* Corresponding author.

E-mail addresses: marek.tarraste@ttu.ee (M. Tarraste), jakob.kubarsepp@ttu.ee (J. Kübarsepp), kristjan.juhani@ttu.ee (K. Juhani), arvo.mere@ttu.ee (A. Mere), mart.kolnes1@ttu.ee (M. Kolnes), mart.viljus@ttu.ee (M. Viljus), birgit.maaten@ttu.ee (B. Maaten).

<https://doi.org/10.1016/j.ijrmhm.2018.02.010>

Received 13 July 2017; Received in revised form 19 January 2018; Accepted 7 February 2018

Available online 08 February 2018

0263-4368/ © 2018 Elsevier Ltd. All rights reserved.

oxidation performance [14].

- Fe and Fe-based alloys, especially those containing also Cr, act as natural grain growth inhibitors. WC grain growth in those composites is greatly retarded even at high temperature [15,16].

Scarce information is available on the WC-FeCr composites. Kambakas and Tsakiroopoulos [17] reinforced high chromium white cast iron with WC which resulted in formation of quite complex microstructure with several eutectic and secondary M_xC_y ($M = Fe, W, Cr$) phase precipitations and overall increase in wear resistance. Sakaguchi prepared WC cemented carbides with Cr-rich cast iron (CI) by means of liquid phase sintering and reported also the formation of addition metal carbides, namely M_7C_3 [18]. Taking into account the high carbon content of cast irons (mostly 2–4 wt%) the formation of other carbides besides WC in WC-CI system is natural. However, due to the relatively high affinity of Fe and Cr for carbon, the precipitation of carbides is possible also in WC cemented carbides with Fe-Cr alloys (steels) as binder [19]. Additionally, considerable dissolution of WC in liquid Fe [20] increases the C content of liquid phase during sintering and therefore favors the formation of other carbide phases upon cooling.

Our aim is to study cobalt and nickel free WC-FeCr cemented carbides. Our choice for the binder metal is ferritic steel AISI430L. Main focus is on phase transformations during sintering and the effect of additional carbon on the phase composition and microstructure of sintered cemented carbides.

2. Experimental

Cemented carbide powder mixtures with the ferritic steel AISI430L (Table 1) binder were prepared by the conventional milling technique: tungsten carbide ($WC_{0.9\mu m}$ supplied by Wolfram Bergbau und Hütten AG) and steel powders were milled in a ball mill with WC-Co lining and balls for 72 h with the ball to powder weight ratio of 10:1. Isopropyl alcohol was used as a milling liquid. Graphite powder (KS6 supplied by Imerys Graphite & Carbon) was employed for carbon addition in the WC-FeCr compositions.

Binder fraction in the starting mixtures was a matter of discussion amongst authors and eventually we decided to prepare WC–30 wt% FeCr. Our initial experiments with the Fe-Cr binder system [21,22] showed that at 15 wt% of chromium steel or mixture of Fe and Cr, the final sintered composite exhibited very high hardness coupled with low toughness. Therefore, we increased the amount of the Fe-Cr binder in the cemented carbide composition drastically. Our additional belief was that increased binder metal content simplifies the detection of possible new phase formations. Table 2 presents the composition of experimental WC cemented carbides studied. Number in grade designation corresponds to the additional carbon (wt%) that was added prior milling.

Milled powders mixed with 3 wt% paraffin were dried at 50 °C and compacted into green bodies with 95 MPa of uniaxial pressure. Conventional liquid phase sintering in vacuum (0.1...0.5 mbar) was carried out in a sinter-HIP furnace FPW 300/400 from FCT Systeme GmbH. Pressed samples were placed on zirconia support in graphite crucibles. Heating rate was 10 °C/min and 30 min dwell at the end temperature, followed by natural cooling with furnace. Different end temperatures were chosen in the range of 600...1300 °C to examine the

Table 1
Chemical composition and particle size of ferritic steel AISI430L powder (Sandvik Osprey Ltd.).

AISI430L (gas atomised)						
Fe wt%	Cr wt%	Mn wt%	Si wt%	Impurities (P, S, C) wt%	Particle size μm	
81.83	16.8	0.69	0.64	0.04	10...45	

Table 2

Calculated chemical composition of studied cemented carbides.

Material	WC		Fe wt%	Cr wt%	C wt%	Others wt%
	wt%	vol%				
W0	70.0	53.9	24.6	5.0	–	0.4
W1	69.3	n/a	24.4	4.9	1.0	0.4
W1.5	69.0	n/a	24.2	4.9	1.5	0.4
W2	68.6	n/a	24.1	4.9	2.0	0.4
W2.4	68.3	n/a	24.0	4.9	2.4	0.4

densification and phase transformations during the sintering cycle.

Sintered specimens were grinded and polished. The porosity of hardmetals was determined by using an optical microscope Axiovert 25 and software Buehler Omnimet. Density was measured by the Archimedes method and compared with the calculated theoretical density. For thermal analysis the cemented carbide grade W0 was analyzed using a NETZSCH STA 449 F3 Jupiter® TG-DSC apparatus. The sample was heated in a pure argon (5.0) atmosphere from 40 °C to 1200 °C with heating rate set 10 °C/min and protective gas flow of 25 mL/min.

SEM (Zeiss EVO MA15) equipped with EDS systems INCA and TEM (FEI Titan Themis 200) systems were used for microstructure observation and assessment of elemental distribution. Specimens for TEM analysis were prepared by FIB cutting (FEI Helios Nanolab 600 SEM-FIB). X-ray diffraction (XRD) measurements of the samples were performed on a Rigaku Ultima IV diffractometer with monochromatic $Cu K\alpha$ radiation ($\lambda = 1.5406 \text{ \AA}$). All samples were studied in the 2θ range of 24–52 deg with the scan step of 0.02 deg.

Vickers hardness and microhardness were measured with Indetec 5030 KV and Micromet 2001, respectively. The indentation fracture toughness (K_{IC}) was determined by measuring the crack length from the tip of the indentation made by Vickers indentation (Palmqvist method) and calculated by the following equation [23]:

$$K_{IC} = 0.15 \sqrt{\frac{HV30}{\Sigma l}}$$

where Σl is sum of crack length of the crack tip from the hardness indent in mm.

3. Results and discussion

3.1. Densification

Fig. 1 represents the densification behavior (density and mass change) and differential scanning calorimetry signal of the experimental WC-FeCr cemented carbide W0. The density percentages given in brackets were calculated from the theoretical full density, which is 12.02 g/cm^3 for WC–30 wt% AISI430L according to the rule of mixture. This value should be considered with caution since it does not take into account density changes from possible phase transformations: formation of the η -phase and intermetallic compounds, solubility of WC in the binder phase etc.

Rapid density increase from 1100 °C to 1200 °C indicates that the liquid phase is formed in the given interval and near full density is achieved at as low as 1200 °C. This is also confirmed by the low residual porosity that was below 0.2% of all specimens sintered at 1200 °C with the exception of material with highest added carbon content (W2.4) where graphite porosity appeared. Low liquid phase formation temperature is in agreement with previous research on the W-C-Fe system, reporting the eutectic melt formation at 1143 °C [19]. It is also very close to the eutectic temperature in the Fe-C system. Importantly, this indicates that the composition of developing liquid phase is close to the eutectic and therefore carbon rich. This means that liquid phase in WC-FeCr system (even in materials without extra carbon) resembles more

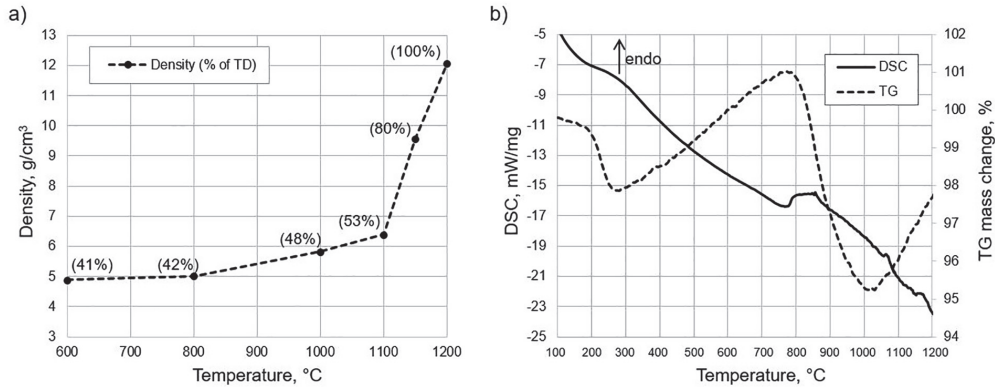


Fig. 1. Density change during sintering in vacuum (a) and results of thermal analysis in Ar flow (b) of the WC-FeCr cemented carbide grade W0.

cast iron, rather than steel. Sintering temperature of 1200 °C is considerably lower as compared to WC-Co where even compositions with a high volume fraction of the binder require temperatures above 1350 °C.

During sintering two noticeable mass losses occur: ~2% mass loss between 200 and 250 °C corresponds to the removal of the paraffin wax and ~5% between 800 and 1000 °C is the result of reduction of oxides and thereby the removal of carbon in form of carbon oxides. Exhibited mass gains are the results of nitrogen pick-up from DSC equipment.

3.2. Microstructure and elemental distribution

3.2.1. Microstructure

The SEM images of the WC-FeCr composite without added C (W0) sintered to near full density at the temperatures 1200 °C and 1300 °C are depicted in Fig. 2. Three different magnifications are presented for better overview of the morphology of the microstructure. Visually, three phases are discernible in the backscatter SEM images: light grey – (ultra)fine WC grains, medium grey – η -phase, and dark grey – binder

phase. Phase distribution and microstructure morphology of WC-FeCr cemented carbides are drastically different from those of well-known WC-Co. Instead of homogeneous distribution of WC particles in the metallic binder matrix, the microstructure of cemented carbides with ferritic chromium steel AISI430L-based binder has distinct areas of dissimilar phase distribution.

Common and generally considered as harmful inclusion, η -phase, is also present in the WC-FeCr grade W0 (Fig. 2). With elemental EDS analysis, it was determined that the η -phase is of M_6C type with the composition of (Fe, W, Cr)₆C where Fe:W:Cr ratio is close to 5:5:1.

Sintering temperature has marked effect on the microstructure and morphology of phases. When composite grade W0 is sintered at higher temperature, solubility of carbides in liquid phase increase and more liquid phase is formed, therefore the Cr-Fe carbide rich binder pools in resulting microstructure are less distinct while on the other hand η -phase regions become more defined, larger and equiaxed (see Fig. 2 e and f).

Fig. 3 exhibits the SEM images of WC-FeCr grades with different

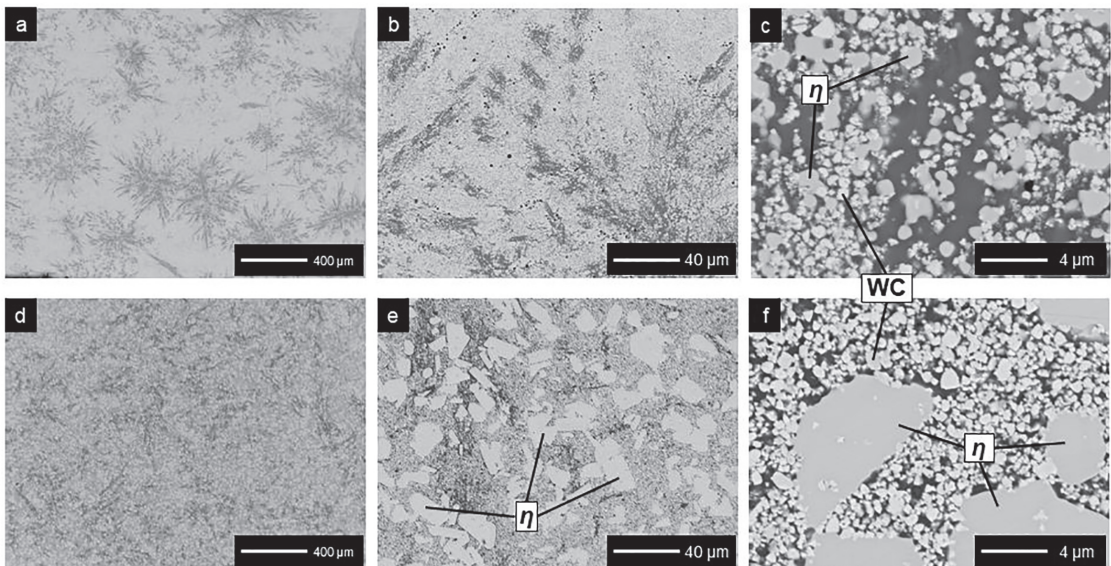


Fig. 2. SEM images of the microstructure of the WC-FeCr cemented carbide grade W0 sintered at 1200 °C (a, b, c) and 1300 °C (d, e, f).

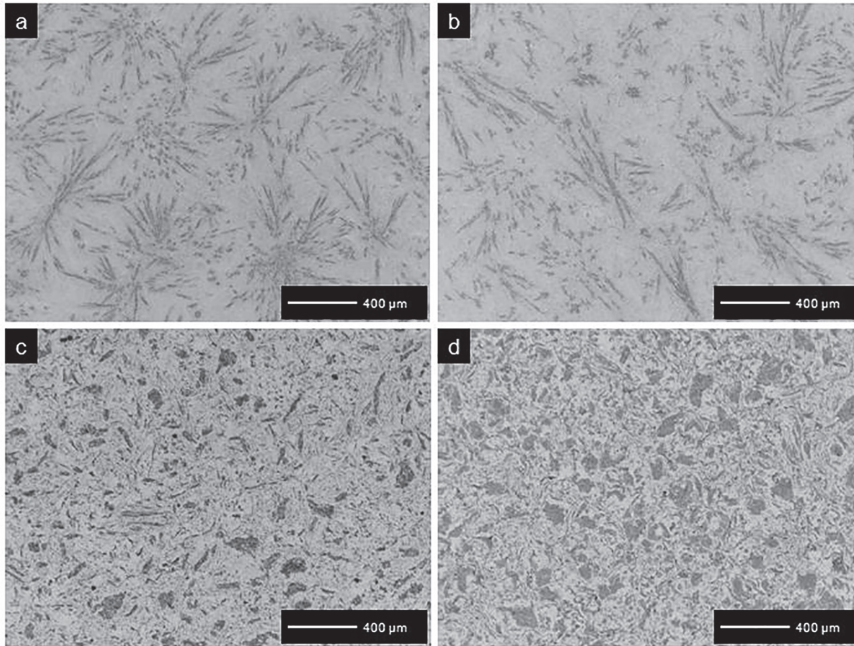


Fig. 3. SEM images of the microstructures of the WC-FeCr cemented carbide grades with added carbon sintered at 1200 °C: a) W1, b) W1.5, c) W2, d) W2.4.

carbon additions. The microstructure and morphology of binder pools change with the increase of carbon additions. Grades with lower added C content W1 and W1.5 (Fig. 3 a, b) resemble grade W0 (Fig. 2 a) exhibiting rather elongated binder pools whereas higher carbon content yields more circular binder rich areas.

3.2.2. Elemental distribution

Large elongated and often needle shaped binder pools are present in the structure and EDS line scan (Fig. 4) reveals that in these regions Cr concentration is increased. In addition, also carbon content in said areas appears to be high. Strong Cr and Fe and somewhat increased C signals indicate the presence of mixed Cr- and Fe-based carbides. TEM image with respective W, C, Fe and Cr elemental mappings (Fig. 5) demonstrate distribution of elements in highly heterogeneous microstructure of the WC-FeCr. In the Fe-Cr-C system ($\text{Cr} > 5 \text{ wt}\%$), where Cr is strongest carbide former, usually Cr-based carbides (Cr_7C_3 and $(\text{Cr}, \text{Fe})_{23}\text{C}_6$ or $(\text{Fe}, \text{Cr})_3\text{C}$ cementite) are formed. The different equilibria dependent on temperature and carbon content between mixed carbides and Fe-based solid solutions ($\alpha\text{-Fe}$ or $\gamma\text{-Fe}$) are presented in phase

diagram (Fig. 6 a). In addition, the C-Cr-W system (Fig. 6 b) exhibits the presence of the $(\text{Cr}, \text{W})_2\text{C}$ besides tungsten mono carbide and Cr-based carbides. In the thermodynamic research of quaternary C-Cr-Fe-W system it is suggested that of the chromium carbide-based phases M_{23}C_6 carbide is more stable than M_7C_3 and solubility of Fe in the M_{23}C_6 can be up to 75% or even higher. Concerning W solubility in M_{23}C_6 the results of different authors vary from 3.8 up to 20 wt% [24].

EDS mappings of grades W1 and W2.4 (Fig. 7) show the difference of Cr and Fe distribution in alloys with different carbon addition. The overlap of Fe and Cr signals in the grade W1 (Fig. 7 a) is virtually non-existent while in the material W2.4 (Fig. 7 b) the elemental signals of Fe and Cr overlap almost completely. This suggests that elemental distribution of Fe and Cr in materials with high carbon content is more homogeneous indicating that the formation $(\text{Cr}, \text{Fe})_x\text{C}_y$ phase could be retarded. The visible fraction of the M_6C (η -phase) decreases when extra carbon is added to the powder mixture. Grades with additional carbon content of 1.5 wt% and higher (W1.5, W2 and W2.4) exhibit marginal fraction of the η -phase grains in the microstructure.

Fig. 8 exhibits the microstructure of WC-FeCr cemented carbide

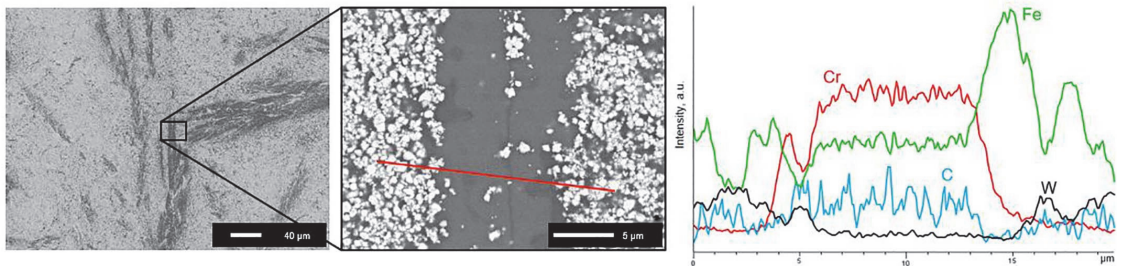


Fig. 4. EDS line scan of binder pool in the material W0 sintered at 1200 °C. The signal of carbon is amplified since it is otherwise relatively low compared with metals (metal \rightarrow y; carbon \rightarrow y^2).

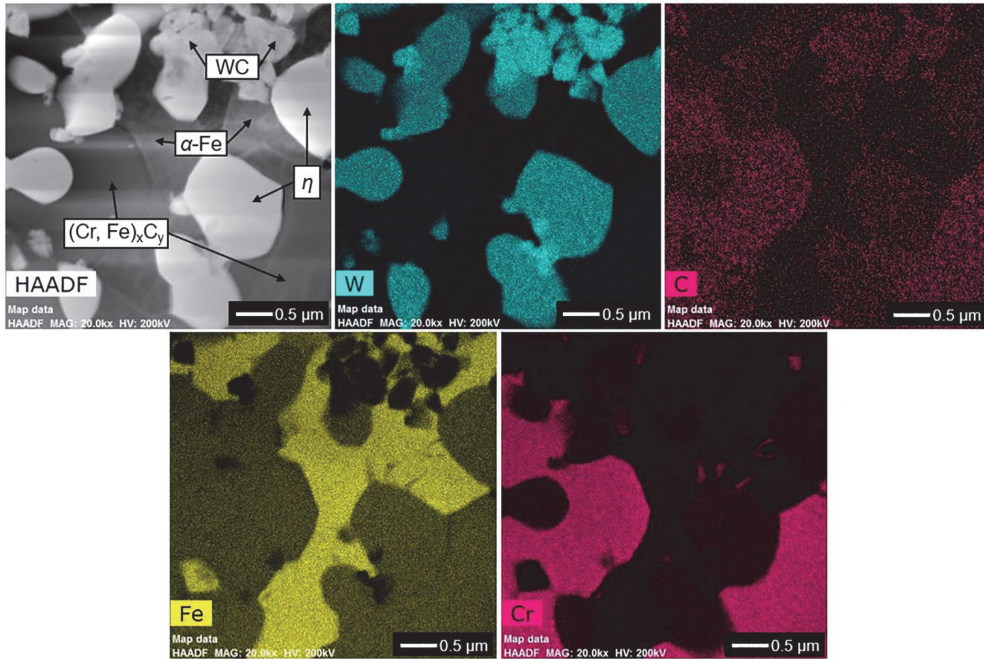


Fig. 5. TEM image of the microstructure and corresponding elemental maps of the WC-FeCr cemented carbide grade W0 sintered at 1200 °C.

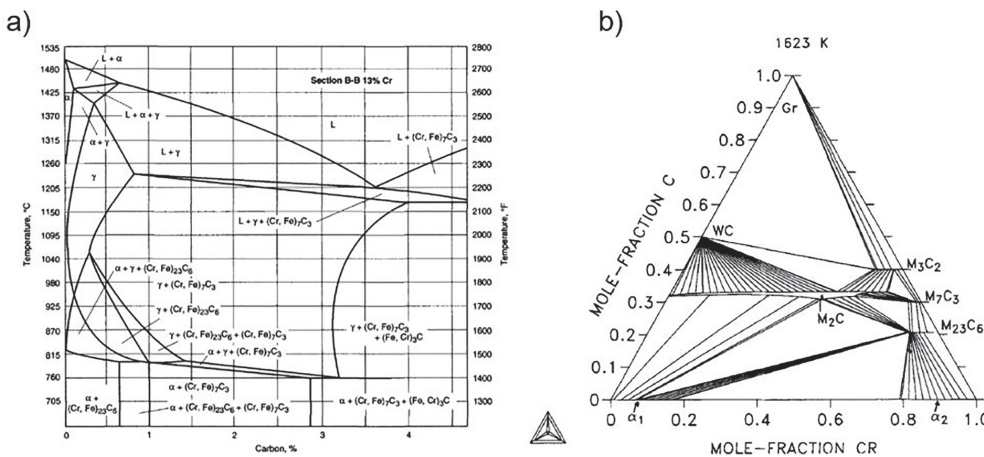


Fig. 6. Vertical section of the Fe-C-Cr system at 13% Cr (a) [25] and calculated isothermal section of the C-Cr-W system at 1350 °C (b) [24].

with 1.5% extra carbon before and after etching with common steel etchant (Nital) and common cemented carbide etchant (Murakami). Nitric acid solution (Nital) attacks α -Fe binder phase between ultrafine WC particles and in $(Cr, Fe)_x C_y$ rich binder pools. From etched surface it is evident that remaining α -Fe fraction in final microstructure is relatively low, especially considering the high steel percentage in initial powder. Etching with Murakami solution reveals large grains of $(Cr, Fe)_x C_y$ carbides forming during liquid phase sintering, contrasting with ultrafine WC grains.

3.3. Phase composition

XRD patterns of the WC-FeCr cemented carbides after sintering at 600–1300 °C are presented in Fig. 9. α -Fe in the current diffractograms should be considered as Fe-Cr solid solution. The M_6C η -phase and Cr-based mixed carbide with lowest possible carbon content $(Cr, Fe)_{23}C_6$ starts to form in the temperature range of 600–800 °C. It is necessary to emphasize, that according to our research, prevalently carbides with enhanced carbon content ($(Cr, Fe)_7C_3$) are formed during sintering of TiC-FeCr cermet at temperatures below 1200 °C. Formation of additional carbide phases in said temperature region is possible since oxide

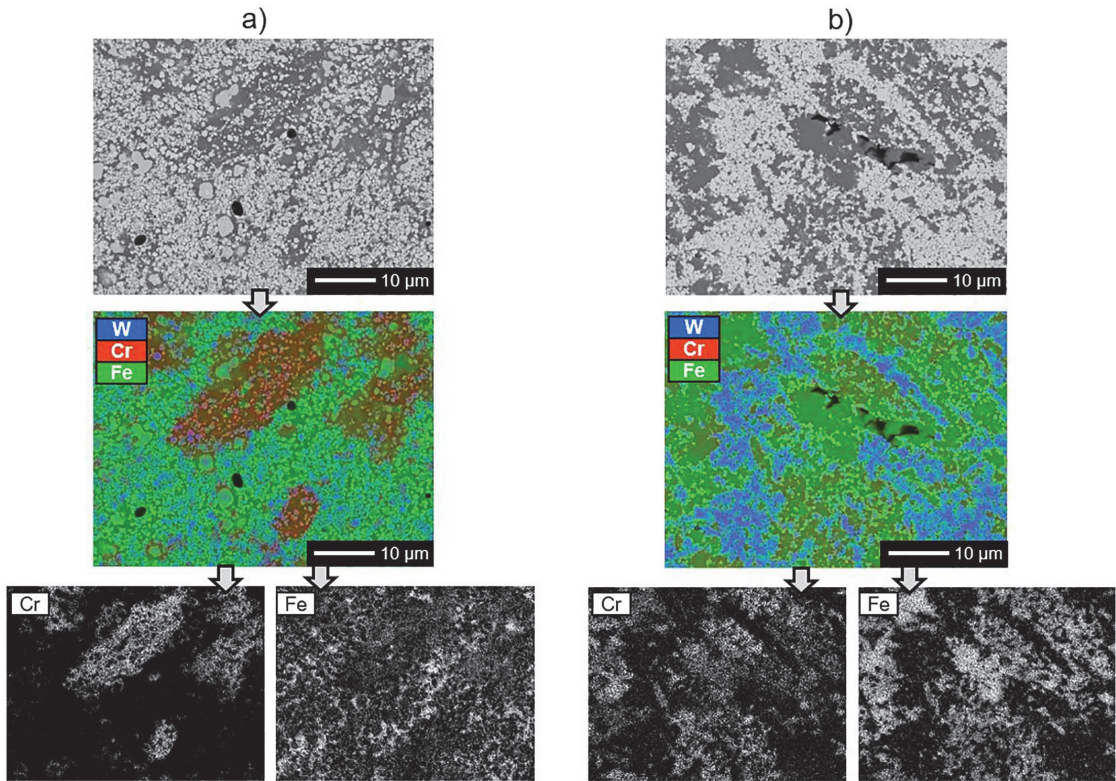


Fig. 7. SEM images of the microstructures and respective EDS mappings of the WC-FeCr cemented carbide grades sintered at 1200 °C with different carbon content: a) W1, b) W2.4.

reduction starts before 800 °C (see TG and DSC signal in Fig. 1) and following reaction can take place: metal oxide + C → metal carbide + carbon oxides. Also, transformation of α -Fe → γ -Fe in C rich Cr-Fe-C system takes place around 800 °C (Fig. 6 a). However, DSC signal does not yield distinct peaks since many processes occur simultaneously and in this, relatively complicated system, phase changes need prolonged time to complete. Changes in DSC signal at around 1150 °C can be attributed to the start of formation of liquid phase.

Initially, W0 is composed of WC and steel powder and carbon content in the latter is marginal, below 0.03 wt%. Therefore, the formation of (Cr, Fe)₂₃C₆ carbide can be possible only when carbon is acquired from WC accompanied by the formation of the η -phase. All phase changes before liquid phase formation are the result of solid-state diffusion and enabled by chromium high affinity for carbon. The fraction of (Cr, Fe)₂₃C₆ carbide in cemented carbide grade W0 decreases when specimens undergo liquid phase sintering at 1200 and 1300 °C (Fig. 9). Thus, it is evident that (Cr, Fe)₂₃C₆ carbide either completely or partially dissolves in liquid phase and after cooling the fraction of this carbide reduces markedly.

Fig. 10 depicts XRD diffractograms of WC cemented carbide grades with different added carbon contents. As expected, the increase of carbon retards the formation of the η -phase since carbon deficiency of WC is avoided. Interestingly (Cr, Fe)₂₃C₆ carbide peaks disappear as well. At 1.5 wt% of added C (material W1.5) prevalently only two phases, WC and α -Fe, yield distinctive peaks in the XRD diffractograms. Only somewhat weak and scattered signal indicated the presence of M_xC carbides, either Fe₃C, Fe₂C or W₂C, in materials with added C content of 1.5 wt% and over (W1.5, W2 and W2.4). Although iron is a weaker carbide former when compared with W and Cr, the presence of

iron carbides at higher carbon contents is quite plausible. Of iron carbides, Fe₃C cementite is most stable, especially at higher temperatures [26] and therefore the weak Fe_xC signal can be attributed to the former. Since Cr and Fe are mutually soluble, Fe-based M_xC carbides can be considered as (Fe, Cr)_xC carbides and large binder pools in grades W1.5, W2 and W2.4 compose of metallic binder and Fe-based carbides, instead of (Cr, Fe)₂₃C₆ carbides that are present in grades with lower carbon content (W0 and W1).

3.4. Mechanical properties

Vickers hardness tests were performed on all cemented carbides with the steel binder. Average hardness of all materials ranged from 1150 to 1400 HV₃₀; however, the standard deviation of results was pronounced (up to ± 90). The high deviation of hardness values is induced by irregular distribution of phases in the microstructure. Fig. 11 presents optical microscope images of hardness and microhardness indentations of the grade W1.5 where the effect of the microstructure on the hardness is evident. The area marked with a dashed circle (Fig. 11 b) is so called Cr-rich binder pool. Higher hardness of the Cr-rich phase confirms the assumption that carbide phase(s) are indeed present. The material with 2% additional carbon (W2), characterised with more homogeneous microstructure (Fig. 6 c), yielded stable results.

Indentation fracture toughness of cemented carbides with a steel binder was measured. It turned out problematic since often multiple cracks emanated from the tip of the indentation corner (Fig. 11 a). Material W2 with more homogeneous microstructure yielded constantly indentations with four measurable cracks and we were able to characterise its fracture toughness. Fig. 12 compares hardness and

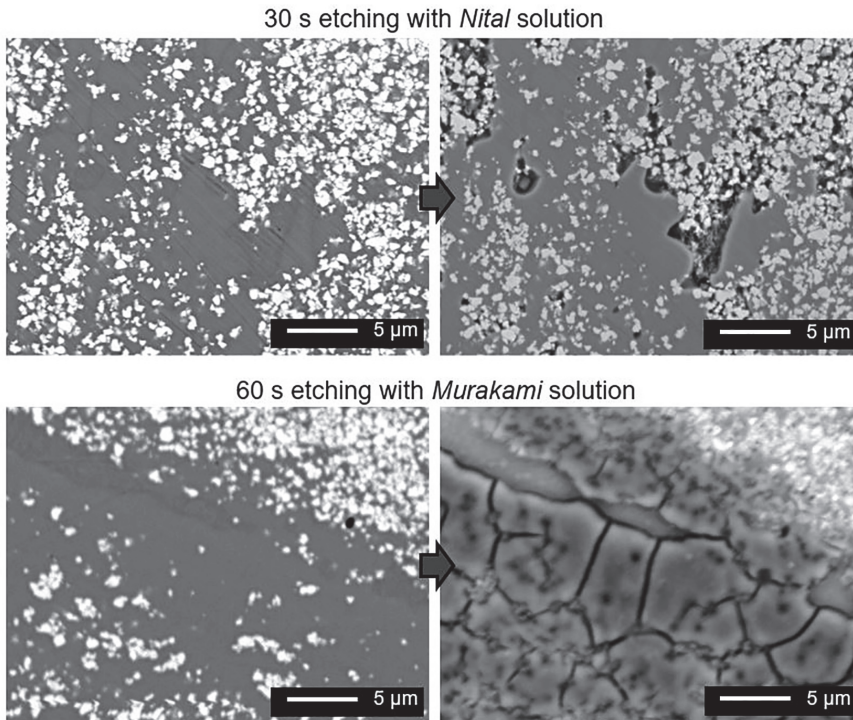


Fig. 8. SEM images of the microstructure of the WC-FeCr cemented carbide grade W1.5 sintered at 1300 °C before and after etching with Nital solution (top) and Murakami solution (bottom).

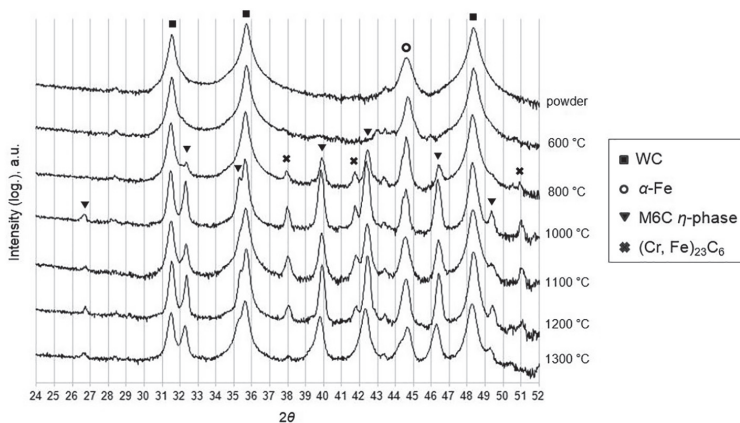


Fig. 9. XRD diffractograms of the WC-FeCr cemented carbide grade without extra carbon (W0) sintered at different temperatures.

toughness of material W2 with WC-Co and WC-FeNi(Cr) properties acquired from literature [9,23]. Although calculated steel fraction of grade W2 is close to 30 wt%, the phase transformations yield cemented carbide with mechanical properties comparable with fine grained WC-Co with considerably lower binder fraction.

4. Conclusions

WC-FeCr cemented carbides with a high volume fraction of ferritic

chromium steel AISI430L were prepared to analyze the influence of sintering temperature and extra carbon addition on the phase composition and microstructure formation. Microstructure analysis (OM, SEM and TEM), X-ray spectroscopy (EDS), scanning differential calorimetry (DSC) and X-ray diffraction (XRD) resulted in the following conclusions:

- Near full density of WC-FeCr cemented carbides was achieved already at the relatively low sintering temperature of 1200 °C. Liquid phase is formed in the range of 1100...1200 °C, which is in

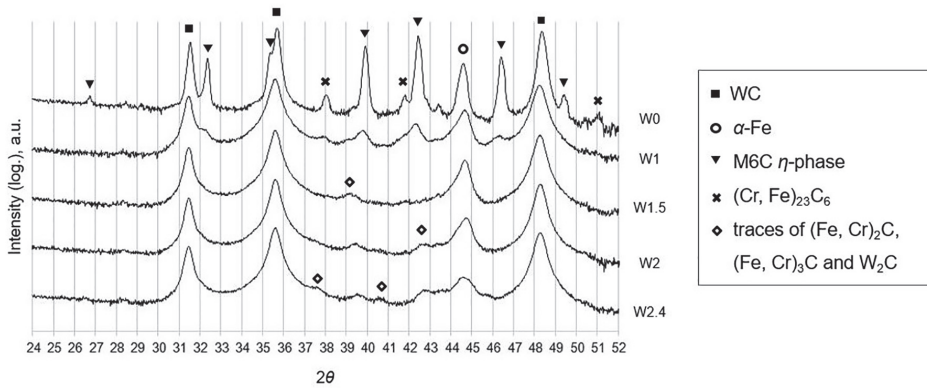


Fig. 10. XRD diffractograms of the WC-FeCr cemented carbide grades with and without extra carbon sintered at 1200 °C.

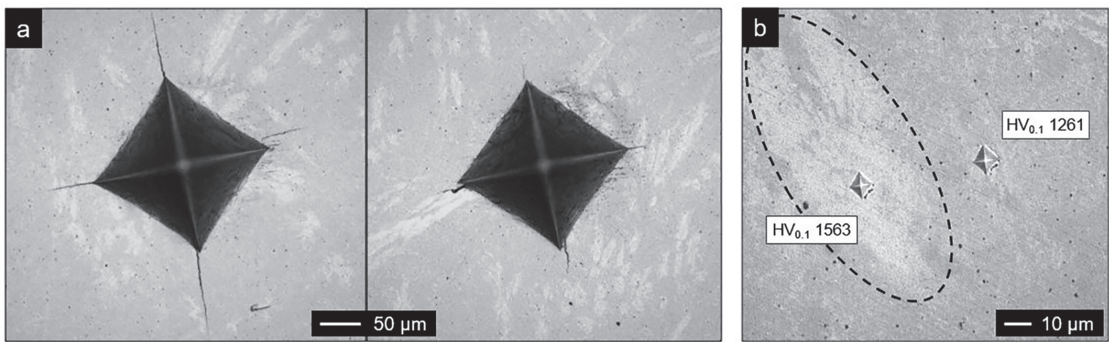


Fig. 11. Optical microscope images of Vickers indentations on the WC-FeCr cemented carbide grade W1.5 after test with 30 kgf (a). Difference in emanating crack length results from highly heterogeneous microstructure. Indentations with 0.1 kgf on harder Cr-rich binder pool compared with Cr-poor area (b).

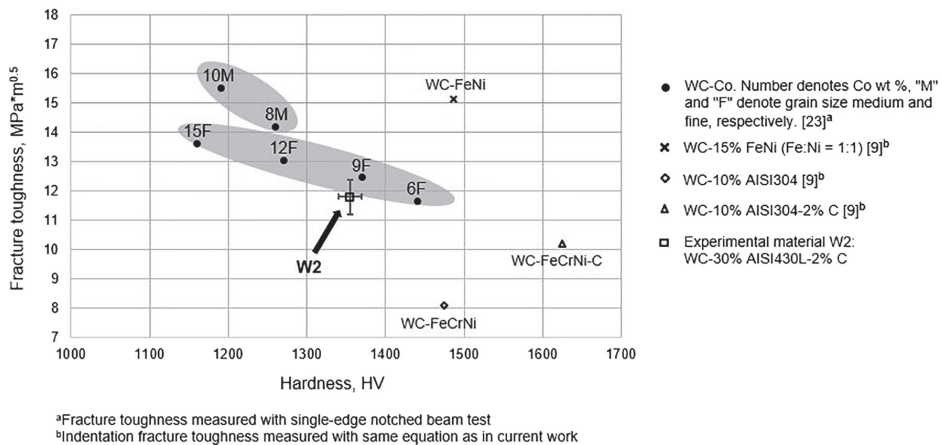


Fig. 12. Hardness and indentation fracture toughness of the WC-FeCr cemented carbide with 2 wt% carbon addition (W2) compared with various WC-Co grades and cemented carbides with Fe-based binder.

agreement with the eutectic temperature in the W-C-Fe system (1143 °C).

- The microstructure of WC-FeCr cemented carbides is dependent on the carbon content and is heterogeneous - WC + binder areas are

interrupted by binder pools. The shape of binder pools change from elongated to more circular ones when increasing carbon addition in alloys.

- In the temperature range of 600–800 °C following processes start:

reduction of oxides, formation of M_6C type η -phase and Cr-based $(Cr, Fe)_{23}C_6$ mixed carbide. η -Phase is present in final microstructure of WC-FeCr without or low extra carbon and is relatively homogeneously dispersed. Addition of extra carbon to the powder mixture retards both η -phase and $(Cr, Fe)_{23}C_6$ formation.

- Binder composed prevalently of Cr-Fe mixed carbides surrounded by α -Fe binder. When overall carbon content is increased $(Cr, Fe)_{23}C_6$ carbides are substituted by Fe-based $(Fe, Cr)_x C$ ones.
- Carbon additions of about 2 wt% in WC-30% FeCr cemented carbides retarding η -phase formation favors homogeneity of microstructure and enhancement of mechanical characteristics (fracture toughness).

It is evident that achieving homogeneous microstructure of the WC-FeCr cemented carbides, in particular corrosion and oxidation resistant ones, is a challenge and requires further research for attainment of improved structural homogeneity and mechanical properties.

Acknowledgements

This work was supported by institutional research fundings IUT (19-29) and IUT (19-4) of the Estonian Ministry of Education and Research and by the European Regional Development Fund project TK141 “Advanced materials and high-technology devices for energy recuperation systems”.

References

- [1] USGS scientific investigations report 2012–5188: metal prices in the United States through 2010, <https://pubs.usgs.gov/sir/2012/5188/>, Accessed date: 30 March 2017(n.d.).
- [2] REACH - Chemicals - Environment - European Commission, http://ec.europa.eu/environment/chemicals/reach/reach_en.htm, Accessed date: 30 March 2017(n.d.).
- [3] Home - National Toxicology Program, <https://ntp.niehs.nih.gov/>, Accessed date: 30 March 2017(n.d.).
- [4] S. Norgren, J. Garcia, A. Blomqvist, L. Yin, Trends in the P/M hard metal industry, *Int. J. Refract. Met. Hard Mater.* 48 (2015) 31–45.
- [5] S. Takeda, A metallographic study of the action of the cementing materials for cemented tungsten carbide, 864 (1936).
- [6] P. Schwarzkopf, R. Kieffer, Cemented Carbides, Collier Macmillan Ltd (1960).
- [7] C. Agte, Die neue Hochleistungshartmetallsorte S6HL, *Neue Hütte* 1 (1956) 333.
- [8] C. Agte, Entwicklung der Hartmetalltechnik während der letzten Jahre in der Deutschen Demokratischen Republik, *Neue Hütte* 2 (1957) 537–544.
- [9] O.J. Ojo-Kupoluyi, S.M. Tahir, B.T.H.T. Baharudin, M.A.A. Hanim, M.S. Anuar, Mechanical properties of WC-based hardmetals bonded with iron alloys – a review, *Mater. Sci. Technol.* 33 (2017) 507–517.
- [10] A.F. Guillermet, Use of phase diagram calculations in selecting the composition of Fe-Ni bonded WC tools, *Int. J. Refract. Met. Hard Mater.* 6 (1987) 24–27.
- [11] A.F. Guillermet, An assessment of the Fe-Ni-W-C phase diagram, *Z. Met.* 78 (1987) 165–171.
- [12] A.F. Guillermet, The Co-Fe-Ni-W-C phase diagram: a thermodynamic description and calculated sections for (Co-Fe-Ni)-bonded cemented WC tools, *Z. Met.* 80 (1989) 83–94.
- [13] W.D. Schubert, M. Fugger, B. Wittmann, R. Useldinger, Aspects of sintering of cemented carbides with Fe-based binders, *Int. J. Refract. Met. Hard Mater.* 49 (2015) 110–123.
- [14] L. Prakash, G. Benno, WC hardmetals with iron based binders, *Proc. 17th Plansee Semin.* 2, 2009.
- [15] B. Wittmann, W.-D. Schubert, B. Lux, WC grain growth and grain growth inhibition in nickel and iron binder hardmetals, *Int. J. Refract. Met. Hard Mater.* 20 (2002) 51–60.
- [16] C.M. Fernandes, A.M.R. Senos, M.T. Vieira, Sintering of tungsten carbide particles sputter-deposited with stainless steel, *Int. J. Refract. Met. Hard Mater.* 21 (2003) 147–154.
- [17] K. Kambakas, P. Tsakiroopoulos, Solidification of high-Cr white cast iron–WC particle reinforced composites, *Mater. Sci. Eng. A* 413–414 (2005) 538–544.
- [18] S. Sakaguchi, S. Imasato, H. Ito, R. Nakamura, Some properties of sintered WC-(Fe-Cr-C) alloys, *J. Jpn. Soc. Powder Powder Metall.* 36 (1989) 908–912.
- [19] C.M. Fernandes, A.M.R. Senos, Cemented carbide phase diagrams: a review, *Int. J. Refract. Met. Hard Mater.* 29 (2011) 405–418.
- [20] H. Palmour, *Sintering '85*, Springer Science & Business Media, 2012, pp. 383–384.
- [21] M. Tarraste, K. Juhani, J. Kübarsepp, J. Pirso, V. Mikli, The effect of Cr and C on the characteristics of WC-FeCr hardmetals, *Proceedings of Euro PM2015*, 2015.
- [22] M. Tarraste, J. Kübarsepp, K. Juhani, T. Suurkivi, J. Pirso, Spark plasma sintering of WC hardmetals with Fe-based binder, *Proceedings of World PM2016*, 2016.
- [23] R. Spiegler, S. Schmauder, L.S. Sigl, Fracture toughness evaluation of WC-Co alloys by indentation testing, *J. Hard. Mater.* 1 (1990) 147–158.
- [24] P. Gustafson, A thermodynamic evaluation of the c-cr-fe-w system, *Metall. Trans. A* 19 (1988) 2547–2554.
- [25] G.A. Roberts, R. Kennedy, G. Krauss, *Tool Steels*, 5th edition, ASM International, 1998, p. 63.
- [26] C.M. Fang, M.A. van Huis, H.W. Zandbergen, Structure and stability of Fe₂C phases from density-functional theory calculations, *Scr. Mater.* 63 (2010) 418–421.

PAPER III

M. Tarraste, J. Kübarsepp, K. Juhani, T. Suurkivi, J. Pirso, Spark plasma sintering of WC hardmetals with Fe-based binder, *Proceedings of World PM2016*. (2016).

Manuscript refereed by Dr Elena Gordo (Madrid University Carlos III)

Spark Plasma Sintering of WC Hardmetals with Fe-based Binder

Marek Tarraste (Tallinn University of Technology, Ehitajate tee 5, 19086 Tallinn, Estonia) marek.tarraste@ttu.ee; Jakob Kübarsepp (Tallinn University of Technology, Ehitajate tee 5, 19086 Tallinn, Estonia) jakob.kubarsepp@ttu.ee; Kristjan Juhani (Tallinn University of Technology, Ehitajate tee 5, 19086 Tallinn, Estonia) kristjan.juhani@ttu.ee; Taavi suurkivi (Tallinn University of Technology, Ehitajate tee 5, 19086 Tallinn, Estonia) taavi.suurkivi@ttu.ee; Jüri Pirso (Tallinn University of Technology, Ehitajate tee 5, 19086 Tallinn, Estonia) juri.pirso@ttu.ee

Abstract

Fe-based binder systems can be an alternative to the well-known binder metal cobalt. Fe as a binder in WC-based hardmetals acts as a carbide grain growth inhibitor. This effect coupled with the fast SPS sintering regime retards greatly the growth of WC grain during sintering. In this work SPS technology was used in the production of WC-Fe and WC-FeCr hardmetals. Powder mixtures were prepared by conventional ball-milling. The effect of temperature as well as pressure during the SPS process was investigated. WC-Co hardmetal was used as reference. Also SPS was compared against liquid phase sintering. Prepared materials were characterized in terms of microstructure and phase composition as well as mechanical properties.

1. Introduction

Tungsten carbide (WC) hardmetals are powder metallurgical composite materials where hard and wear resistant tungsten carbide phase is embedded in the softer and ductile metallic phase from the iron group of metals (Co, Ni, Fe). Metal acts as a binder phase for carbide grains. Cobalt is the most favored choice as a binder due to its very good wetting with WC, notable solubility of WC in cobalt and excellent strength and ductility of WC-Co composites [1-3]. The applications of WC-Co include machining tools for metallic and nonmetallic materials, chipless forming tools, mining tools, various wear parts etc. [4].

The motivation to find alternatives to cobalt was initially triggered by its high price coupled with limited availability [5] and later by its toxicity [6]. Nickel is often used as a total or partial substitute to Co in applications where corrosion or oxidation resistance is important [1, 7]. Like Co, Ni is cancerogenic and declared as a health hazard for humans [8]. The possibility to employ Fe as an alternative to Co was elaborated as early as in the 1930's, yet it was concluded that in an iron system it is difficult to avoid the formation of the brittle η -phase (M₆C) during sintering [9]. In 1956 Agte suggested that a desired two phase microstructure in the W-Fe-C system can be achieved through precise carbon control [10]. In the last decades of the 20th century worldwide research to find suitable Fe-based alloys as alternative binders was intensified. Alloy systems like Fe-Co-Ni, Fe-Ni, Ni-Cr and Fe-Ni-Cr have been studied [11-13]. Ni and Co free non-toxic binders have also been investigated to some degree. Hardmetals bonded with Fe-Mn alloy have shown similar characteristics to WC-Co [14] and Fe-Cr binder systems have been used in niche applications e.g. hardmetal coatings on a steel substrate [15]. The authors of this work have elaborated on the effect of Cr and C content on the WC-15FeCr hardmetals [16]. Ferro-chromium binder has found more extensive use in TiC-based cermets [17, 18]. Iron as a binder metal acts also as an efficient grain growth inhibitor when compared to Ni or Co [19].

Hardmetal powders are consolidated into near net shape products traditionally by mechanical or isostatic pressing, followed by solid state and liquid phase sintering (LPS) [3]. During LPS, the temperature exceeds the eutectic temperature of the W-C-M (M = binder metal or alloy) system and a liquid melt of binder is formed. Rapid densification at the beginning of LPS is caused by rearrangement of particles by the capillarity force [20]. Carbide grain growth – microstructure coarsening (Oswald ripening) while the liquid melt is present is an important phenomenon [21]. By retaining a finer microstructure, the mechanical properties such as hardness and transverse rupture strength as well as wear resistance can be increased [3]. Spark plasma sintering (SPS) is a powerful consolidation method to acquire WC hardmetals with ultrafine and near-nano microstructure. SPS employs very high heating rates coupled with external pressure to consolidate powders in a short time and at low temperatures. Temperatures of the powder compact do not exceed the eutectic temperature, instead, electrical discharge generates sparks between particles, which in turn, leads to localized melting and

World PM2016 – HM – Alternative Binders

formation of necks between contacting powders [22]. Therefore, carbide grain growth is greatly retarded.

The aim of this work is to examine the effect of spark plasma sintering parameters on the densification, mechanical and microstructure characteristics of WC-Fe hardmetals. Furthermore, SPS was used to compare prepared WC-Fe and WC-FeCr with traditional WC-Co and liquid phase sintered counterparts. The carbon pick-up from the surrounding graphite mold during SPS is also addressed.

2. Experimental

Hardmetal powder mixtures with different binders were prepared by the conventional ball milling technique: tungsten carbide (WC0.9 μ m - Wolframite) and binder metal powders were milled in a ball mill with hardmetal lining and balls for 72h with the ball to powder weight ratio of 10:1. Isopropyl alcohol was used as a milling liquid. Iron powder HP1001 from ATOMET with a particle size of 20-45 μ m and cobalt powder from PPM Ltd. with a particle size of 5-6 μ m were used to preparing WC-Fe and WC-Co compositions, respectively. For the FeCr binder system, the ferritic chromium-steel powder (10-45 μ m) grade AISI430L was employed. Calculated chemical composition of the prepared hardmetals and detailed composition of AISI430L steel are presented in Table 1.

Table 1. Chemical composition and theoretical density of prepared hardmetals.

Material	WC		Binder		Binder composition, wt%				
	wt%	vol%	wt%	vol%	Co	Fe	Cr	Mn	Si
WC-Fe	85	74.1	15	25.9	–	100	–	–	–
WC-S*	85	73.9	15	26.1	–	81.83	16.8	0.69	0.64
WC-Co	85	76.4	15	23.6	100	–	–	–	–

*WC-S is a hardmetal with AISI430L ferritic steel binder.

Milled powders were dried at 50 °C and stored at glovebox (N₂ gas) for SPS. For LPS, dried powders were mixed with 3 wt% paraffin and compacted into green bodies with 95 MPa of uniaxial pressure. For consolidation of the powders via the SPS method, the furnace HPD 10-GB from FCT Systeme GmbH was used. The powders were placed in graphite die between two graphite punches. Pulsating current and uniaxial pressure were applied simultaneously. Vacuum level in the sintering chamber was kept around 2 mbar. The temperature was measured from the hole inside the top graphite punch using a pyrometer. The effect of temperature and pressure on the densification and properties of WC-Fe was investigated. The temperature ramp speed and the dwell time at end temperature were kept the same, 100 °C/min and 5 min, respectively. The combination of 1200 °C and 50 MPa (regime 4) yielded optimal results and materials with steel and Co binder were prepared using the same parameters (see Table 2). Figure 1 exhibits an example of the SPS regime with a relative piston movement due to shrinkage.

Table 2. SPS regimes and properties of prepared hardmetals.

Material	Regime	Temperature, °C	Uniaxial pressure, MPa	Porosity, %	Hardness, HV ₃₀	Fracture toughness, MPa·m ^{1/2}
WC-Fe	R1	1100	10	31.0	228	5.2
	R2	1100	50	0.3	1229	7.5
	R3	1200	10	1.4	720	8.3
	R4	1200	50	< 0.1	1469	9.3
	R5	1300	10	< 0.1	1607	7.4
	R6	1300	50	1.7	1468	8.3
WC-S	R4	1200	50	0.4	1651	8.3
WC-Co	R4	1200	50	0.2	1489	10.4

Table 3. LPS regime and properties of prepared hardmetals.

Material	Temperature, °C	Ar isostatic pressure, MPa	Porosity, %	Hardness, HV ₃₀	Fracture toughness, MPa·m ^{1/2}
WC-Fe	1450	3	< 0.1	1645	6.6
WC-S			0.1	2016	4.2
WC-Co			0.1	1274	14.9

Liquid phase sintering was carried out in a sinter-HIP furnace FPW 300/400 from FCT Systeme GmbH. Pressed samples were placed on zirconia support in graphite crucibles. Heating rate was 10 °C/min and 30 min dwell at the end temperature, 1450 °C, followed by natural cooling was employed. 3 MPa Ar pressure was applied at the end temperature during the last 15 min of dwelling.

Both SPS and LPS samples were cut in half and cast into polymer. Cross-sections of sintered parts were ground and polished. The porosity of hardmetals was determined by using an optical microscope Axiovert 25 and software Buehler Omnimet. A Zeiss Ultra 55 FEG-SEM scanning electron microscope (SEM) was used for microstructure observation and phase identification. Vickers hardness was measured with Indetec 5030 KV and microhardness was measured with Micromet 2001. The fracture toughness (K_{Ic}) was determined by measuring the crack length from the tip of the indentation made by Vickers indentation (Palmqvist method) and calculated by the following equation [23]:

$$K_{Ic} = 0.0726 \frac{P}{C^{3/2}},$$

where P is the load of Vickers indenter (N) and C is half of the diagonal + crack length (mm).

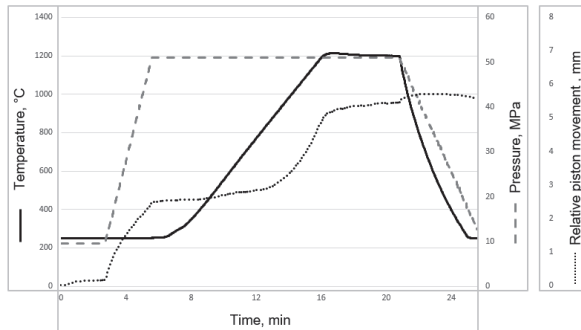


Figure 1. Optimal SPS regime (R4) for preparing WC-Fe.

3. Results and discussion

3.1. Densification

One of the main goals was to examine the effect of SPS parameters on the characteristics of WC-Fe hardmetals. The densification was determined by the residual porosity of the sintered samples. The best results were obtained with regimes R4 (1200 °C; 50 MPa) and R5 (1300 °C, 10 MPa). The lowest temperature, 1100 °C, and high mechanical pressure gave also an almost satisfactory result in terms of porosity – 0.3%. It might be possible to achieve comparable porosity with regimes R4 and R5 at 1100 °C when even higher pressures are used. Unfortunately for the graphite dies used in this research, the 50 MPa pressure was a limit. With 1300 °C and 50 MPa (regime R6), a small amount of material had flown between the punch and the mould, thus damaging the graphite die. SPS regime R4 was chosen to prepare the materials WC-S and WC-Co. The residual porosity of specimens prepared by conventional sintering was satisfactory – 0.1% or less.

3.2. Microstructure

The SEM images of the microstructures of the prepared hardmetals are exhibited in Figures 2-4. Microstructures of hardmetals with Fe and chromium steel binder showed similar characteristics – spark plasma sintered specimens yielded a two-phase structure where WC grains (light phase) were unevenly cemented in the Fe-based metal binder (dark phase); liquid phase sintered specimens exhibited a three-phase structure with WC grains, the Fe-based binder and the η -phase (light gray).

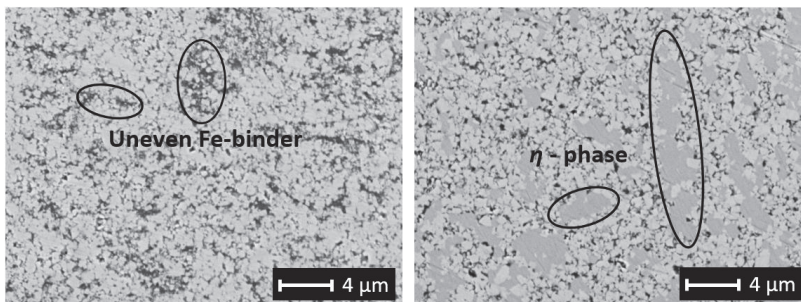


Figure 2. Microstructure of WC-Fe prepared by SPS-R4 (left) and LPS (right).

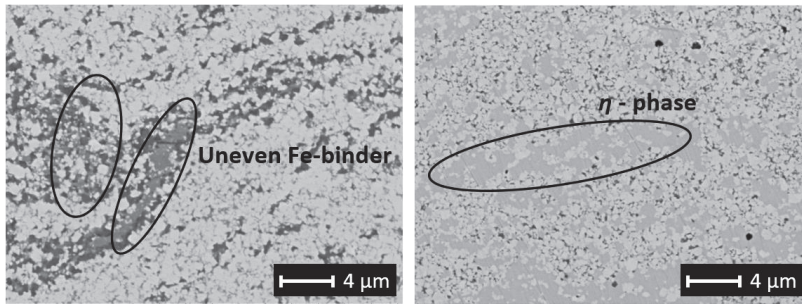


Figure 3. Microstructure of WC-S prepared by SPS-R4 (left) and LPS (right).

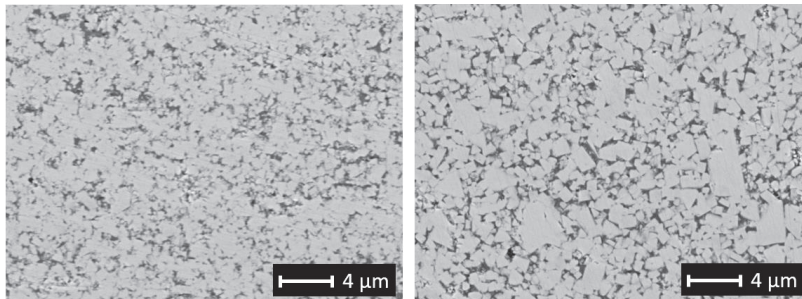


Figure 4. Microstructure of WC-Co prepared by SPS-R4 (left) and LPS (right).

The formation of various hard and brittle η -phases in Fe containing hardmetals during sintering is caused by its thermodynamical stability in W-C-Fe and W-C-Fe-Cr systems [5]. A well-known practice is to introduce extra carbon to increase the carbon level over the stoichiometric level, thereby inhibiting the formation of the η -phase. However, it should be noted that no considerable formation of the η -phase occurred during SPS. It can be attributed to the fact that SPS takes place at lower temperatures and the process is much shorter. The WC-Co hardmetal exhibited even distribution of two phases with both sintering technologies.

The rapid SPS process yields finer grained microstructure than LPS. The most evident difference of the two processes in terms WC grain size is with WC-Co hardmetal. The WC-Fe and WC-S hardmetals exhibit even finer microstructure since Fe and Cr act as grain growth inhibitors.

Noteworthy gradient layers were formed on the surface of WC-Fe during spark plasma sintering (Fig. 5). This layer (~0.7 mm) on the surface of the sintered specimen exhibited more uniform distribution of WC and Fe-binder phases. Since no such formation was noticed in the liquid phase sintered WC-Fe, the formation of this outer layer can be attributed to the carbon pick-up from the graphite die during SPS. This indicates that although the SPS of WC-Fe yielded two-phase structures, extra carbon can contribute to the formation of a more uniform structure. WC-S and WC-Co prepared via SPS did not exhibit difference in microstructure when comparing specimen surface and core.

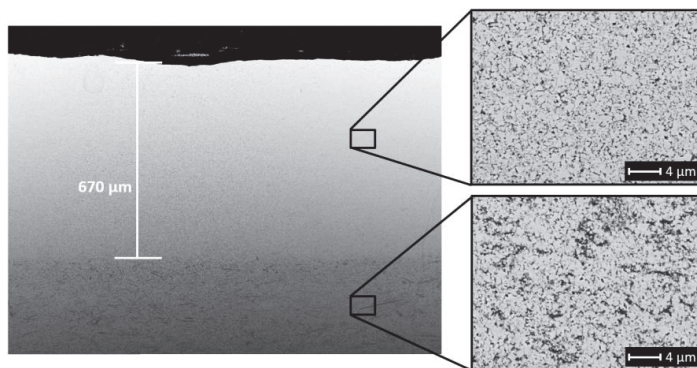


Figure 5. Gradient layer on the surface of SPS'ed WC-Fe.

3.3. Mechanical properties

Hardness and toughness values of the prepared hardmetals are presented in Table 2 and in Figure 6. Materials prepared by a traditional sintering method show clear difference in mechanical properties. WC-Co exhibited lowest hardness and highest indentation fracture toughness values while WC-S showed opposite results: highest hardness and very low toughness. WC-Fe falls in-between of WC-Co and WC-S in terms of properties. It is well known that WC-Co can display unparalleled high toughness values against binder systems without Co. Moreover, the higher toughness of WC-Co can be attributed to the more uniform and coarser grained microstructure (Fig. 4). The materials prepared by the SPS method displayed far more similar hardness and toughness. This is directly connected to the nature of SPS - due to fast sintering cycle various processes, such as formation of brittle the η -phase (WC-Fe and WC-S) and WC grain growth (WC-Co), are diminished.

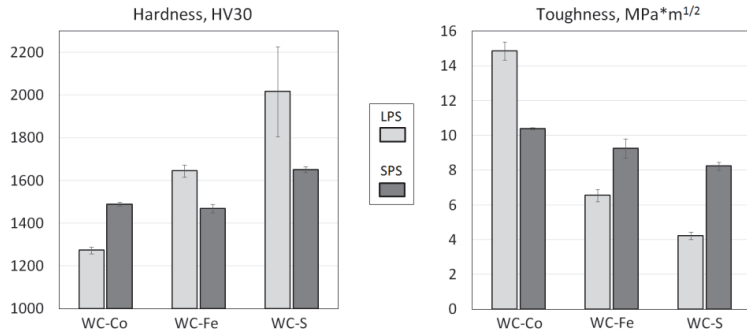


Figure 6. Hardness and indentation fracture toughness of prepared hardmetals.

Figure 7 displays the microhardness of the hardmetals as a function of the distance from the sintered specimen surface. All three hardmetal compositions exhibit higher hardness values near surface when prepared by SPS. The hardmetal with an Fe binder shows the highest discrepancy of hardness measured from the surface and the core. WC-Fe is also the only one that exhibited considerable gradient layer near the surface (Fig. 5).

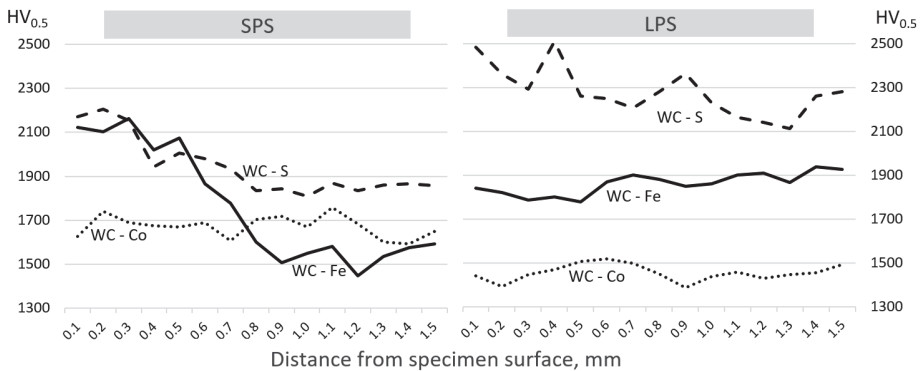


Figure 7. Microhardness of prepared hardmetals dependent on the distance from specimen surface.

4. Conclusions

- WC hardmetals with a Fe, Co and chromium steel (AISI430L) binder were prepared by a traditional liquid phase sintering and fast spark plasma sintering.
- The effect of different SPS regimes on the densification of WC-Fe was investigated. The temperature/pressure combinations of 1200°C/50 MPa and 1300°C/10 MPa yielded materials with the lowest residual porosity, under 0.1%.
- The binder phase distribution of the spark plasma sintered WC-Fe and WC-S is uneven against the LPS counterparts and WC-Co.

World PM2016 – HM – Alternative Binders

- The fast nature of SPS cycle diminishes the formation of hard and brittle η -phase (with a Fe and steel binder) and WC grain growth (with a Co binder). For that reason, the mechanical properties of hardmetals prepared by SPS are more similar when compared with results obtained with LPS.
- During SPS, the gradient layers are formed on the surface of WC-Fe. This layer is around 0.7 mm thick and displays more uniform distribution of phases and higher hardness. Although a two phase structure is achieved without extra carbon, the increase in the carbon content can alter the microstructure of the spark plasma sintered WC-Fe.

Acknowledgments

This work was supported by institutional research funding IUT (19-29) of the Estonian Ministry of Education and Research.

References

- [1] R. Edwards, et al. Proceedings of the Plansee Seminar (1953), p. 232.
- [2] J. Whalen, M. Humenick, Progress in Powder Metallurgy, MPIF (1962), pp. 85-98.
- [3] Comprehensive Hard Materials, Volume 1, Elsevier (2014).
- [4] G. S. Upadhyaya, Cemented Tungsten Carbides: Production, Properties and Testing, Noyes Publications (1998).
- [5] W.D. Schubert, M. Fugger, B. Wittmann, R. Useldinger, Aspects of sintering of cemented carbides with Fe-based binders, Int. Journal of Refractory Metals and Hard Materials, 49 (2015), pp. 110-123.
- [6] D. Lison, R. Lauwerys, The interaction of cobalt metal with different carbides and other mineral particles on mouse peritoneal macrophages, Toxic Vitro, 9(3) (1995), 341-7.
- [7] ASM Handbook, volume 13 Corrosion, ASM International (1987), p. 846.
- [8] ECHA (European Chemicals agency) homepage - substance information: <http://echa.europa.eu/substance-information/-/substanceinfo/100.028.283> (16.04.2016).
- [9] S. Takeda, A Metallographic Study of the Action of the Cementing Materials for Cemented Tungsten Carbide. Sci. Rep. Tohoku Univ., Honda-Festband (1936), 864-61.
- [10] C. Agte, Die neue Hochleistungshartmetallsorte, Neue Hütte 1 (1956), pp. 333-338.
- [11] L. Prakash, H. Holleck, F. Thümmler, P. Walter, Influence of the Binder Composition on the Properties of WC-Fe/Co/Ni Cemented Carbides, Modern Dev. Powder Metall. 14 (1981), pp. 255-268.
- [12] D. Moskovitz, M.J. Ford, M. Humenik. High Strength Tungsten Carbides. Int J Powder Metall, 6(4) (1970), pp. 55-64.
- [13] C.M. Fernandes, L.M.Vilhena, C.M.S. Pinho, F.J. Oliveira, E. Soares, J. Sacramento, A.M.R. Senos, Mechanical Characterization of WC-10wt%AlSi304 Cemented Carbides, Materials Science & Engineering A, 618 (2014) pp. 629-636.
- [14] C. Hanyaloglu, B. Aksakal, J.D. Bolton, Production and Indentation Analysis of WC/Fe-Mn as an Alternative to Cobalt-bonded Hardmetals, Materials Characterization, 47 (2001), pp. 315-322.
- [15] I. Konyashin, D. Hlawatschek, B. Ries, D. Park, T. Weirich, J. Mayer, Superior Cemented Carbides Obtained by Plasma Spraying – Dream or Reality, Proceedings of Euro PM2015.
- [16] M. Tarraste, K. Juhani, J. Kübarsepp, J. Pirso, V. Mikli, The Effect of Cr and C on the Characteristics of WC-FeCr Hardmetals, Proceedings of Euro PM2015.
- [17] J. Kübarsepp, Steel-Bonded Hardmetals, PhD thesis, Tallinn University of Technology (1992).
- [18] M. Kolnes, J. Kübarsepp, L. Kollo, M. Viljus, Characterization of TiC-FeCrMn Cermets Produced by Powder Metallurgy Method, Materials Science (Medžiagotyra), 21 (2015), pp. 353-357
- [19] B. Wittmann, W.-D. Schubert, B. Lux, WC Grain Growth and Grain Growth Inhibition in Nickel and Iron Binder Hardmetals, International Journal of Refractory Metals & Hard Materials, 20 (2002), pp. 51-60.
- [20] V. Smolej, S. Pejovnik, W.A. Kaysser, Rearrangement during Liquid Phase Sintering of Large Particles, Powder Met. Int., 14 (1981), pp. 126-128.
- [21] W.D. Kingery, Densification during Sintering in the Presence of a Liquid Phase, J. Applied Phys., 30 (3) (1959), pp. 301-306.
- [22] M. Tokita, Mechanism of Spark Plasma Sintering, Sumitomo Coal Mining Company, Ltd., Kawasaki-shi Kanagawa, Japan (1999).
- [23] H.R. Lawn, E.R. Fuller, Equilibrium Penny-like Cracks in Indentation Fracture, J. Mater. Sci., 10 (1975), pp. 2016-2024.

PAPER IV

M. Tarraste, J. Kübarsepp, K. Juhani, A. Mere, M. Viljus, Effect of Carbon Stabilizing Elements on WC Cemented Carbides with Chromium Steel Binder, *Materials Science (Medžiagotyra)*, (XXXX) XX. (Accepted)

Effect of Carbon Stabilizing Elements on WC Cemented Carbides with Chromium Steel Binder

Marek TARRASTE^{1*}, Jakob KÜBARSEPP¹, Kristjan JUHANI¹, Arvo MERE²,
Mart VILJUS¹

¹ Department of Mechanical and Industrial Engineering, Tallinn University of Technology, Ehitajate tee 5, 19086 Tallinn, Estonia

² Department of Materials and Environmental Technology, Tallinn University of Technology, Ehitajate tee 5, 19086 Tallinn, Estonia

crossref <http://dx.doi.org/10.XXXX/j01.xxxxxxx>

Received 07 December 2017; accepted 25 April 2018

High price, limited availability and toxicity of cobalt motivates researchers and material engineers to find alternative binder systems for WC cemented carbides. Iron and iron alloys are promising candidates for complete cobalt substitution. Ferritic steels alloyed with chromium can offer an inexpensive binder system to acquire cemented carbides with enhanced oxidation and corrosion resistance. Since Fe and Cr are carbide formers, production of WC-FeCr cemented carbides with a desirable two-phase structure can be problematic. Niobium and titanium are strong carbide formers and well-known alloying elements in steels used to stabilize carbon, preventing formation of unwanted chromium carbide phases. In our work, WC-FeCr was alloyed with elemental Nb and Ti. The phase composition, structure morphology and mechanical properties of prepared cemented carbides were characterized and discussed. As a result, additions of carbon stabilizing elements enabled us to improve structural homogeneity and wear resistance of WC cemented carbides with ferritic a steel binder.

Keywords: cemented carbides, alternative binder, erosion resistance, microstructure evolution.

1. INTRODUCTION

The necessity to reduce or even avoid toxic elements such as cobalt and nickel in engineering materials is intensified by various regulations [1, 2]. However, these elements are preferred as binder in tungsten cemented carbides. WC-Co system show exceptional mechanical and tribological performance and WC-Ni offers enhanced oxidation/corrosion resistance. Iron as a potential binder metal was excluded in the early 1930s due to its inferior mechanical properties, but in the recent decades, studies have increasingly focused on Fe-binder. Several complications with Fe as a base binder metal have been resolved by addressing the crucial effect of carbon balance [3] and the usage of calculated phase diagrams [4]. With binder systems such as FeNi, FeCoNi, FeNiCr, FeMn, etc., researchers have achieved positive and often superior results, even surpassing those of WC-Co [5–7].

Co and Ni free WC cemented carbides with the FeCr-based binder have received limited attention. Hinners et al. prepared hardfacing where WC and M_xC_y particles were embedded in Fe(Cr) matrix [8]. Sakaguchi et al. and Kambakas et al. focus on the high chromium grey cast irons with WC reinforcement [9, 10]. Our studies of the FeCr binder system have shown that it is challenging to achieve a uniform structure without using very fast consolidation processes (e.g. SPS) [11, 12], due to carbon activity, Fe and Cr mixed metal carbides form (Fig. 1). Kambakas et al. have shown how active the cast iron and WC system is in terms

of phase formations. According to their study, during casting, various M_xC_y primary and eutectic carbides were formed. M_xC_y carbides can have a detrimental effect on the properties of bulk WC cemented carbides.

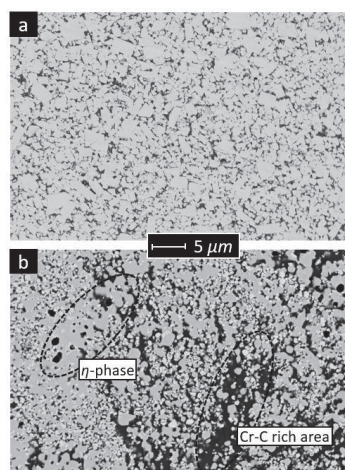


Fig. 1. WC-Co microstructure: a – exhibits favourable uniform two phase structure with WC grains in Co matrix. In the WC-FeCr microstructure; b – presence of secondary metal carbides yields heterogeneous microstructure

* Corresponding author. Tel.: +372-6203357.

E-mail address: marek.tarraste@gmail.com (M. Tarraste)

The most prevalent method to retard the formation of Fe- and Cr-based metal carbides in steels is the addition of strong monocarbide forming elements [13].

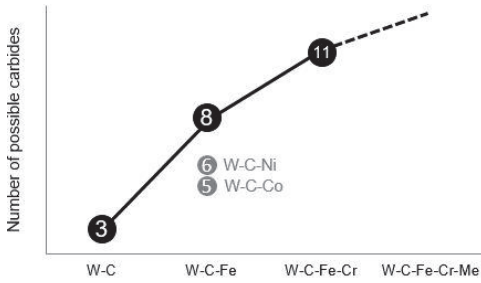


Fig. 2. Number of possible carbides in WC hardmetal systems according to [14, 15]

However, due to the carbon active nature of Fe and Cr the number of possible carbide phases in WC-Fe(Cr) cemented carbides is already greater than in conventional WC-Co/Ni systems (Fig. 2). The addition of active carbide formers to the W-C-Fe-Cr system could complicate the final phase composition even further.

Our aim of this research is to study the effect of carbide-forming elements Ti and Nb on the microstructure and properties of WC-FeCr cemented carbides.

2. EXPERIMENTAL

Cemented carbide powder mixtures with a ferritic chromium steel AISI430L ($Fe_{81.8}Cr_{16.8}Mn_{0.7}Si_{0.7}$) binder and Ti/Nb additions were prepared by the conventional milling technique: WC, steel, Ti/Nb and graphite powders were milled in a ball mill with hardmetal lining and balls for 144 h with the ball-to-powder weight ratio of 10:1. Isopropyl alcohol was used as a milling liquid. Chemical composition of prepared mixtures and reference materials are presented in Table 1. Graphite powder as an extra carbon source was included to minimize decomposition of the WC phase due to the formation additional M_3C_2 phases, especially after liquid phase sintering. As compared with traditional WC-Co cemented carbides, experimental WCS-Ti and WCS-Nb as well as WCS mixtures were prepared with drastically increased metal fraction to guarantee the presence of metal matrix after the formation of various additional carbide phases.

Milled powders mixed with 3 wt.% paraffin were dried at 50 °C and compacted into green bodies with 95 MPa of uniaxial pressure. Conventional liquid phase sintering in

vacuum (0.1...0.5 mbar) was carried out in a sinter-HIP furnace FPW 300/400 from FCT Systeme GmbH. Pressed samples were placed on zirconia support in graphite crucibles. Heating rate was 10 °C/min and 30 min dwell at the end temperature, followed by natural cooling with the furnace. WCS-(Ti/Nb) materials were sintered at 1300 °C while WC-Co reference materials were sintered at 1400–1450 °C. Respective sintering temperatures yielded specimens with near full density and minimal porosity (< 0.2 %). Zeiss EVO MA15 scanning electron microscope (SEM) equipped with an Oxford Instruments INCA Energy EDS system was used for microstructure observation and assessment of elemental distribution. X-ray diffraction (XRD) measurements of the samples were performed on a Rigaku Ultima IV diffractometer with monochromatic Cu K α radiation ($\lambda = 1.5406 \text{ \AA}$) at 40 kV and 40 mA using the silicon strip detector D/teX Ultra. All samples were studied in the 2θ range of 28 – 55 deg with the scan step of 0.02 deg. Vickers hardness was measured with Indetec 5030. The indentation fracture toughness (K_{IC}) was determined by measuring the crack length from the tip of the indentation made by Vickers indentation (Palmqvist method) and calculated by the following equation [16]:

$$K_{IC} = 0.15 \sqrt{\frac{HV_{30}}{\sum l}}, \quad (1)$$

where $\sum l$ is the sum of the crack length of the crack tip from the hardness indent in mm. The erosion wear of prepared cemented carbides in room and in elevated temperatures was measured with the help of the four channel centrifugal high temperature erosion wear tester described in [17]. Silica particles with a mean size 0.3 mm were chosen as erodent. Particles with the velocity of 80 m/s hit specimens at the angle of 30°. During all tests the atmosphere was air to simulate erosion-oxidation conditions.

3. RESULTS AND DISCUSSION

3.1. Microstructure and phase composition

Backscatter SEM images of WCS-(Ti/Nb) cemented carbides with respective Cr mappings are presented in Fig. 3. Small magnification renders a good overview of phase distribution and with the corresponding Cr elemental signal, it is evident that addition of Ti and Nb promotes the development of more a homogeneous structure. Large elongated Cr-rich binder pools, often over several hundred micrometre long, are not present in materials WCS-(Ti/Nb). The η -phase, almost not present in WCS, is formed in materials alloyed with Ti and Nb (Fig. 4 and Fig. 5).

Table 1. Composition of prepared powder mixtures and mechanical properties of respective sintered cemented carbides

Material designation	Composition, wt.%									Hardness, HV30 kgf/mm ²	Indentation fracture toughness MPa*m ^{1/2}
	WC	Co	Fe	Cr	Mn	Si	C	Ti	Nb		
WCS-Ti	69	–	20.2	4.1	0.2	0.2	1.5	4.9	–	1237 ± 13	8.7 ± 0.1
WCS-Nb	69	–	20.2	4.1	0.2	0.2	1.5	–	4.9	1340 ± 28	8.5 ± 0.2
WCS	69	–	24.2	5.0	0.2	0.2	1.5	–	–	1204 ± 49	n/a*
WC-11Co	89.0	11.0	–	–	–	–	–	–	–	1489 ± 24	13.8 ± 0.3
WC-15Co	85.0	15.0	–	–	–	–	–	–	–	1274 ± 16	17.5 ± 1.1

□ reference materials
*not possible to measure fracture toughness due to severely uneven microstructure

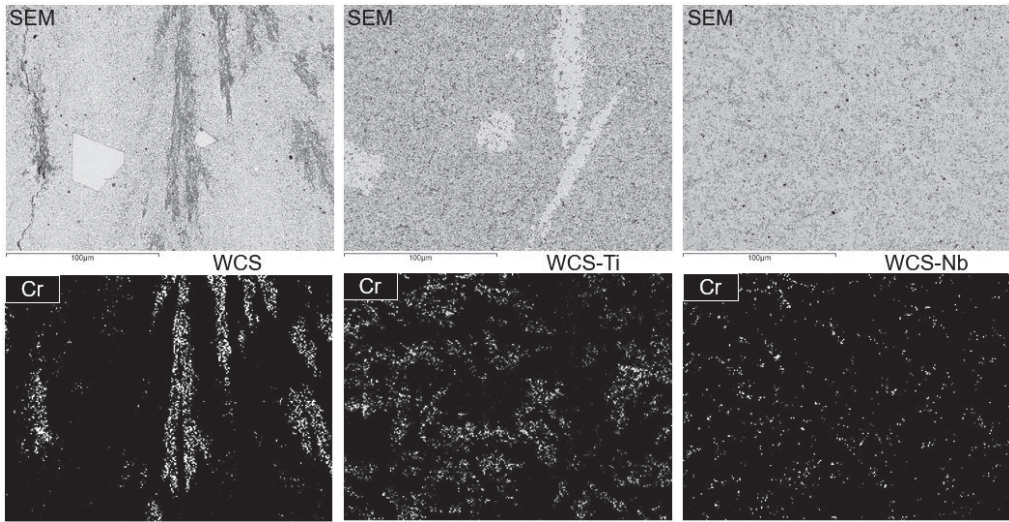


Fig. 3. BS-SEM images and elemental maps of Cr: WCS (left), WCS-Ti (middle) and WCS-Nb (right). Areas with increased Cr concentration are marked as white on elemental maps

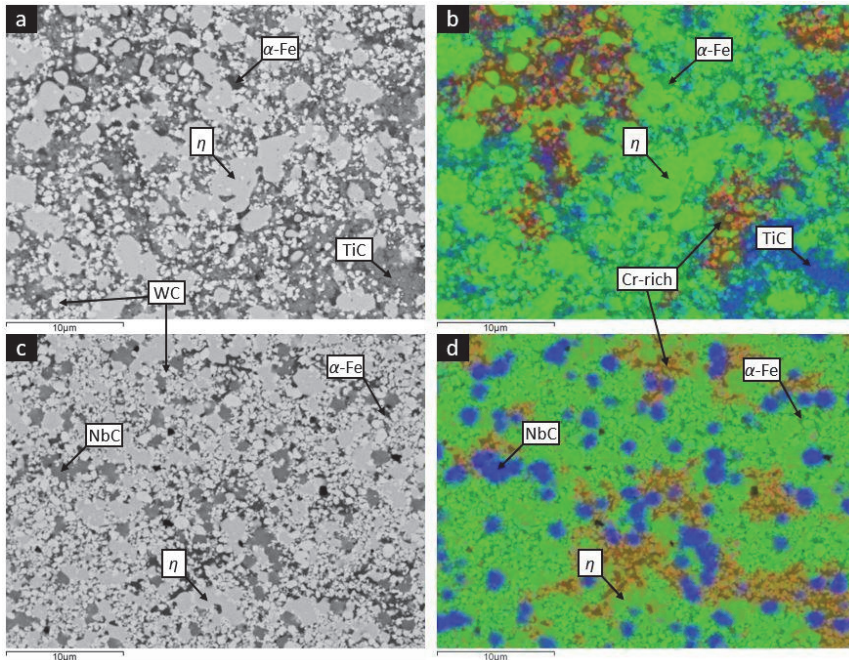


Fig. 4. BS-SEM images coupled with EDS mappings of WCS-Ti (a, b) and WCS-Nb (c, d) (green = Fe, red = Cr, blue = Ti/Nb)

With the help of the EDS and XRD analysis, it was determined to be the type of $(Fe,W,Cr)_6C$ with the Fe:W:Cr ratio close to 5:5:1. The shape of that phase depends on the material. Only in the microstructure of WCS-Nb η -phase appears as uniformly distributed 1–3 μm sized grains (Fig. 3 and Fig. 4 c). BS-SEM microstructure images and respective EDS elemental mappings of experimental cemented carbides (Fig. 4) with higher magnification demonstrate three distinguishable areas with different

elemental composition: three carbide phases (WC, η -phase, TiC or NbC) and two metal rich phases. Due to the relatively large interaction volume of EDS analysis method ($\geq 1 \mu m \text{ } \varnothing$) coupled with submicron structure of experimental materials, we were unable to employ EDS spot analysis to acquire precise quantitative elemental data of other phases besides η -phase. TiC and NbC are both cubic carbides and other refractory metals (W, V, Mo, Cr) are soluble in them. In the current work with EDS, a dissolution

of 16...20 wt.% of W in Ti and Nb carbides was approximated.

According to the XRD results Fe-rich phase is ferrite, α -Fe with the bcc crystal structure. The presence of α -Fe instead of fcc structured γ -Fe is in good accordance with literature [18]. Cr is soluble in α -Fe, thus forming Fe-Cr solid solution. However, in the materials, Cr content in solid solution was not over 5 wt.% and even taking account high uncertainty of EDS, it is still considerably lower than the in starting material (16.8 wt.% in AISI430L steel), thus confirming the formation of Cr-carbides. In the Fe-Cr-C system during cooling from liquid phase, eutectic transformation follow $L \rightarrow fcc + M_7C_3$ and later fcc starts decomposing into bcc and $M_{23}C_6$ [19]. Thus, a Cr-rich phase in the WCS material consists mainly of Cr carbides with their shape similar to the $(Cr, M)_x C_y$ carbides reported by Kambakas [10]. In the WCS-Ti/Nb materials, the formation of large elongated Cr-rich areas is retarded, which indicates that upon solidification eutectic-like mixture of $M_x C_y$ and α -Fe based solid solution is formed. This confirms that the addition of Ti and Nb had a desired effect on the microstructure, i.e., TiC and NbC as more stable carbides form preferably and thereby the fraction of Cr-based carbides is reduced. Traces of γ -Fe were also detected in the WCS-Ti material. This residual fcc phase indicates that decomposition of fcc was not finished during the cooling cycle and metallic phase could be in a metastable condition.

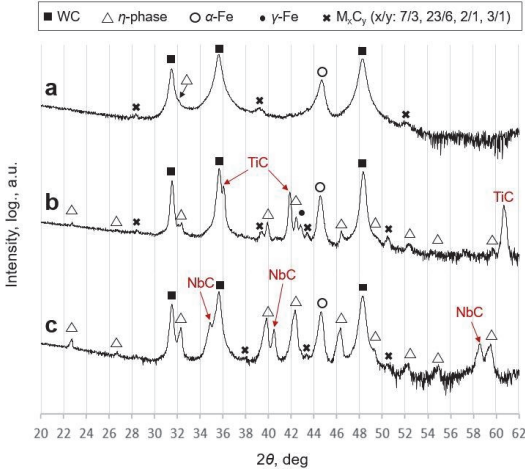


Fig. 5. XRD results of materials: a–WCS; b–WCS-Ti; c–WCS-Nb

3.2. Mechanical properties and wear performance

Mechanical properties presented in Table 1 reveal that while hardness of WCS-(Ti/Nb) cemented carbides is comparable with that of WC-15Co, the indentation fracture toughness is considerably lower even, when compared with that of WC-11Co. Achieving good toughness values with the Fe-based binder is complicated even with relatively straightforward WC-Fe system because of the stability of the M_6C phase [20]. With the materials discussed in our work, it is especially difficult because of the high total fraction of carbides and the low fraction of completely carbide free binder phase. However, an improvement was

achieved with the addition of Ti and Nb since their absence results in a microstructure too disturbed by Cr-rich areas to enable the measurement of fracture toughness with indentation (Palmqvist method).

Erosion wear tests at room and elevated temperatures were carried out to investigate the performance of cemented carbides with the FeCr based binder system in erosion-oxidation environment and compare them with regular WC-Co grades (Fig. 6). At room temperature, WC-11Co and WC-15Co exhibit superior wear resistance; however, their performance begins to deteriorate when the temperature is increased. The advantage of the materials with a steel binder and with and without additional carbide forming elements can be explained with a lower fraction of WC and higher fraction of more oxidation resistant Ti-, Nb- and Cr-carbides [21]. The WCS-Ti material with TiC in the microstructure showed particularly good wear resistance at higher temperatures.

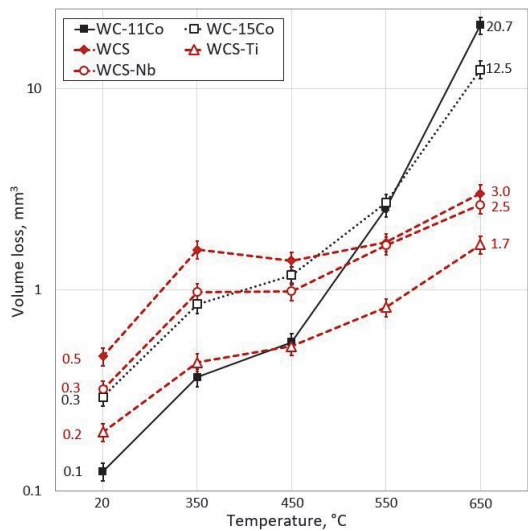


Fig. 6. Erosion wear at room and elevated temperatures of cemented carbides with FeCr and Co binder

4. CONCLUSIONS

WC-based cemented carbides with a ferritic chromium steel binder alloyed with carbon active elements Ti and Nb were prepared. The following conclusions can be drawn:

1. The addition of active monocarbide formers promotes the formation of a more homogeneous microstructure. The formation of Cr-carbide rich areas that disturb the microstructure is retarded.
2. Phase composition of experimental materials is relatively complex – besides W and Ti or Nb monocarbides the structure consists of M_6C type η -phase and different $M_x C_y$ metal carbides.
3. Materials with FeCr binder show improved erosive wear resistance at elevated temperatures when compared with conventional WC-Co cemented carbides.
4. Fracture toughness of materials with a FeCr binder system suffers due to the carbide rich microstructure.

Acknowledgments

This work was supported by institutional research fundings IUT (19-29) and IUT (19-4) of the Estonian Ministry of Education and Research and by the European Regional Development Fund project TK141 "Advanced materials and high-technology devices for energy recuperation systems".

REFERENCES

1. "REACH-Chemicals-Environment-European Commission." http://ec.europa.eu/environment/chemicals/reach/reach_en.htm. [30.5.2017].
2. "National Toxicology Program." <https://ntp.niehs.nih.gov/>. [30.5.2017].
3. Agte, C. Die Neue Hochleistungshartsmetallsorte S6HL. Neue Hütte 1, 1956: p. 333.
4. Gustafson, P. A Thermodynamic Evaluation of the C-Cr-Fe-W System *Metallurgical Transactions A* 19 1988: pp. 2547–2554. <https://doi.org/10.1007/BF02645482>
5. Fernandes, C.M., Vilhena, L.M., Pinho, C.M.S., Oliveira, F.J., Soares, E., Sacramento, J., Senos, A.M.R. Mechanical Characterization of WC–10 wt% AISI 304 Cemented Carbides *Materials Science and Engineering A* 618 2014: pp. 629–636. <https://doi.org/10.1016/j.msea.2014.09.064>
6. Prakash, L., Holleck, H., Thümler, F., Walter, P. The Influence of the Binder Composition on the Properties of WC-Fe/Co/Ni Cemented Carbides *Modern Developments in Powder Metallurgy* 14 1981: pp. 255–268.
7. Hanyaloglu, C., Aksakal, B., Bolton, J.D. Production and Indentation Analysis of WC/Fe–Mn as an Alternative to Cobalt-bonded Hardmetals *Materials Characterization* 47 (3–4) 2001: pp. 315–322. [https://doi.org/10.1016/S1044-5803\(02\)00181-X](https://doi.org/10.1016/S1044-5803(02)00181-X)
8. Hinners, H., Konyashin, I., Ries, B., Petrzhik, M., Levashov, E.A., Park, D., Weirich, T., Mayer, J., Mazilkin, A.A. Novel Hardmetals with Nano-grain Reinforced Binder for Hard-facings *International Journal of Refractory Metals and Hard Materials* 67 2017: pp. 98–104. <https://doi.org/10.1016/j.ijrmhm.2017.05.011>
9. Sakaguchi, S., Imasato, S., Ito, H., Nakamura, R. Some Properties of Sintered WC-(Fe-Cr-C) Alloys *Journal of the Japan Society of Powder and Powder Metallurgy* 36 (8) 1989: pp. 908–912. <https://doi.org/10.2497/jjpspm.36.908>
10. Kambakas, K., Tsakirooulos, P. Solidification of High-Cr White Cast Iron–WC Particle Reinforced Composites *Materials Science and Engineering A* 413–414 2005: pp. 538–544. <https://doi.org/10.1016/j.msea.2005.08.215>
11. Tarraste, M., Juhani, K., Kūbarsepp, J., Pirso, J., Mikli, V. The Effect of Cr and C on the Characteristics of WC-FeCr Hardmetals *Proceedings of Euro PM2015* 2015.
12. Tarraste, M., Kūbarsepp, J., Juhani, K., Suurkivi, T., Pirso, J. Spark Plasma Sintering of WC Hardmetals with Fe-based Binder *Proceedings of World PM2016* 2016.
13. Lo, K.H., Shek, C.H., Lai, J.K.L. Recent Developments in Stainless Steels *Materials Science and Engineering: R: Reports* 65 (4) 2009: pp. 39–104. <https://doi.org/10.1016/j.mser.2009.03.001>
14. Fernandes, C.M., Senos, A.M.R. Cemented Carbide Phase Diagrams: A Review *International Journal of Refractory Metals and Hard Materials* 29 (4) 2011: pp. 405–418. <https://doi.org/10.1016/j.ijrmhm.2011.02.004>
15. Upadhyaya, G.S. Cemented Tungsten Carbides: Production, Properties and Testing, Noyes Publications, 1998.
16. Spiegler, R., Schmauder, S., Sigl, L.S. Fracture Toughness Evaluation of WC-Co Alloys by Indentation Testing *Journal of Hard Materials* 1 (3) 1990: pp. 147–158.
17. Antonov, M., Hussainova, I., Pirso, J., Volobueva, O. Assessment of Mechanically Mixed Layer Developed During High Temperature Erosion of Cermets *Wear* 263 (7) 2007: pp. 878–886. <https://doi.org/10.1016/j.wear.2006.12.035>
18. Khvan, A.V., Hallstedt, B., Broeckmann, C. A Thermodynamic Evaluation of the Fe–Cr–C System *Calphad* 46 2014: pp. 24–33. <https://doi.org/10.1016/j.calphad.2014.01.002>
19. Wiengmoon, A., Pearce, J.T.H., Chairuangri, T. Relationship Between Microstructure, Hardness and Corrosion Resistance in 20wt.%Cr, 27wt.%Cr and 36wt.%Cr High Chromium Cast Irons *Materials Chemistry and Physics* 125 (3) 2011: pp. 739–748. <https://doi.org/10.1016/j.matchemphys.2010.09.064>
20. Schubert, W.D., Fugger, M., Wittmann, B., Useldinger, R. Aspects of Sintering of Cemented Carbides with Fe-based Binders *International Journal of Refractory Metals and Hard Materials* 49 2015: pp. 110–123. <https://doi.org/10.1016/j.ijrmhm.2014.07.028>
21. Huang, S., Xiong, J., Guo, Z., Wan, W., Tang, L., Zhong, H., Zhou, W., Wang, B. Oxidation of WC-TiC-TaC-Co Hard Materials at Relatively Low Temperature *International Journal of Refractory Metals and Hard Materials* 48 2015: pp. 134–140. <https://doi.org/10.1016/j.ijrmhm.2014.08.002>

CURRICULUM VITAE

Personal data

Name	Marek Tarraste
Date of birth	04.11.1987
Place of birth	Tartu
Citizenship	Estonian

Contact data

E-mail	marek.tarraste@ttu.ee, marek.tarraste@gmail.com
--------	---

Education

2013–2018	Tallinn University of Technology – PhD
2011–2013	Tallinn University of Technology – MSc
2007–2011	Tallinn University of Technology – BSc
1995–2007	Tallinna Arte Gümnaasium – High school

Language competence

Estonian	Native speaker
English	Fluent
German	Basic
Russian	Basic

Professional employment

2016–2018	Tallinn University of Technology, early stage researcher
2011–2016	Tallinn University of Technology, engineer

Projects in progress

IUT19-29 "*Multi-scale structured ceramic-based composites for extreme applications (1.01.2014–31.12.2019)*"; Principal investigator: Jakob Kübarsepp, Tallinn University of Technology, School of Engineering, Department of Mechanical and Industrial Engineering.

Industrial property

Invention: *Method of making a double-structured bimodal tungsten cemented carbide composite material*; Owners: Tallinn University of Technology; Authors: Marek Tarraste, Der-Liang Yung, Maksim Antonov, Irina Hussainova, Renno Veinthal, Jüri Pirso, Philippe Kapsa, Vincent Fridrici, Ousseini Marou-Alzouma, Alexandre Taboulet, Thomas Camus; Priority number: PCT/IB2017/050505; Priority date: 31.01.2017.

Invention: *Method and device for manufacturing sintered material products*; Owners: Tallinn University of Technology; Authors: Lauri Kollo, Kaspar Kallip, Zorjana Mural, Hans Vallner, Renno Veinthal, Märt Kolnes, Marek Tarraste, Marek Jöeleht; Priority number: P201500021; Priority date: 13.05.2015.

ELULOO KIRJELDUS

Isikuandmed

Nimi	Marek Tarraste
Sünniaeg	04.11.1987
Sünnikoht	Tartu
Kodakondsus	Eesti

Kontaktandmed

E-post	marek.tarraste@ttu.ee, marek.tarraste@gmail.com
--------	---

Hariduskäik

2013–2018	Tallinna Tehnikaülikool – PhD
2011–2013	Tallinna Tehnikaülikool – MSc
2007–2011	Tallinna Tehnikaülikool – BSc
1995–2007	Tallinna Arte Gümnaasium – Keskkharidus

Keelteoskus

Eesti keel	Emakeel
Inglise keel	Kõrgtase
Saksa keel	Algtase
Vene keel	Algtase

Teenistuskäik

2016–2018	Tallinna Tehnikaülikool, nooremteadur
2011–2016	Tallinna Tehnikaülikool, insener

Jooksvad projektid

IUT19-29 "*Mitmeastmeliselt struktureeritud keraamika-baasil komposiitmaterjalid kasutamiseks ekstreemtingimustes (1.01.2014–31.12.2019)*"; Vastutav täitja: Jakob Kübarsepp, Tallinn Tehnikaülikool, Inseneriteaduskond, Mehaanika ja tööstustehnika instituut.

Tööstusomand

Patentne leiutis: *Meetod topelt-struktuuriga bimodaalsete volframkarbiid kõvasulamite valmistamiseks*; Asutus: Tallinna Tehnikaülikool; Autorid: Marek Tarraste, Der-Liang Yung, Maksim Antonov, Irina Hussainova, Renno Veinthal, Jüri Pirso, Philippe Kapsa, Vincent Fridrici, Ousseini Marou-Alzouma, Alexandre Taboulet, Thomas Camus; Prioriteedi number: PCT/IB2017/050505; Prioriteedi kuupäev: 31.01.2017.

Patentne leiutis: *Meetod ja seade pulbermaterjalist toodete valmistamiseks*; Asutus: Tallinna Tehnikaülikool; Autorid: Lauri Kollo, Kaspar Kallip, Zorjana Mural, Hans Vallner, Renno Veinthal, Märt Kolnes, Marek Tarraste, Marek Jõelet; Prioriteedi number: P201500021; Prioriteedi kuupäev: 13.05.2015.